REPORT NO. 30-5

EXPERIMENTAL INVESTIGATION OF FLAME STABILIZATION IN A DEFLECTED JET

GUNNAR ERIK BROMAN

JET PROPULSION LABORATORY
CALIFORNIA INSTITUTE OF TECHNOLOGY
PASADENA, CALIFORNIA

SEPTEMBER 30, 1959

National Aeronautics and Space Administration
Contract No. NASw-6

REPORT NO. 30-5

EXPERIMENTAL INVESTIGATION OF FLAME STABILIZATION IN A DEFLECTED JET

Gunnar Erik Broman

Frank E. Marble

Frank E. Marble, *Chief*
Combustion Research Section

JET PROPULSION LABORATORY
California Institute of Technology
Pasadena, California
September 30, 1959

PREFACE

Portions of the following report were originated under studies conducted for the Department of Army Ordnance Corps under Contract No. DA-04-495-Ord 18. Such studies are now conducted for the National Aeronautics and Space Administration under Contract No. NASw-6.

CONTENTS

FIGURES

FIGURES (Cont'd)

FIGURES (Cont'd)

ABSTRACT

An experimental investigation has been made of flame stabilization in a two-dimensional deflected jet of a propane–air mixture at a temperature of 70°F and atmospheric pressure. By a 90-deg deflection of the jet entering a combustion-chamber duct through a slot, a recirculation zone is created which serves as a heat source in the flow. The chemical reaction in a mixing zone between the fresh mixture in the jet and the hot gas in the recirculation zone supplies heat for the stabilization of a flame in the flow.

The influence of the flow parameters on the stability was determined by changing the burner size and geometry. When the geometry was changed by variation of the ratio between slot width and burner height, two types of flow were observed. First, for large ratios, the mixing zone was covered by the flow of fresh mixture along the complete length of the mixing zone. This type of flow, with a free mixing zone, shows a great deal of similarity to the flow of the bluff body flameholder. The characteristic time introduced for the bluff body flameholder was also found to be a satisfactory correlation parameter for the stability of burners of different sizes and geometries.

In the second type of flow found for small slot-to-height ratios, the mixing zone reached the burner wall before the end of the recirculation zone. A detailed study of the flow showed that the actual residence time in the mixing zone was the primary parameter for stability. Comparisons between burners with small slot-to-height ratios and the can burner also suggest that the same concept can be applied to the can burner.

The results of the present investigation show that the ignition delay concept, on which the characteristic time for the bluff body flameholder is based, can be extended to flame stabilization in a deflected jet.

I. INTRODUCTION

Modern jet engines require combustors capable of stabilizing a flame at flow speeds considerably higher than the speed of flame propagation. Two different types of combustors have been developed to meet this requirement. The first type, the bluff body flameholder, makes use of the wake behind the body as a heat source from which the flame can propagate through the flow, as illustrated by Fig. 1a. The second combustor design, the so-called can-type combustion chamber, also operates with a hot wake created by a deflection of the flow, as indicated in Fig. 1b. Both of these combustors are presently in common use in the turbojet and ramjet engines.

The performance quality of primary interest in these combustors is the relationship between the speed of the flow and the range of fuel–air ratios for which a stable operation can be maintained. The limits of the range of stable operation are, as a rule, determined by blowoff experiments. It is, however, desirable to find the similarity laws for stability, so that the stability limits of combustors can be predicted without necessitating actual tests in every case. Because of the complexity of the stabilization process, the actual mechanism of flame stabilization must be understood before these similarity laws can be developed in a rational manner.

A large number of experimental as well as theoretical investigations have been carried out in order to explain the stabilization process and to provide material for the development of stability parameters. The most common approach has been to establish the correlation parameter from the results of blowoff experiments with combustors of different size and geometry. By considering the character of these rather general empirical parameters, attempts have been made to determine the stabilization mechanism.

A brief summary of some of the investigations concerning the flame stabilization in the bluff body flameholder and the can-type combustion chamber is now presented. Since the bluff body flameholder exhibits a considerably less complex flow field than the can burner, most of the work in flame stabilization has been concentrated on the former type of combustor.

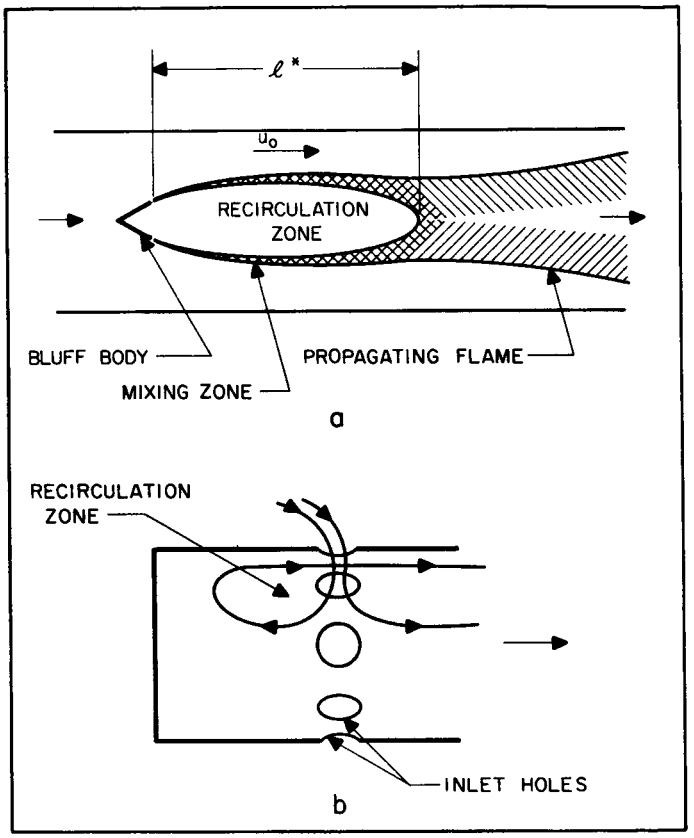

Fig. 1. Schematic Flow Diagram for (a) Bluff Body Flameholder and (b) Can-Type Combustion Chamber

The theories developed for the bluff body flame stabilization can be divided into two groups, depending upon what region of the flow field is considered to be significant in the blowoff mechanism. The investigators working with theories in the first group have concentrated their attention on the recirculation zone and have concluded that the energy balance in this zone is the primary factor determining the stability of the flame.

The second approach, originated by Zukoski and Marble (Ref. 1) has been to consider the chemical reaction process in the mixing zone as the limiting factor for the stability. Some examples will further illustrate the nature of the different approaches taken to the problem.

In the first group, various factors influencing the energy balance of the recirculation zone have been considered. Longwell, *et al* (Ref. 2), Mullins (Ref. 3), and De Zubay (Ref. 4), have assumed the recirculation zone to be a region sufficiently well mixed to be considered a homogeneous reaction region. The stability of this zone is then determined by the chemical kinetics of the reaction. Blowoff occurs when the amount of heat released by the chemical reaction is not sufficient to keep the temperature up in the homogeneous mixture of hot gas and fresh fuel–air mixture presumed to be present in the recirculation zone. It is interesting to note that the consideration of stability in this case involves a time concept. As the mass flow entering the recirculation zone is increased, less time is available for the reaction; hence, less heat will be evolved, and, at some critical mass flow rate, blowoff will occur. The stability limits predicted by these theories can be made to agree with the dependence of the observed stability limits on certain of the parameters of interest. However, the analyses are not based on a detailed knowledge of the actual flow field. Indeed, certain features of the flow implied by the analyses are in direct disagreement with observed facts.

The second approach, involving a consideration of the ignition process in the mixing zone, was a result of a thorough study of the wake gas properties and wake geometry. It has led to a considerable clarification of the process and, in particular, to a simple separation of the effects on stability of flow parameters on one side and of chemical parameters on the other. Zukoski and Marble have shown that the stability limits can be correlated by a characteristic time parameter

$$\tau_c = \frac{l^*}{u_0}$$

where l^* is the length of the wake, and u_0 is the blowoff speed of the fresh mixture past the wake as shown in Fig. 1a. It was found that this parameter is determined exclusively by the factors affecting the combustion chemistry. The corresponding stabilization mechanism is based on the concept of a continuous ignition process taking place in the mixing zone between the stream of fresh fuel–air mixture and the hot gas in the wake. It is interesting to notice that the recirculation zone is considered as an independent steady heat source in the flow field, not only under normal stable operation, but also through the blowoff process. Blowoff of the flame propagating through the mixture downstream from the wake occurs when the material involved in the continuous ignition process is not given a long enough residence time in contact with the hot wake. Thus the characteristic time τ_c is a measure of a chemical ignition delay time. The question of stability has been reduced to a question of whether or not the time available in the flow field is longer than the minimum chemical time required for ignition. The influence of the different parameters on the stability follows immediately from this consideration. Experiments by Wright (Ref. 5) further illustrated the usefulness of the ignition delay time as a correlation parameter for bluff body flameholders.

In the study of the can-type combustor, most investigators have only determined the over-all stability parameters. The detailed structure of the flow field in this burner is not very well known, and the theories for the stabilization mechanism have therefore been given a rather general formulation.

Weiss and Longwell (Ref. 6) studied the stability of a large number of can burners of different geometry and size. The stability of the burners was found to be correlated by a parameter similar to the stability parameter for a well-stirred chemical reactor. It was assumed that the recirculation zone of the can burner had an intensely mixed region and that the stability of this region depended on the over-all kinetics of a homogeneous reaction. Of interest is the fact that the correlation parameter for stability found by Weiss and Longwell is based on the rate of mass flow rather than the jet speed.

Other investigators, e.g., Way (Ref. 7) and Herbert (Ref. 8), have reached similar conclusions about the flame stabilization mechanism in the can burner. However, Way has given the stability criterion a somewhat different formulation. He proposes that for geometrically similar burners working with gaseous mixtures, the ratio of the residence time to a chemical reaction time is the correlation parameter for stability. However, this residence time is rather ambiguous and is not related to the details of the flow. In addition, Way discusses some probing experiments which show that the flow pattern in the can has the same general character as indicated in Fig. 1b.

Clearly, the theories for flame stabilization in the can burner have been given a rather vague formulation as compared with the ignition delay time theory for the

bluff body flameholder. In both cases, the chemical reaction rates are the ultimate factors determining the stability. However, the ignition delay time introduced by Zukoski and Marble is directly related to the flow picture by its characteristic time. Furthermore, the concept that the continuous ignition process is the basic element of the stabilization mechanism is in complete agreement with the observed physical processes and scaling laws.

The can burner theories, on the other hand, do not very clearly relate the stability parameter to the actual flow picture. Nor is the stabilization mechanism explained by the structure of the flow field. The basic reason for this situation is that, because of its complexity, the flow picture in the can burner is not well known. Therefore, it was decided to study some of the aspects of the flame stabilization process in the can burner by use of a relatively simple model which permitted a determination of the flow parameters. A two-dimensional deflected jet of fuel–air mixture was chosen as a suitable model for this purpose. By variation of geometry, a model of this type can be made to exhibit some of the characteristics of the bluff body flameholder as well as the can burner. The objective of the present investigation, then, was to study the flame stabilization in a deflected jet with particular reference to the concept of an ignition delay time.

II. EXPERIMENTAL EQUIPMENT AND TECHNIQUE

A number of combustion chambers based on a simplified model of a burning jet of fuel–air mixture were designed and studied during the course of the investigation. The experiments were carried out in a test facility providing a fuel–air mixture supply system. The system delivered a homogeneous mixture over the wide range of mass flow rates and fuel–air ratios required to cover the stable region of operation for combustion chambers of various sizes and geometrical configurations.

A. Combustor Model

As mentioned previously, it was decided that a two-dimensional jet of fuel–air mixture deflected at a right angle would constitute a suitable model. The general features of this model are shown in Fig. 2. By the deflection of the jet, a recirculation zone is created between the initial undeflected part of the jet and the downstream part of the deflected flow. Consequently, a flame can be stabilized in the jet and the flow parameters can easily be determined in the resulting two-dimensional flow pattern.

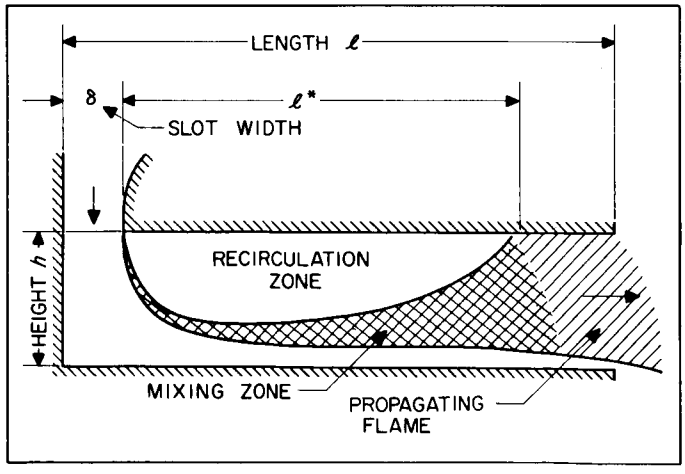

Fig. 2. Schematic Diagram of Geometry and Flame Configuration of Two-Dimensional Slot-Type Combustion Chamber; Burner Geometry Is Specified by Standard Notation ($\delta \times h \times l$)

The geometrical configuration of this model is defined by the ratio between the slot width δ and the combustion chamber height h. For the sake of brevity, this ratio will be denoted by the expression "slot ratio." Given a certain slot ratio, the length l^* of the recirculation zone would be expected to depend primarily on the height h. Consequently, h is a convenient parameter defining the combustion chamber size. The length l of the chamber is a less significant dimension. The only requirement of the length l is the obvious requirement that it be long enough to cover the complete length of the recirculation zone.

The combustion chamber size and geometrical configuration are defined by the notation

$$\delta \times h \times l$$

The model chosen covers a variety of flow configurations. As will be shown, it will be possible to exhibit some of the characteristics of the bluff body as well as the can burner flame stabilization processes by varying the slot ratio over a wide range.

To make it possible to find similarity laws for stability, the slot width as well as the burner height should be variable over sufficient ranges. It follows that the actual combustion chamber design must incorporate a great deal of flexibility.

In order to study the influence of the chemical parameters, it is also desirable to control the temperatures of the fresh mixture as well as the recirculation zone. For the latter purpose the combustion chamber should have provisions for changing the heat transfer from the recirculation zone.

The remaining chemical parameter, the type of fuel, was held constant during all experiments. As the major part of the investigation was carried out with the fresh mixture at room temperature, propane was selected as the standard fuel to insure homogeneity of the mixture. Another reason for this choice was that the propane was readily available in the quantities desired. In liquid form, propane also offers an automatic pressurization of the fuel system.

B. Combustion Chambers

Two combustors featuring two-dimensional slot-type combustion chambers were designed and built for the present investigation. The first combustor, designated type A, was primarily designed for linear scaling of the combustion chamber geometry. The second combustor, type B, was basically arranged to permit a considerable variation of the geometrical configuration for a combustor of intermediate size.

1. Combustor type A. The main features of combustor type A are shown in Figs. 3 and 4. The inlet duct has a square cross section of 4 × 4 in. One side wall of the duct is extended below the others to serve as a back wall of the combustion chamber. The entrance to the chamber is formed by a slot between the extended side wall and a steel block attached to the other three side walls of the duct. The block has a rounded profile on the approach side of the slot, and the lower surface serves as the top wall of the combustion chamber. The bottom wall is formed by a steel plate attached at right angles to the back plate by a support.

In order to provide facilities for visual observation of the two-dimensional flow pattern, the chamber is equipped with side walls consisting of ¼-in.-thick vycor glass plates. The glass is pressed directly against the side surfaces of the steel block and the back and bottom plates by flat springs.

It is possible to vary the chamber height in the range of ½ to 2 in. by moving the support for the bottom plate along the back wall. Accordingly, the length of the bottom plate has to be adjusted in order to maintain the exit section fairly close to the end of the recirculation zone. In combustion chamber experiments it is commonly

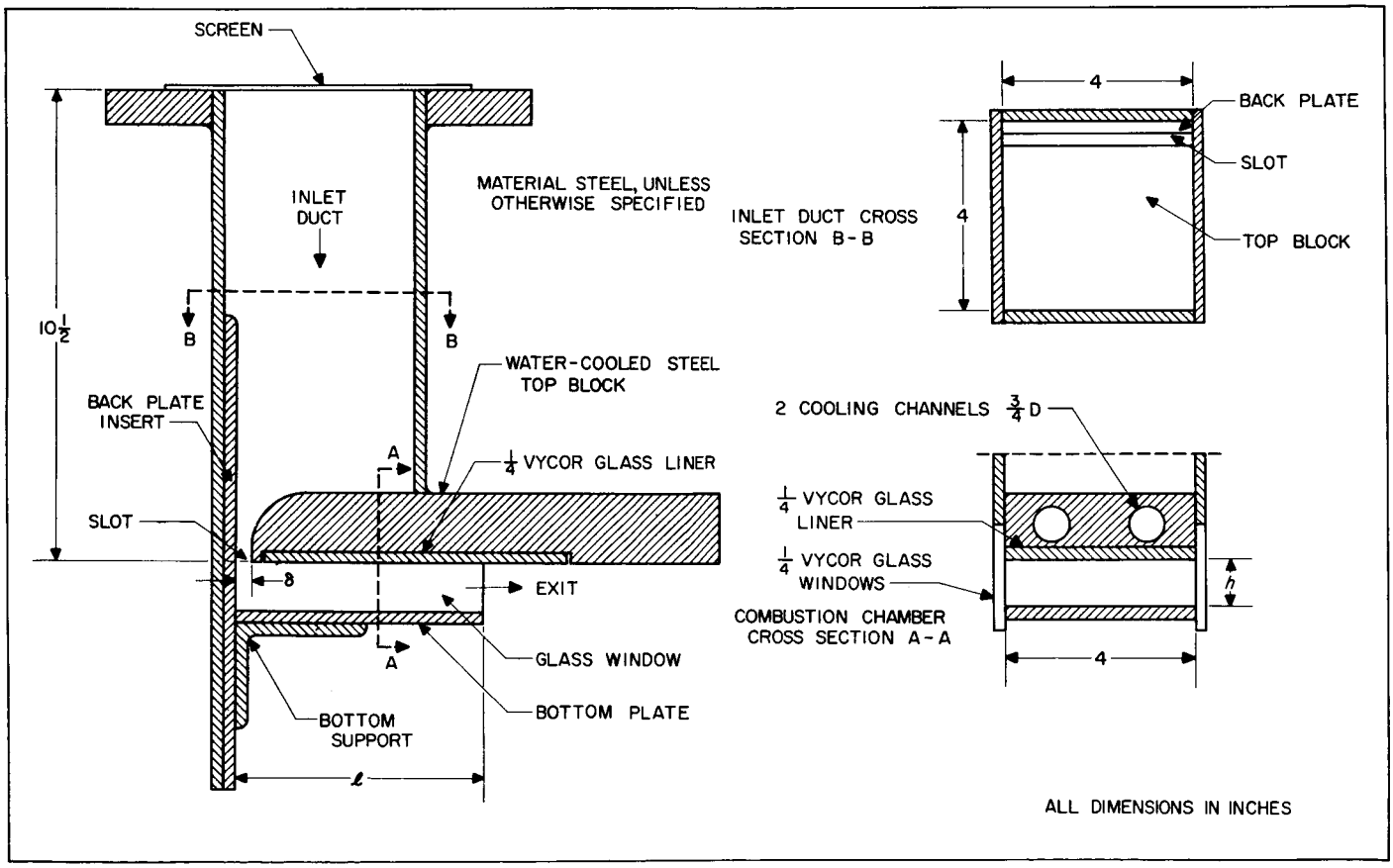

Fig. 3. Combustor Type A; Combustion Chamber Height and Slot Width Variable in Ranges h = ½–2 in. and δ = 0–½ in.

Since the combustion chamber was designed primarily for scaling experiments, an attempt was made to reduce the effects of heat transfer from the recirculation zone as much as possible. Therefore, the top wall of the burner is covered by a ¼-in.-thick vycor glass liner. To protect the top steel block itself from excessive heating, a number of passages for cooling water were introduced.

observed that long tailpipes lead to instabilities in the flame stabilization process. Such instabilities were actually encountered during the initial tests, which were carried out using relatively long bottom plates. It was found that a length about 5 times the height of the chamber gave a satisfactory operation from the point of view of stability and at the same time was long enough to cover

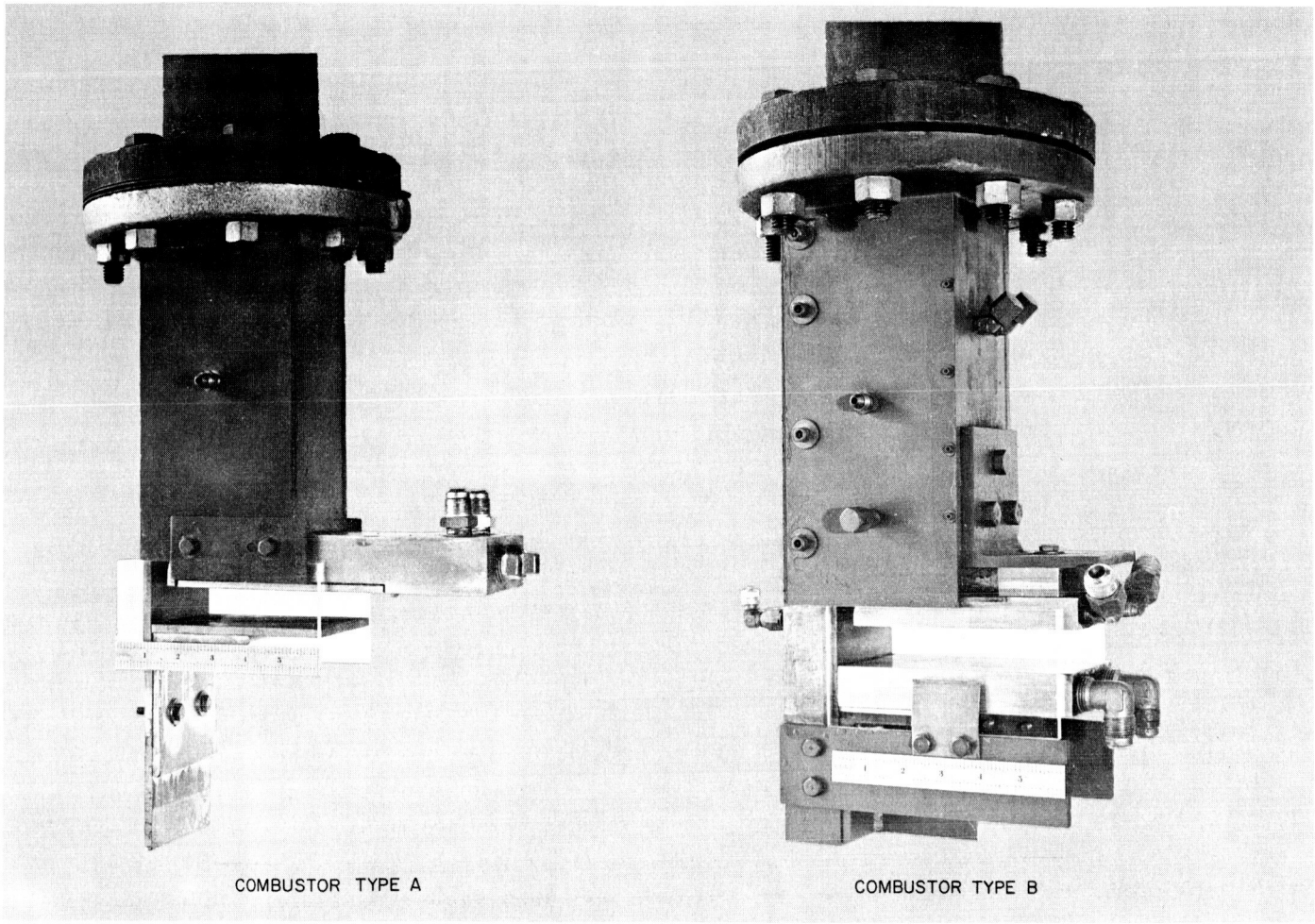

Fig. 4. Side View of Combustors

the recirculation zone. The standard length of the present combustion chamber was therefore set at 5 h. The length is measured from the back wall to the exit section. It will be noticed that the top block extends considerably outside this section. This is a matter of practicality. The length of the top block cannot be changed as easily as is the case for the other combustion chamber walls. Because the overshooting part of the block does not affect the stability of the flame, the block was kept at a length sufficient to cover the largest combustion chambers to be tested.

The slot width δ is adjustable in the range of 0 to 0.5 in. by inserting plates of uniform thickness (0.5–δ in.) into the slot. The plate insert is pressed against the back wall by the support for the bottom plate.

In terms of the code notation defined earlier in this report, the combustion chambers in combustor type A are denoted by ($\delta \times h \times 5h$) A.

2. Combustor type B. The purpose of combustor type B is to provide facilities for changing the slot ratio over a wide range for a combustion chamber of an intermediate size. The design, shown in Figs. 4 and 5, has the same general features as the previous model except for the arrangement for changing the slot width. This is accomplished by sliding the top block in an axial direction.

The inlet duct of combustor type B has a square cross-section of 3×3 in., which was made smaller than that used for type A to reduce the requirements on fuel flow rates for large slot widths. The back plate consists of a steel channel profile to provide a very rigid mount for the bottom plate.

To make it possible to study the effect of heat transfer from the recirculation zone, the top block is made of aluminum and equipped with passages for cooling water. Thus, the lower surface of the block, which serves as the

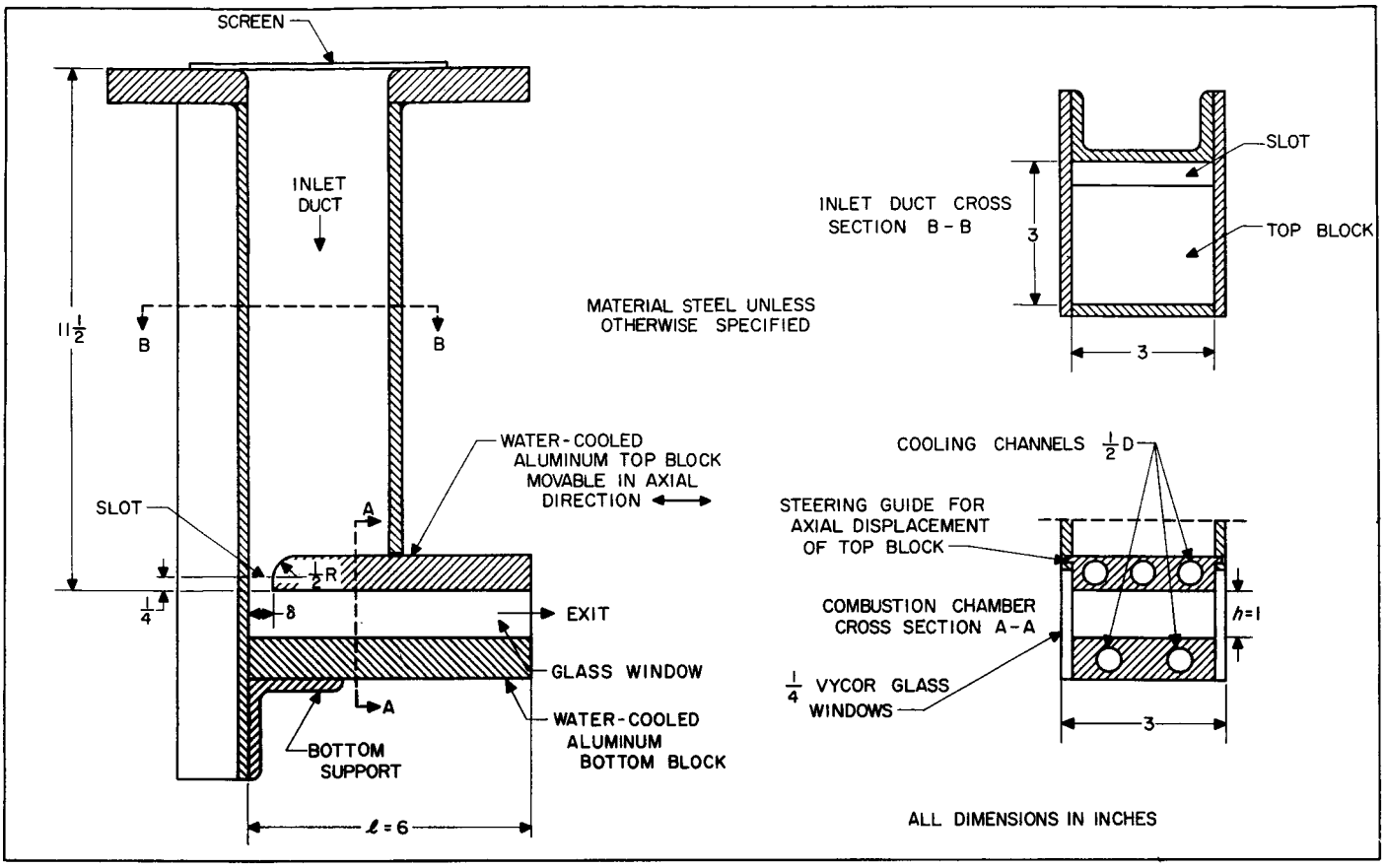

Fig. 5. Combustor Type B; Slot Width Variable in Range 0–1 in. by Axial Displacement of Top Block

top wall of the combustion chamber, acts as a strong heat sink along the boundary of the recirculation zone.

The adjustment of the top block is governed by axial guides at the sides of the block which slide in grooves along the edges of the inlet-duct side plates. The slot width can easily be adjusted in the range of 0 to 1 in. The top block is fixed in the position desired by a lock screw on the upper surface of the block as shown in Fig. 4.

The intermediate burner size chosen has a height of 1 in. and a length of 6 in. In this case, the reason for making the length larger than 5 h is that longer recirculation zones will be encountered when the slot width is reduced to smaller ratios than those used in combustor type A.

The standard notation for the combustion chambers in combustor type B is $(\delta \times 1 \times 6)$ B.

C. *Mixture Supply System*

The facility used during the experiments includes a test cell equipped with a mixture supply system and a control room from which the combustion chamber can be operated and observed. The mixture is supplied from separate systems for controlling and metering the air and fuel flow rates, as shown in Figs. 6, 7 and 8.

1. Air system. The air used in the test cell is supplied by two 2-stage rotary-vane-type compressors. The compressors have a total capacity of 3300 ft^3/min and charge a receiver tank to a constant pressure level of about 90 psia. The air delivered to the test facility passes through a pressure level to a constant value of about 76 psia.

The metering of the air flow rate is carried out at the latter pressure by means of sharp-edged orifices designed according to ASME Standards (Ref. 9). The metering system has two parallel lines of 2- and 4-in. diameter, respectively, each carrying an orifice section. At high flow rates, the 4-in. line is used. Lower flow rates are metered by the 2-in. line. The orifice holders are of a design permitting rapid exchange of orifice plates. The pressure drop over the orifices is measured by manometers located in the control room.

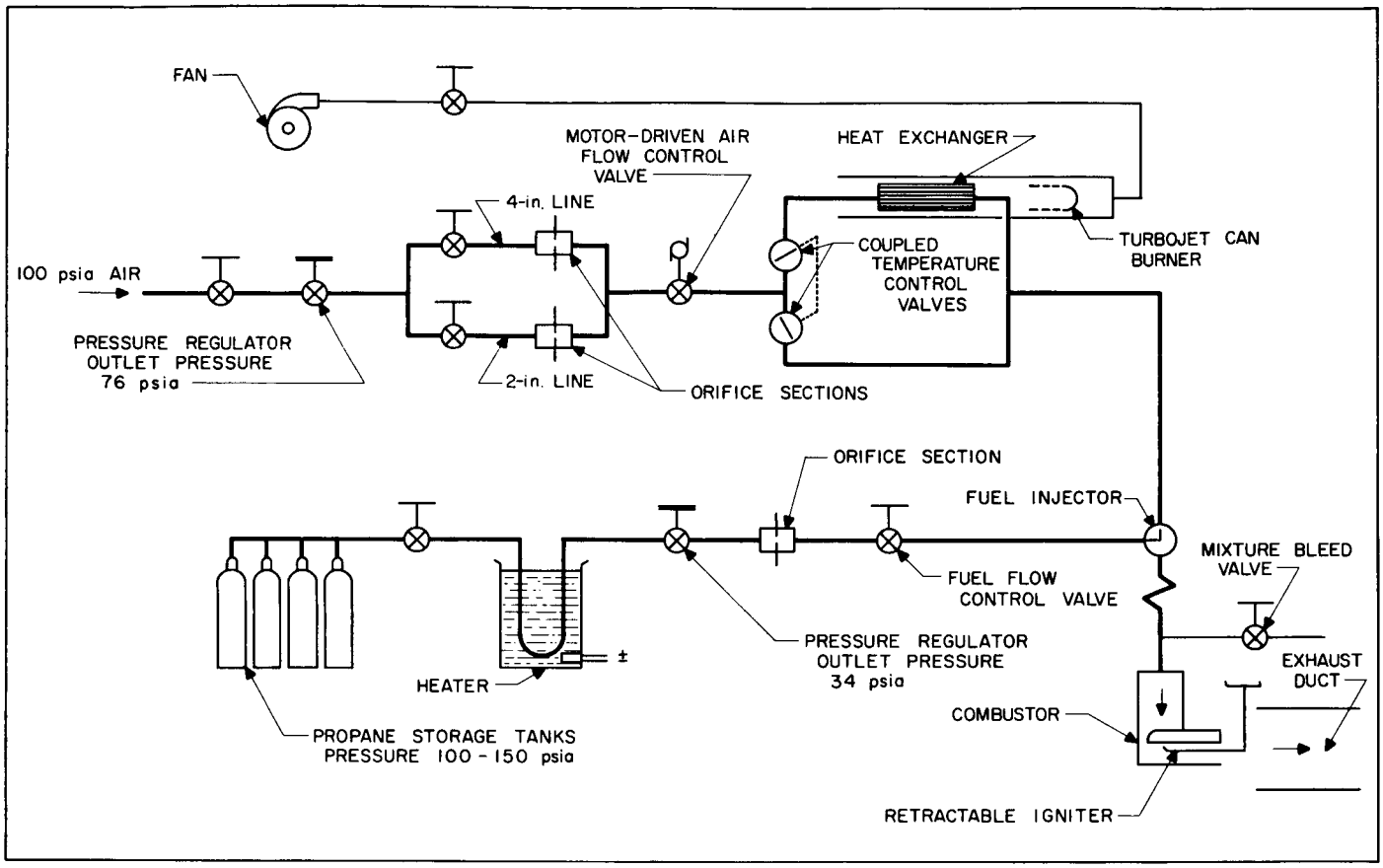

Fig. 6. Schematic Diagram of Fuel–Air Mixture Supply System

The flow coefficients of the orifices in the Reynolds region of interest have been determined by calibration with weighted flows of water. The calibrated values agree closely with the coefficients tabulated in the ASME Standards.

The air-flow control valve, located downstream from the metering sections, is driven by an electric motor operated from the control room. The valve always works with a sonic pressure drop; consequently, the mass flow for a certain valve setting remains constant, independent of changes in the pressure level at the inlet of the combustor.

When no preheating is required, the air passes directly from the control valve to the combustor. The fuel is injected at a certain distance upstream from the combustor, as described in the next section.

If preheating is desired, a smaller or larger part of the air can be passed through a counter-flow heat exchanger. The hot gas stream for this exchanger is generated by a turbojet can burner. Two coupled butterfly valves, controlled by a thermostat, balance the ratio between heated and bypassed air in such a way that the temperature of the resulting mixed air remains at a preset value.

The heat exchanger and air line downstream are insulated in order to reduce the heat losses. Maximum temperature available at the combustor inlet is about 500°F.

2. Fuel system. The fuel used during all experiments was propane gas supplied under the commercial name, "Rockgas." The exact fuel composition is 97.8% propane and 2.2% ethane.

The fuel system constructed for the experiments is shown in Figs. 6 and 8. The design and operation of this system are described as follows: Liquid propane is stored in four tanks. If subjected to a pressure drop by the opening of a shutoff valve in the fuel line, the propane will start to boil off in the storage tanks and the saturated propane gas will then be forced to flow through a heater. As the gas passes through the heater (which consists of a copper spiral submerged in electrically heated water) its temperature is raised by about 40°F. This temperature increase is sufficient to prevent condensation of the gas

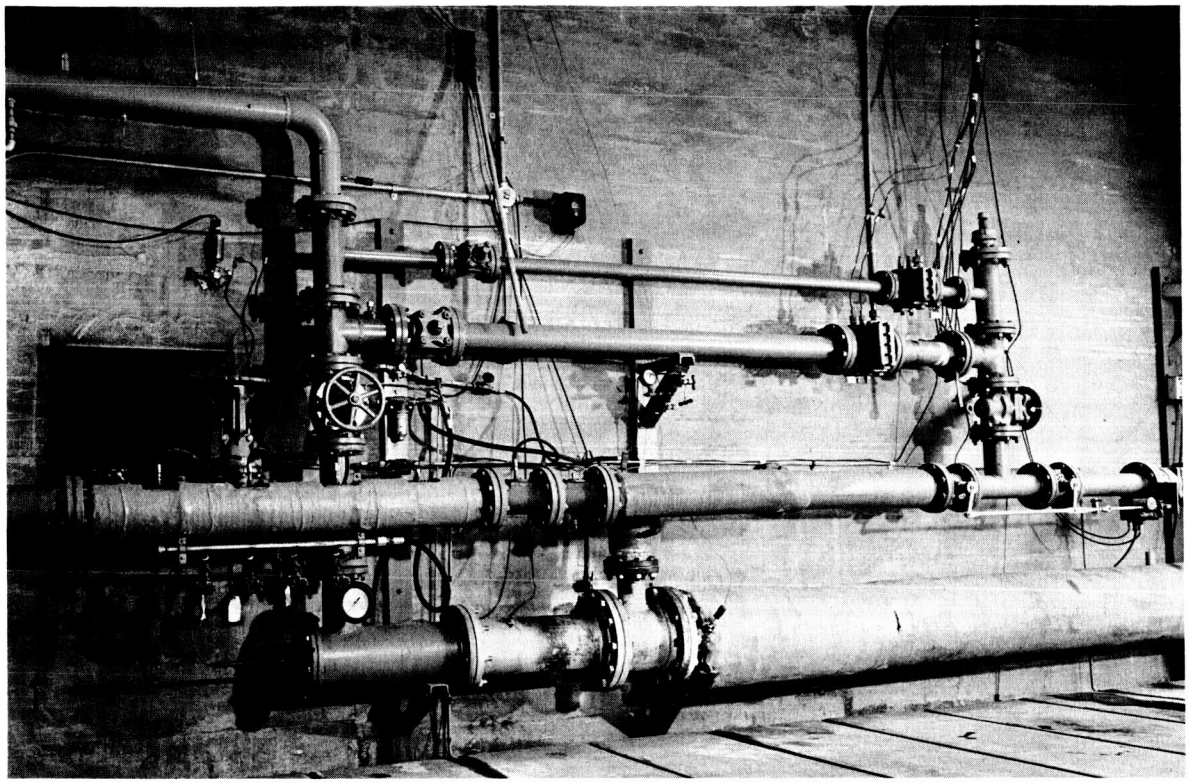

Fig. 7. Air Metering and Heating System

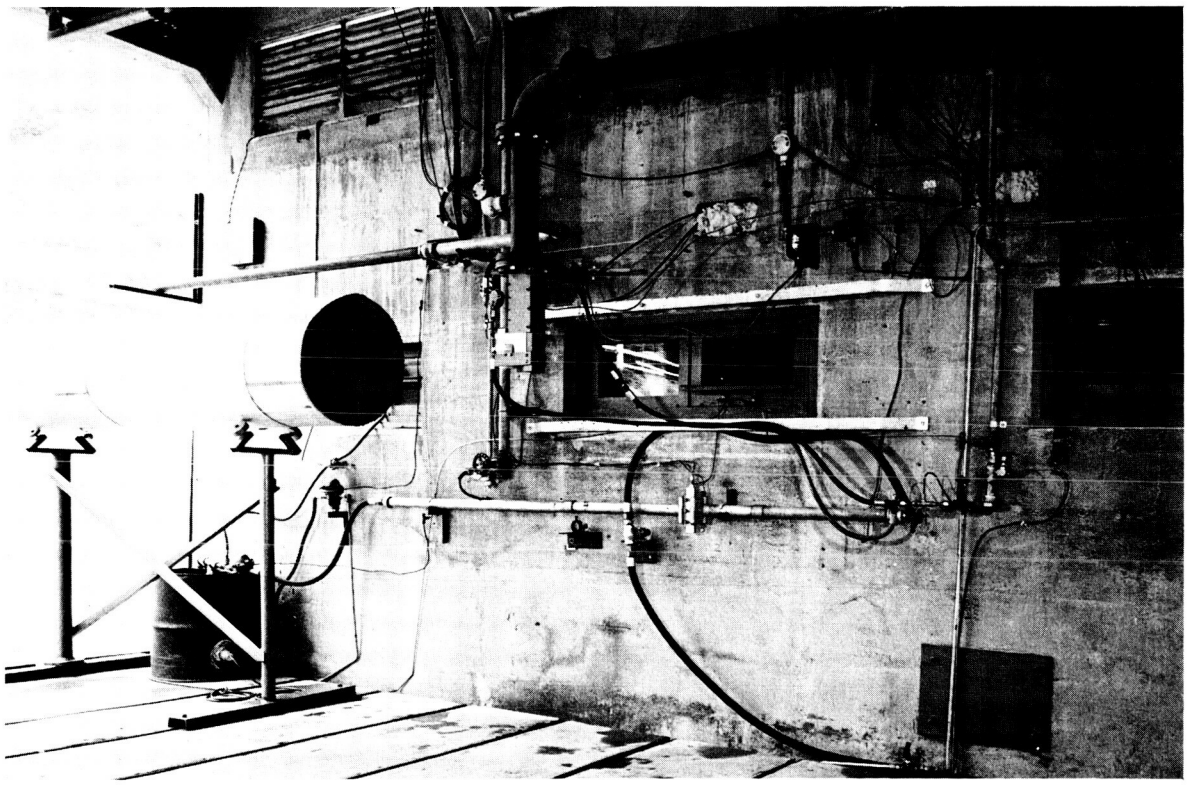

Fig. 8. Combustor Test Area and Fuel Metering System

when the storage temperature is higher than the ambient temperature in the test cell.

Immediately after the heating process, the propane pressure is reduced from the saturation value of 100–150 psia in the storage tanks to 34.0 psia, which was selected as a standard pressure level for the metering system. The pressure regulator can be adjusted from the control room to the exact standard value by means of a pneumatic system.

The metering section immediately downstream carries in a 1½-in. line a sharp-edged orifice made according to the same standards as the air orifices. The pressure drop over the orifices is measured by a 10-ft water manometer located in the test cell within a readable distance from the control room window. The fuel flow orifices have undergone the same water flow calibration used with the air flow orifices. The fuel flow control valve, placed downstream from the metering section, permits the metering to take place at a constant standard pressure level. The valve is manually operated from the control room.

Finally, the fuel is introduced into the air stream through an injector tube. The tube, located at the center of the 4-in. air pipe, has a number of small radial holes through which the fuel is distributed over the cross section of the air stream. The injection takes place at a distance of about 60 pipe diameters from the inlet to the combustor. In order to further secure a homogeneous fuel–air mixture, two perforated plate sections have been introduced in the main line, one at the fuel injector, the other close to the inlet to the combustor. The last plate also serves as a protection from flashback from the combustion chamber.

3. *Auxiliary equipment.* As shown in Fig. 6, the main line has a bleed connection a short distance upstream from the combustion inlet section. The bleed line carries a 2½-in. gate valve manually operated from the control room. The mixture bled off is exhausted to the atmosphere outside the test cell.

The bleed arrangement is very useful for determining the high-speed part of the stability limits. With slots of intermediate size, it is possible to increase the jet speed by a factor of 4 at a constant fuel–air ratio by going from open to closed position on the bleed valve.

To start the combustion chamber, an insulated wire is introduced through the exit of the combustion chamber. The tip of the wire is brought into the upstream part of the recirculation zone and placed at a distance of about ¼ in. from the top wall. The wire is connected to one terminal of an ignition transformer with an output of 10,000 v. The other terminal is grounded. The discharge between the wire tip and the grounded top block ignites the fresh mixture in the recirculation zone, and the combustion chamber starts.

The exhaust gases are conducted outside the test cell by a large duct downstream from the combustor exit. A powerful fan placed on the upstream side of the combustor assists in removing exhaust products not captured by the duct.

D. Instrumentation

The instrumentation used during the experiments includes equipment for measuring the recirculation zone temperature by the line reversal technique, thermocouple probes for temperature measurements in the mixing zone, and, finally, a schlieren system for studies of the flow configuration.

1. Line reversal equipment. The well-known arrangement of the optical system is shown by Fig. 9. The image of the lamp filament, reproduced in scale 1:1, is focused in a plane through the middle of the combustion chamber cross section. In order to facilitate displacement of the image to other locations in the same plane, the lamp and the first lens are mounted on a lathe compound in the test cell. The second lens and the spectroscope form another unit on a similar mount inside the control room. The optical axes of the two units are made colinear by moving the compounds in a plane perpendicular to the axes. By this arrangement the optical beam can easily be located at any desired point of the recirculation zone.

The voltage of the tungsten ribbon filament is adjusted by a voltage regulator located at the spectroscope in the control room and measured by an rms voltmeter. The spectroscope is a standard instrument with fairly low resolution.

The sodium D-lines are used in the reversal measurements since sodium vapor could be easily introduced into the flame by adding sodium chloride to the recirculation zone gas. Several methods for introducing the salt were tried. Injection in liquid form led to undesirable deposits on the glass windows. The best results were obtained with a flat metal probe inserted along the top wall of the combustion chamber. The tip of the probe is perforated and dipped into a mixture of sodium silicate and sodium

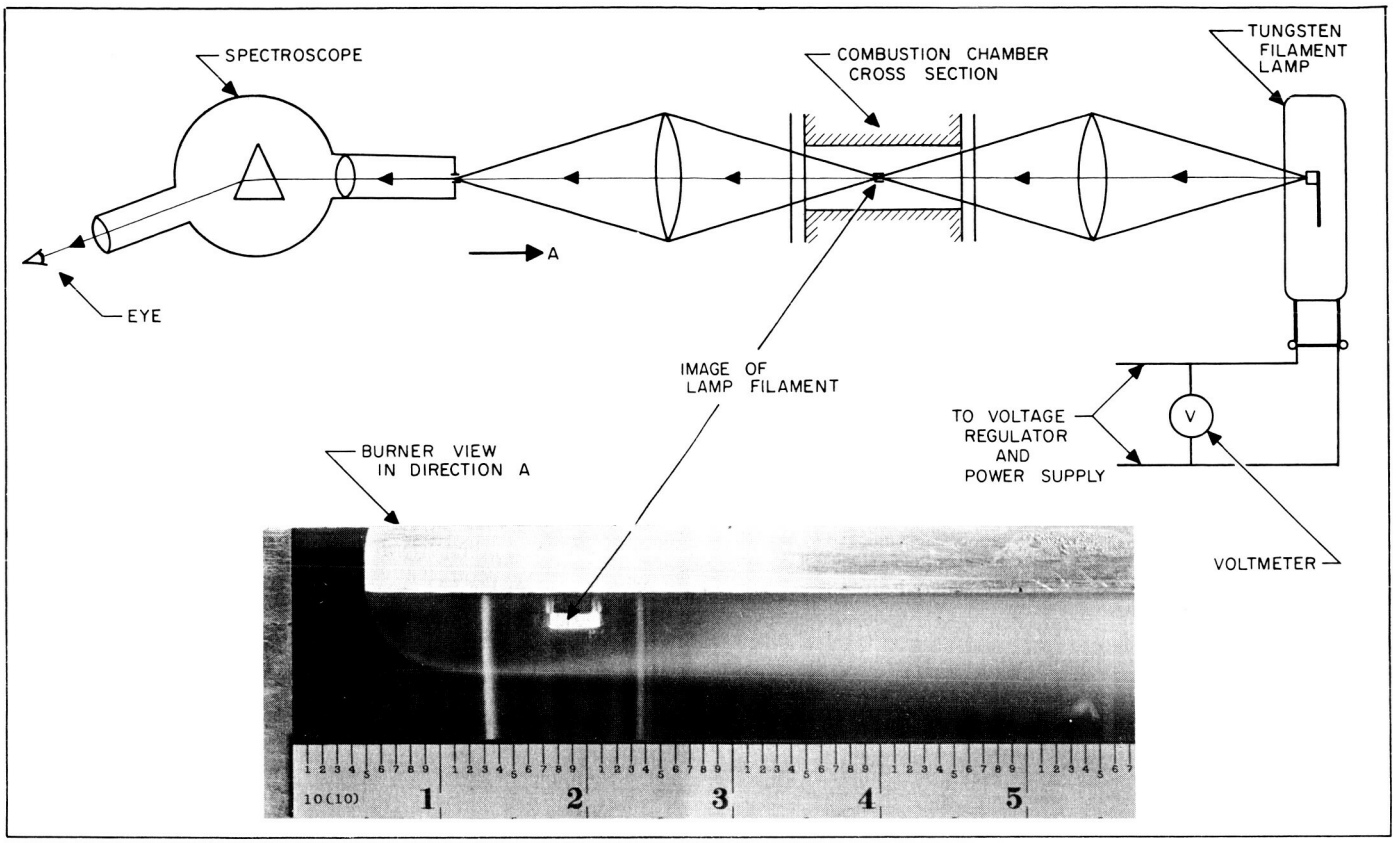

Fig. 9. Schematic Diagram of Apparatus for Line Reversal Temperature Measurements

chloride. The salt on the tip sublimes because of the heat transfer from the hot gas in contact with the probe. The gaseous salt products spread throughout the recirculation zone emitting D-line light with a brightness corresponding to the local gas temperature. The salt deposited in the cavities of the perforated probe tip lasts sufficiently long for a series of temperature measurements. Furthermore, the amount of salt introduced can be limited to a level such that deposits on the windows are minimized.

The tungsten filament of the light sources was calibrated by an optical pyrometer after each experiment. Calibrations of the image in the combustion chamber as well as the real filament were made. In the first case, losses occur in the first lens and the first glass window. These losses were not found to have any effect of practical importance. Even a slightly dimmed window did not affect the temperature reading by more than 0.5% in the temperature range considered.

2. Thermocouple probes. Chromel-alumel thermocouples were used for measuring low and intermediate temperatures in the mixing zone. The temperature in this zone varies from the cold flow temperature to a value close to the adiabatic flame temperature. Because of radiation heat losses, the thermocouples could also be used, although with less accuracy in the high temperature regions. Corrections of the readings were taken from Ref. 10.

The thermocouples were made from wires of 0.02-in. diameter inserted into a water-cooled tubular holder. The thermoelectric potential was measured on a Brown self-balancing potentiometer.

3. Schlieren system. The schlieren system set up for studies of the flow configuration is of the conventional double-mirror, single-pass type which uses two spherical, 6-in.-diameter mirrors with a 48-in. focal length. The light source consists of a BH-6 mercury lamp. Single exposures were taken with a spark having a duration of about 5 μsec.

4. Pressure instrumentation. All pressures below 2 atmospheres were measured by water and mercury manometers. Standard Bourdon-type pressure gauges were

used for higher values. These instruments were calibrated against precision gauges.

E. The General Procedure for Blowoff Experiment

The experimental procedure including the standard measurements taken during a blowoff experiment is described in the following material.

1. Blowoff technique. The stability limits of a combustion chamber are usually defined in terms of the blowoff speed of the fresh mixture for various fuel–air ratios. The general character of the stability limits is shown in Fig. 10. Here, the fractional blowoff speed is presented as a function of the equivalence ratio ϕ, which is defined as the ratio between the actual and stoichiometric fuel–air ratios. Maximum blowoff speed occurs at about the stoichiometric fuel–air ratio.

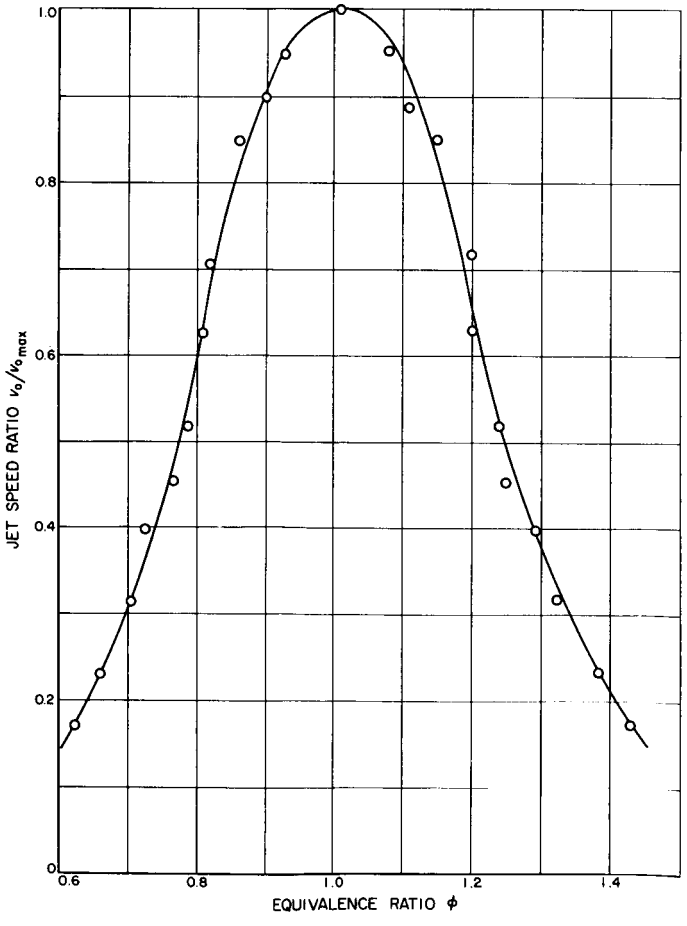

Fig. 10. Blowoff Limits for Combustion Chamber (½ × 1 × 6) B; Maximum Blowoff Speed $v_{0\,max}$ = 650 ft/sec

The region inside the blowoff curve is the field of stable operation of the combustion chamber. To determine the blowoff curve, the burner is started inside the stable region and brought out to the lean or rich blowoff limit by changing the fuel–air ratio or the speed of the flow.

The first technique was used at low and intermediate speeds by controlling the fuel flow rate at constant air flow rate. In the high-speed region of the stability curve, the second technique was applied by using the mixture bleed valve mentioned previously. By this procedure, the stability limits are approached at approximately right angles for all blowoff experiments.

2. Standard measurements. In a blowoff experiment, all quantities required to determine the fluid mechanics, as well as the chemical parameters of the system, have to be measured.

Flow parameters: The characteristic dimensions of the flow configuration are determined by direct measurements. As will be shown, most of the mixing zone has a clear optical definition in a two-dimensional model. Consequently, the geometry of this zone can be studied by taking direct flame photographs as well as schlieren pictures in a direction perpendicular to the two-dimensional plane.

The dimensions of the recirculation zone are less obvious, although the height of the zone can be estimated from the location of the mixing zone. Another technique must be applied in order to determine the length of this region, since the end of the zone is usually obscured by flames. A probing technique, successfully applied to bluff body experiments by Zukoski and Marble, provided the answer. A probe with a 1/16-in. tungsten wire tip is prepared with the same salt mixture as used during the sodium D-line reversal measurements. The probe is introduced through the burner exit and can be moved along the top wall of the chamber. The sodium light emitted by the gaseous salt products indicates the direction of the flow around the tip of the probe. At the downstream end of the duct, the sodium light only appears in a region downstream from the probe tip. However, as the probe is introduced further upstream, the tip eventually will touch the boundary of the recirculation zone. At this moment, the sodium light suddenly flickers through the entire recirculation zone. After moving the probe slightly further upstream, a steady sodium light is emitted through-

out the recirculation zone. The lengths corresponding to the first light and the steady light contact are measured in order to reduce errors due to the fluctuations of the flow at the downstream end of the recirculation zone.

The speeds in the isentropic regions of the flow field are based on the total pressure in the inlet duct of the combustor and the local static pressures. The static pressure in the upstream part of the recirculation zone was chosen as reference pressure for the jet speed; it is measured by a tap hole located in the top wall about ½ in. from the edge of the slot. The static pressure gradients within the relatively stagnant recirculation zone are negligible compared with the corresponding gradients in the jet. Consequently, the reference velocity based on the inlet total pressure and the reference static pressure defines the initial speed of the jet. As will be shown, this reference velocity is representative of the speed in the cold flow along the complete boundary of the mixing zone.

In order to get more complete information about the flow field, traverses of total pressure, static pressure, and temperature through the nonisentropic regions were made for certain test series. Since these measurements are not to be considered standard procedure, they will be discussed in connection with the experiments in question.

Chemical parameters: The state of the fresh mixture entering the combustion chamber is determined by its temperature, pressure, and fuel–air ratio. The temperature is measured by a standard temperature gauge located in the inlet duct of the combustor.

The fuel–air ratio is determined by separate measurements of the fuel and air flow rates as described previously. By choosing orifices of suitable size, mass flow corrections due to Reynolds number and compressibility effects could be limited to a reasonable size. It is estimated that the maximum error in the measured fuel–air ratio is $\pm 2\%$.

III. GENERAL CHARACTERISTICS OF THE FLOW FIELD IN TWO-DIMENSIONAL SLOT-TYPE COMBUSTION CHAMBERS

The present investigation will cover a number of two-dimensional combustion chambers of varying sizes and geometrical configurations. Before the effects resulting from a variation of the geometrical parameters are studied, the general features of the flow field in a burner of intermediate size and geometric configuration are discussed.

The combustion chamber considered belongs to combustor type B (Fig. 5). Its geometry is ½ × 1 × 6, i.e., slot width ½ in., height 1 in., and over-all length 6 in. The top wall consists of a water-cooled aluminum block. Consequently, the case discussed also demonstrates the effects of heat transfer.

A. Flow Configuration

Figure 11a shows a photograph of a flame stabilized in the combustion chamber at stoichiometric mixture ratio and a jet speed of approximately half of the maximum blowoff speed. The different zones of the flow are easily distinguishable in the two-dimensional pattern. The mixing zone between the fresh mixture in the entering jet and the hot gases in the recirculation zone appears as a band of high light intensity which gradually becomes wider. After the deflection of the flow by the bottom wall, the mixing zone broadens considerably until it nearly fills the cross section of the combustion chamber at the end of the recirculation zone. The boundary of the recirculation zone, determined by the probing technique described previously, is marked by a dotted line in Fig. 11a.

A schlieren photograph of the same flow field (Fig. 11b) confirms the impressions obtained from the flame photograph. The schlieren picture has been taken with a horizontal edge, since the density gradients of major interest are vertical. The mixing layer is indicated by a dark line that is in sharp contrast to the surrounding transparent fields, which correspond to the cold mixture flow and the hot recirculation zone. As the mixture moves toward the exit, the dark line is split up into more diffuse regions, which indicates less pronounced temperature gradients and a larger scale of the turbulent mixing. At the end of the recirculation zone, the lower surface of the mixing zone appears at a short distance above the bottom plate.

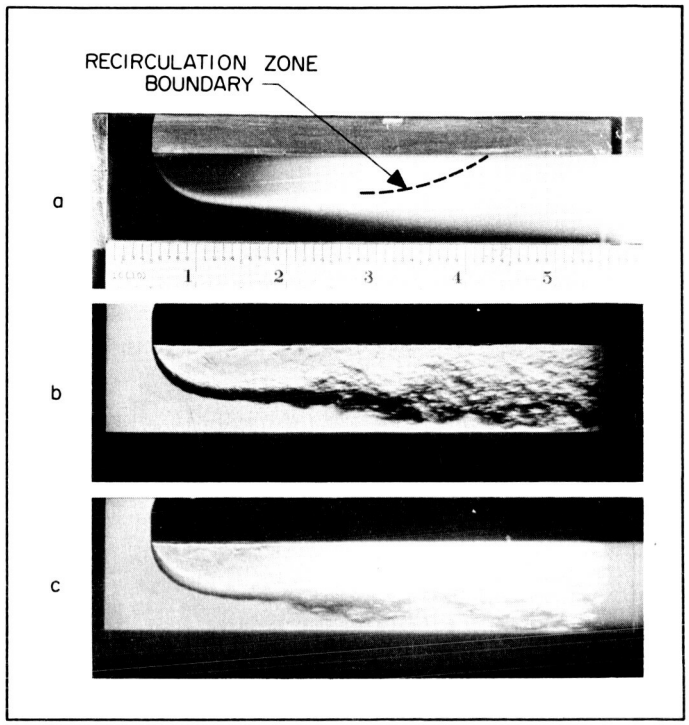

Fig. 11. Photographs of Combustion Chamber (½ × 1 × 6) B Operating at Stoichiometric Mixture Ratio and Jet Speed Ratio $v_0/v_{0\,max} = 0.5$; (a) Direct Flame Picture, (b) Schlieren Picture, (c) Schlieren Picture with Flame Superimposed

The schlieren photograph also reveals that most of the recirculation zone is a region of relatively small temperature gradients. This is interesting, since the flame picture shows some flames in the downstream end of the zone. These flames are evidently very weak as compared with the flames in the mixing zone.

Figure 11c shows the flame superimposed on the schlieren picture. The superposition reveals that the thermal mixing zone extends slightly outside the visible flame front in the deflection region of the jet.

The basic features of the flow field remain unchanged within the stable region of burner operation. However, the appearance of the mixing layer and the recirculation zone is influenced slightly by the jet speed as well as the fuel–air ratio of the fresh mixture.

In addition, the actual dimensions of the recirculation zone are also fairly independent of speed and fuel–air ratio. The length has a minimum value at stoichiometric operation, and a minor increase in length occurs when the jet speed is increased.

B. Velocity Distribution

The velocities in the flow field of the combustion chamber (½ × 1 × 6) B are discussed in the following material. The significance of the reference velocity chosen for the system is also discussed.

It will be recalled that the reference velocity v_0 is based on the total pressure p_{t_0} in the inlet duct and the reference static pressure p_{ref} measured at the wall in the upstream part of the recirculation zone.

The flow speeds in the mixing layer between the fresh mixture and the hot gases in the recirculation zone are determined by the speed in the isentropic flow of fresh mixture along the boundary of the mixing layer. The speed at this boundary was based on measurements of the static pressure distributions made at the side wall of the burner. The flow picture obtained from these measurements is now discussed, starting from the slot.

The static pressure measurements made across the slot indicate that the streamlines have a certain curvature at the very entrance of the jet into the burner. The previously presented photographs of the flame show a slight initial deflection of the entering jet. This evidence and extensive static pressure measurements show that the presence of the deflecting bottom wall is felt through the subsonic flow field up to the slot section.

Figure 12 shows the velocity distributions in the isentropic flow of fresh mixture at several different sections of the flow. Traverse A is taken in the deflection region. An outer wake is formed in the flow at the corner of the back and bottom walls. Even though the speed along the outer wake is only 60% of the reference speed, it will be noticed that the speed along the inner wake is within a few per cent of the reference speed. Traverses B and C, taken further downstream, show fairly flat velocity profiles with speeds about the same as the reference speed.

The conclusion is, then, that the speed all along the boundary of the mixing zone is close to the reference speed. This is a consequence of the fact that the recirculation zone is a stagnant region of almost uniform pressure.

C. Temperature of the Recirculation Zone

The larger part of the recirculation zone is filled with completely burnt material except in the downstream region where some weak flames appear. If the zone were not subjected to any heat transfer to the surroundings, the gas temperature would presumably be the same as the adiabatic flame temperature. However, in the present case, the top wall acts as a strong heat sink. Since the gas inside the recirculation zone describes a vortex motion, the hot gas in the downstream part (indicated as B in the following sketch) of the zone travels in an upstream direction along the cool top wall. The heat losses to the wall will result in a drop to a minimum temperature at the end A of the cooling path.

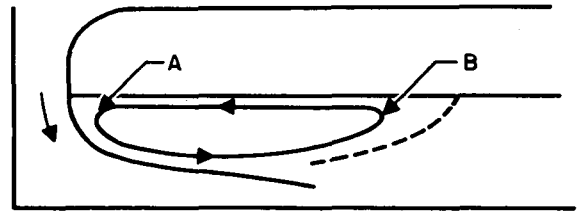

After turning down in the direction of the jet, part of the gas diffuses into the mixing layer at the same time as newly burnt material enters the recirculation zone. Following the path A→ B indicated in the sketch, the gas temperature should increase to a maximum value in region B.

The line reversal temperature measurements substantiate the picture presented above. Figure 13 illustrates the temperature distribution in the present combustion chamber at stoichiometric mixture ratio and maximum blowoff speed. Starting from a level of about 85% of the adiabatic flame temperature, there is a temperature drop of about 10% along the cooling path B→ A. Figure 13 also shows that the gas rapidly recovers its original temperature along the return path A→ B. At about half of the recirculation zone length the temperature has reached 84%, only 1% less than at the end of the path A→ B.

Actually, the temperature was not measured quite at the end of the recirculation zone in the present case. As shown by Fig. 13 the point farthest downstream is located at about ⅔ of the zone length. Judging from other measurements, the temperature in the very end of the region is a few per cent higher than that at the point discussed.

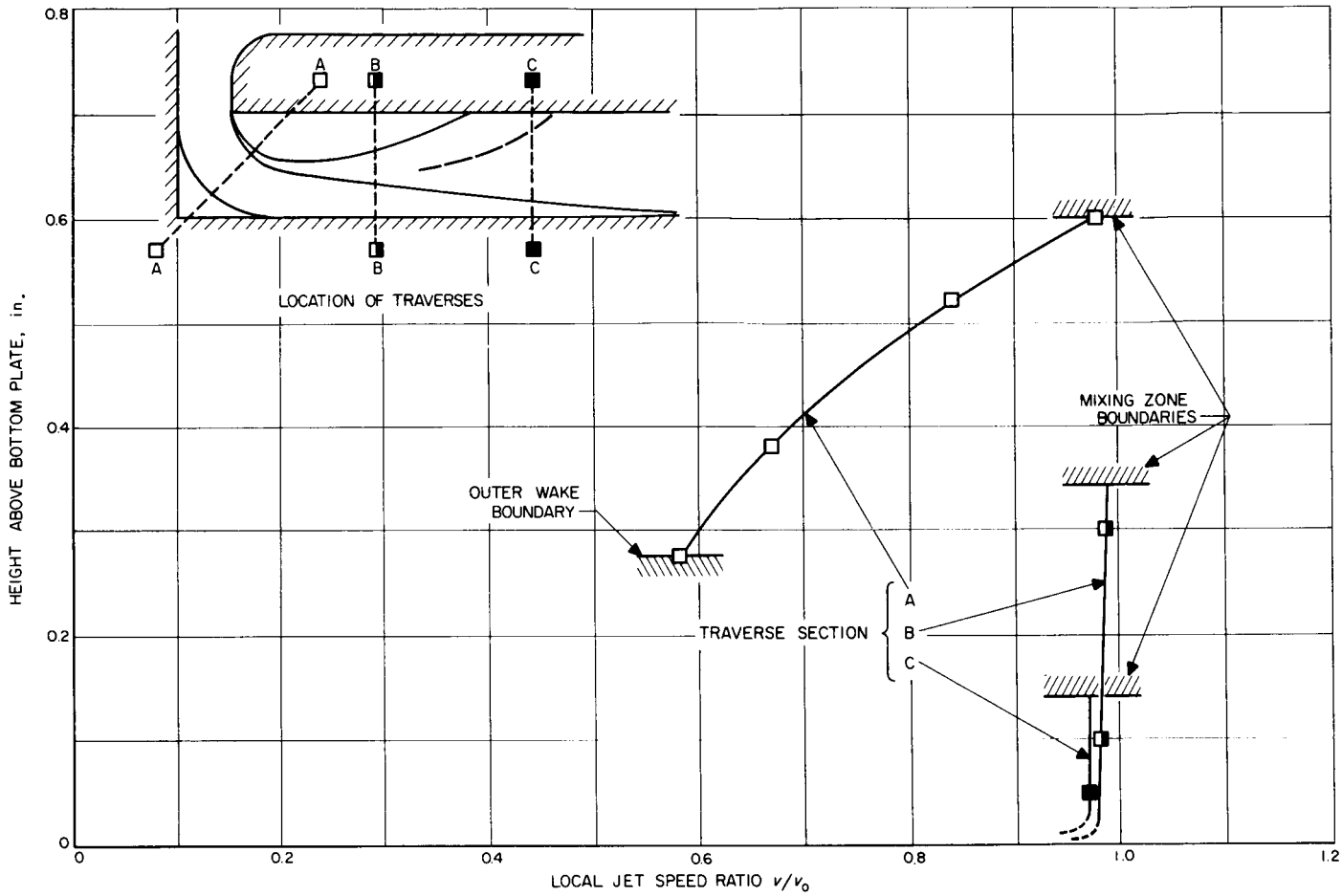

Fig. 12. Velocity Distributions in Fresh Mixture Flow Field of Combustion Chamber (½ × 1 × 6) B at Jet Speed Ratio $v_0/v_{0\,max} = 0.5$

Another consequence of the heat transfer situation is that the gas temperature at a certain location and fuel–air ratio will depend somewhat on the jet speed, since the speeds within the recirculation zone are determined by the speed along the boundary of the zone. As will be demonstrated, the temperature at the upstream end of the recirculation zone rises slightly with an increased jet speed, because the residence time along the cooling path B → A is reduced. At the downstream end of the zone, on the other hand, it was found that the temperature is practically independent of the jet speed.

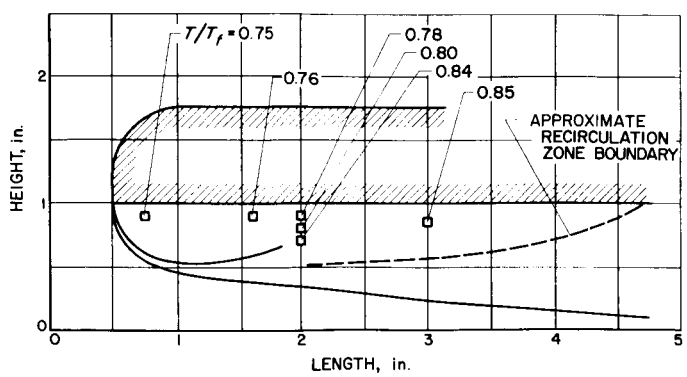

Fig. 13. Temperature Distribution in Recirculation Zone of Combustion Chamber (½ × 1 × 6) B at Maximum Blowoff Speed $v_{0\,max} = 650$ ft/sec

D. Blowoff Characteristics

The blowoff limits of combustion chamber (½ × 1 × 6) B are shown in Fig. 10. A maximum speed of 650 ft/sec is reached slightly on the rich side of the stoichiometric mixture ratio.

The behavior of the flame when the stability limit is approached and reached is of particular interest with respect to the stabilization mechanism. It was generally observed that the lower surface of the visible flame at

the end of the recirculation zone lifts to a higher position above the bottom wall when the blowoff limit is approached.

At the very moment of blowoff, two different types of behavior were observed. In most burners the flame suddenly disappeared throughout the flow field. Under certain circumstances, however, some of the thermally insulated burners showed a residual flame in the recirculation zone after blowoff of the flame propagating downstream from the zone.

Several investigators have made the same observation for other types of combustors. The presence of a residual flame with the bluff body flameholder was described by Zukoski (Ref. 11). Wright and Becker (Ref. 12) also found a residual flame in the mixing zone between two parallel streams.

The two types of blowoff behavior observed in the present combustion chambers are discussed separately in the following paragraphs.

1. Blowoff with steady residual flame. The burner families tested in combustor type A exhibited steady residual flames at intermediate and high speeds. Figure 14 shows direct flame and schlieren photographs of a steady residual flame at the rich limit of combustion chamber (½ × 1 × 5) A operating at 60% of maximum speed. The residual flame fills about half of the original length of the recirculation zone, and the boundary of the wake appears to be the same as before blowoff. Temperature measurements indicate that the temperature levels in the recirculation zone of the residual flame are the same as those observed at the same location before blowoff.

The schlieren photographs in Fig. 14 support the picture presented above. The normal flame exhibits a wide region of strong temperature gradients caused by the mixing and reaction in the mixing zone. The residual flame shows only minor gradients due to mixing, without reaction in the same zone. The dark region along the top wall is due to temperature gradients in the glass walls which, in turn, are due to the longer running time required for reaching the residual flame state.

2. Blowoff with transient residual flame. As mentioned, most burners—and in particular all water-cooled burners of combustor type B—had a blowoff of the complete flame without any observable residual flame.

In order to investigate the different phases of the blowoff process, some high-speed motion pictures were taken. Figure 15 shows a sequence of the blowoff of the flame at the rich limit in a combustion chamber with water-cooled top wall. For comparison, the picture also includes

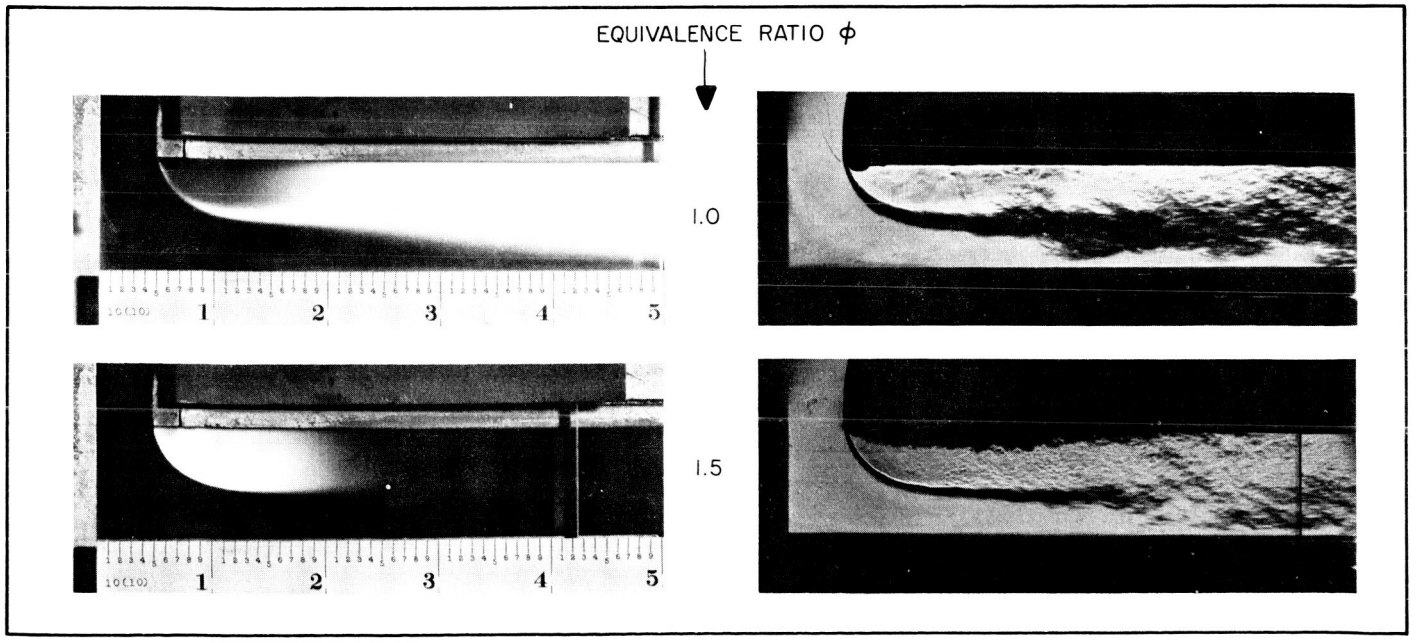

Fig. 14. Propagating and Residual Flames in Combustion Chamber (½ × 1 × 5) A Operating at Jet Speed Ratio $v_0/v_{0\,max} = 0.6$

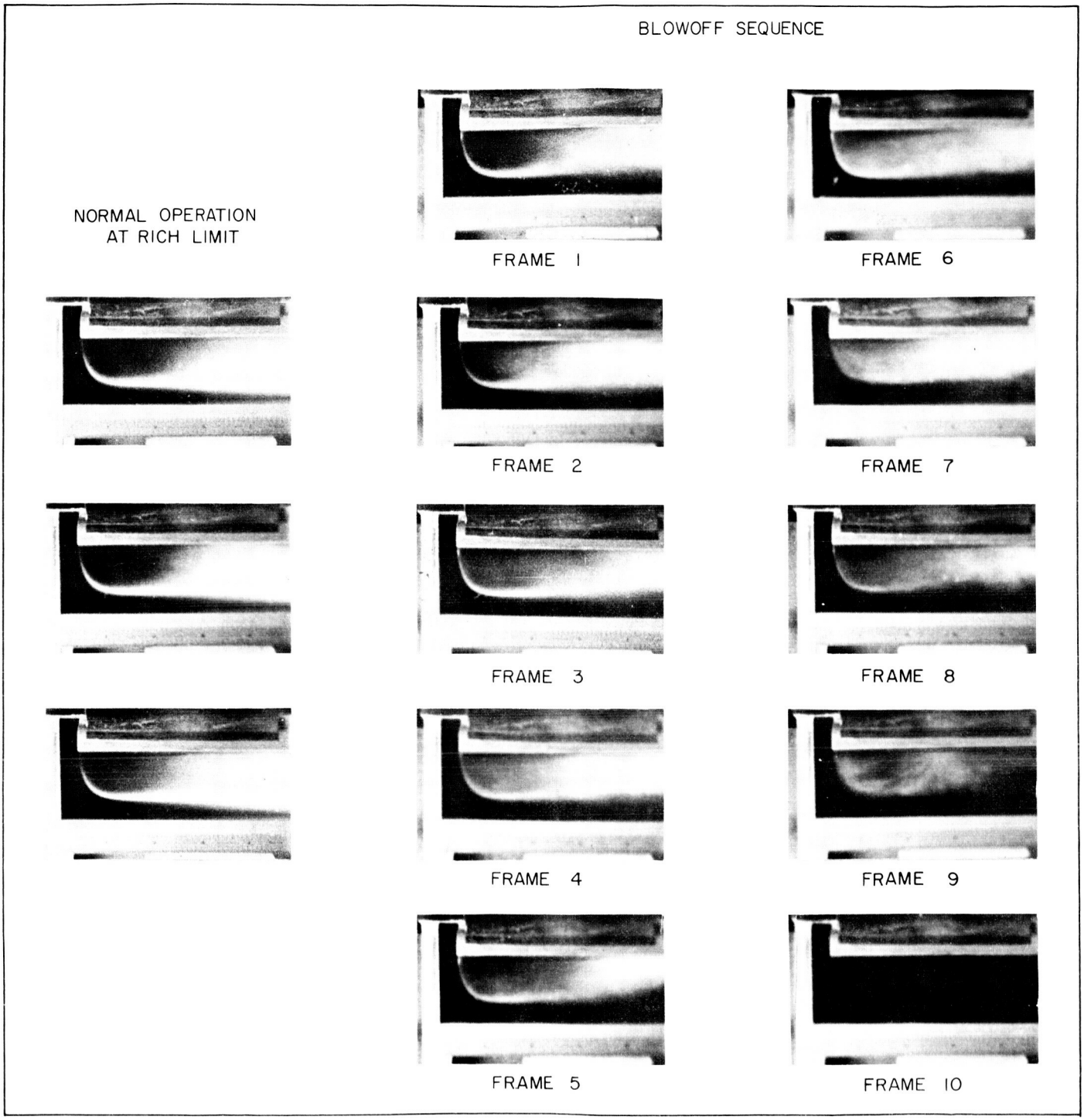

Fig. 15. High-Speed Motion Picture Frames Showing Blowoff of the Flame at the Rich Limit in Combustion Chamber (⅜ × 1 ½ × 7 ½) B Operating at Jet Speed Ratio $v_0/v_{0\,max} = 0.5$ and Equivalence Ratio $\phi = 1.25$; Camera Speed, 600 fps

a few frames of the flame as it appears at normal operation close to the rich limit. The camera speed is 600 frames per sec.

It will be noticed that the downstream part of the normal flame appears quite close to the bottom wall. However, the first frames of the blowoff sequence show a lifted flame surface in accordance with the visual observation during the approach to blowoff.

The motion pictures also reveal an unsteady character of the flame immediately before blowoff. Actually, the propagating flame appears to be almost blown off in frame 5. Frames 6 and 7, however, show a temporary recovery of the flame in the mixing zone. This cycling of the flame position brings to mind the behavior observed in the transition to a residual flame, which was discussed previously.

The final blowoff is illustrated by frames 8 and 9. It is very interesting to notice that frame 9 shows the presence of a residual flame. Consequently, it can be concluded that the blowoff process shown in these frames is in fact the same as for the insulated burners exhibiting steady residual flames.

IV. CORRELATION OF STABILITY LIMITS FOR GEOMETRICALLY SIMILAR COMBUSTION CHAMBERS OF VARYING SIZES

The flame stabilization process is governed by a number of fluid mechanical and chemical parameters. In order to determine the scaling laws and to elucidate the mechanism for stabilization, it is desirable to carry out experiments in which only one of these parameters is changed at a time. By this process, it will be possible to separate the influence of the various parameters and to determine clearly which parameters have a strong effect.

It was decided to study the influence of the flow parameters first. Of these variables, the two which appear to be most important in fixing the flow field are the burner size and geometry. It is reasonable to assume that these may be characterized by the duct height and the slot ratio, respectively.

In this section, the influence of burner size is determined for three different values of the slot ratio. Thus, the effect of changing both of these fluid dynamic parameters is illustrated. Experimental evidence will be presented to show that the other parameters remain constant during the various changes of scale and geometry.

A. Equipment and Experiments

Combustor type A provides a convenient tool for carrying out scaling experiments of the nature indicated above, since the combustion chambers in this model can be linearly scaled by a factor of 4 in the burner height range ½–2 in. Furthermore, the recirculation zone is insulated by a glass liner which reduces heat transfer. This is a desirable feature since the relative heat transfer from the recirculation zone is likely to change with the burner size; by reducing the heat losses as much as possible, the temperature maintained in the zone will be less dependent on variations in burner size.

In order to make the scaling experiment cover a wide range of geometry as well as scale, it was decided to study three different families of combustion chambers. The size and geometry of these burners are illustrated in Fig. 16 in a diagram of height vs slot width. The first family of geometry $(\frac{1}{2}h \times h \times 5h)$ A has the same slot ratio as the burner previously described. Judging from the earlier results, a slot ratio of ½ creates a flow field in which the complete length of the recirculation zone is covered by a cold flow of fresh mixture.

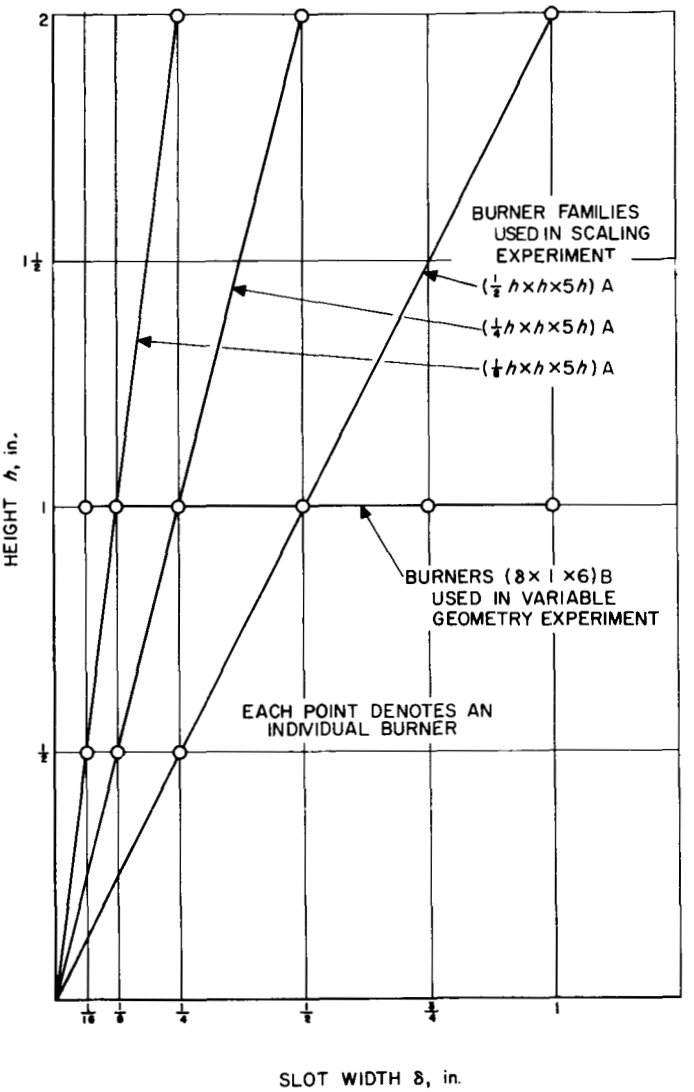

Fig. 16. Height and Slot Width of Combustion Chambers Used During Scaling and Variable Geometry Experiments

For the second family, which has the geometry $(\frac{1}{4}h \times h \times 5h)$ A, less, if any, of the fresh mixture is left outside the mixing zone at the end of the recirculation zone.

The third slot ratio to be studied is ⅛ in burner family $(\frac{1}{8}h \times h \times 5h)$ A. In this case, all of the fresh mixture enters the mixing zone far upstream from the end of the recirculation zone.

As indicated by Fig. 16, the standard heights chosen for each of the burner families are $h = \frac{1}{2}$, 1, and 2 in.

Each combustion chamber was tested in accordance with the previously described general procedure. However, the recirculation zone temperatures were measured only in the combustion chambers of the family $(\frac{1}{2}h \times h \times 5h)$ A. The objective of the temperature measurements was to make sure that there are no pronounced temperature differences between burners of different size due to heat transfer effects. If this is true for one family of burners, it can be concluded that the temperature similarity is satisfactory also in the other two families.

B. Results and Discussion

The experiments yield, primarily, information about the flow configuration, the temperature of the recirculation zone, and, finally, the stability limits of the burners. The data concerning these different parameters are presented and discussed in the following paragraphs.

1. Flow configuration. The geometrical configuration of the flow fields for the burners with the family $(\frac{1}{2}h \times h \times 5h)$ A is illustrated by Fig. 17. There, the flame as well as the schlieren pictures is shown for a jet speed of about half of the maximum blowoff speed. In order to facilitate a direct comparison between burners of different scale, the pictures have been enlarged so that the burner height appears to be the same size in all pictures.

The flame pictures show a high degree of geometrical similarity of the mixing zone boundary. The schlieren pictures also demonstrate that the rest of the flow field exhibits similar geometry. The other two burner families also show geometrical similarity of the flow field for different burners within the same family.

A comparison made between the flow field in different families confirmed that the slot width has a strong influence on the location of the mixing zone boundary. Figure 18 shows schematically how the mixing zone in the burners of family $(\frac{1}{2}h \times h \times 5h)$ A does not reach the lower wall before the end of the recirculation zone. Figure 18 also indicates that in family $(\frac{1}{4}h \times h \times 5h)$ A the mixing zone reaches the bottom wall at a point a short distance upstream from the end of the recirculation zone. Finally, family $(\frac{1}{8}h \times h \times 5h)$ A has a mixing zone that reached the bottom boundary a short distance downstream from the deflection of the jet.

From the observations made above, it can be concluded that even though the flow has geometrical similarity for different burners within the same family, this similarity in the flow does not apply to the different families.

2. Recirculation zone geometry. The recirculation zone length l^* at the lean blowoff limit is shown as a function of the jet speed in Fig. 19. The length is expressed in terms of the ratio l^*/h, and the speed is given as a fraction of maximum blowoff speed.

As indicated previously, the recirculation zone length is measured for two locations of the sodium probe tip: the first, corresponding to the appearance of intermittent light in the zone, is shown as an open point in Fig. 19; the second, corresponding to a steady light appearing in the zone, is shown as a solid point. The lengths in Fig. 19 show a fairly wide scatter, somewhat amplified by the illustration of the two lengths measured. The recirculation zone length is by definition the arithmetic average of these two values. Considering the average length, Fig. 19 indicates a maximum variation of $\pm 20\%$ about $l^*/h = 4.0$ for burner family $(\frac{1}{2}h \times h \times 5h)$ A, $\pm 15\%$ about $l^*/h = 4.2$ for the next family, $(\frac{1}{4}h \times h \times 5h)$ A, and, finally, $\pm 10\%$ about $l^*/h = 5.0$ for the last family, $(\frac{1}{8}h \times h \times 5h)$ A.

The scatter in the data presented above has several origins. First, the geometry of the approach channel to the slot throat has not been scaled. This lack of perfect scaling causes a smaller burner, within a certain family, to have a larger length-to-width ratio of the parallel part of the slot channel, and hence causes the initial state of the jet to vary with scale. Second, compressibility effects may also change the flow field between geometrically similar burners of different size, since, for the same fuel–air ratio, larger burners are operated at considerably higher Mach numbers than are the smaller ones.

The results indicate that the relative recirculation zone length increases when the slot ratio is reduced. This effect is a direct result of the changes in the flow field which are associated with a reduction of the maximum height of the zone as the slot ratio is increased. Again, it is evident that the geometry of the recirculation zone is affected by variations in the slot ratio parameter.

3. Recirculation zone temperature. The recirculation zone temperature for burner family $(\frac{1}{2}h \times h \times 5h)$ A is presented in Fig. 20, which shows (at three different

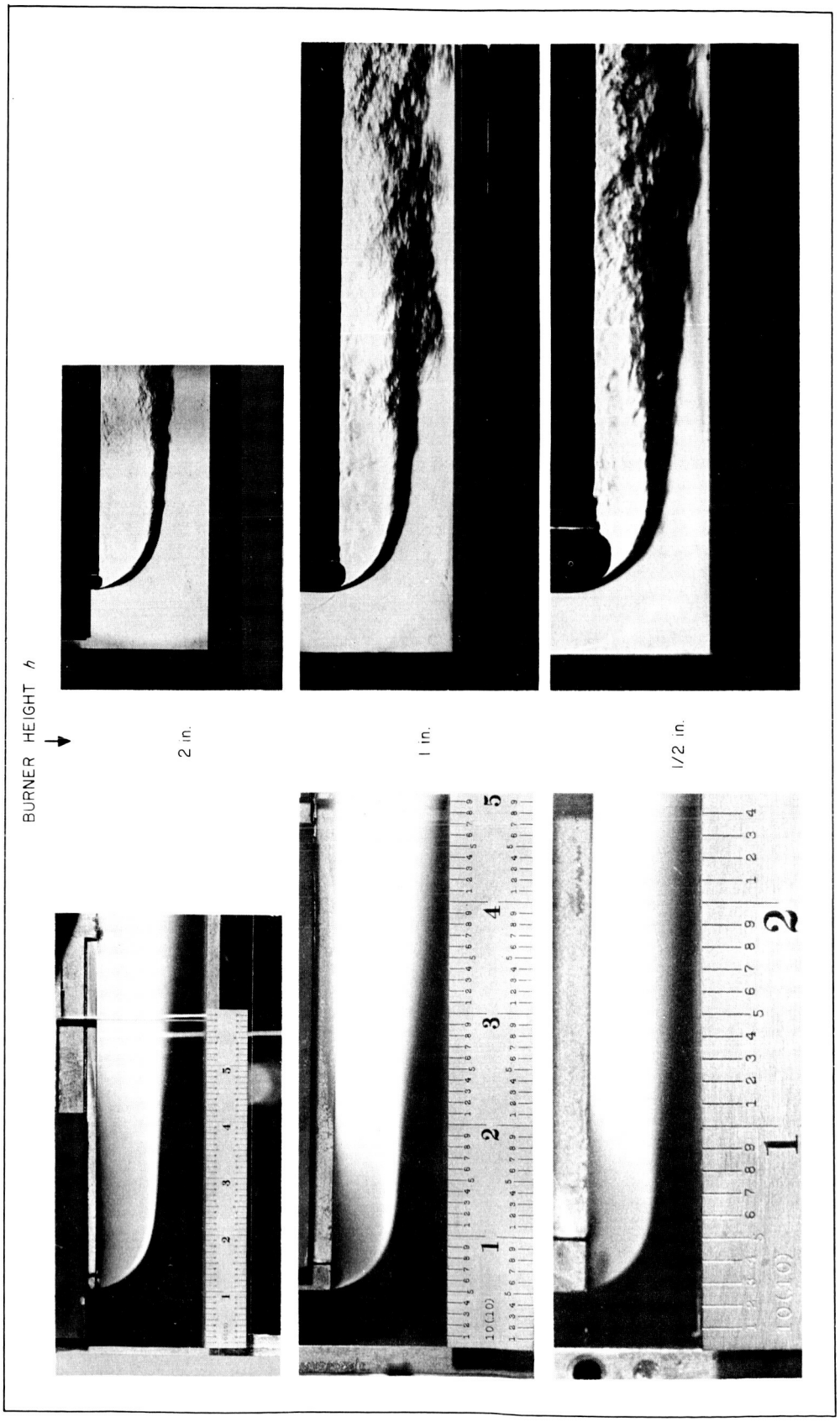

Fig. 17. Direct Flame and Schlieren Photographs of Burner Family ($\frac{1}{2}h \times h \times 5h$) A Operating at Stoichiometric Mixture Ratio and Jet Speed Ratio $v_0/v_{0\,max} = 0.5$

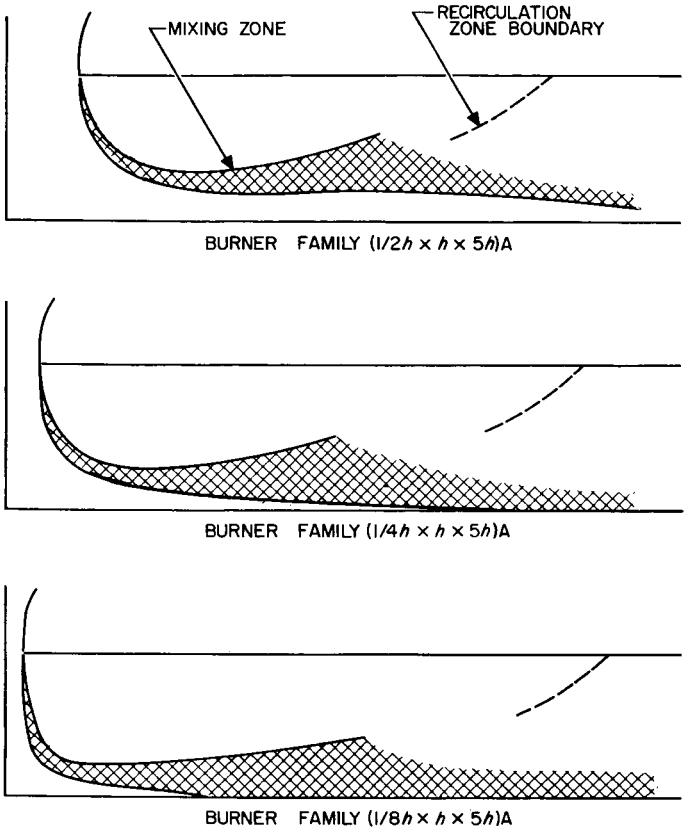

Fig. 18. Schematic Diagram of Flow Field for Three Different Burner Families in Combustor Type A

locations) the temperatures, divided by the adiabatic flame temperature, plotted as functions of jet speed divided by maximum blowoff speed.

Figure 20 shows that the temperature at location 1 in the upstream part of the recirculation zone is fairly strongly influenced by the jet speed. For example, when the velocity ratio is changed from 0.1 to 1.0, the temperature increases by about 20%. On the other hand, the temperature for any given speed ratio seems to depend only slightly on the burner size. Although at low speed ratios the temperature apparently increases slightly with burner size, the temperature ratios are, in the range of high speed ratios, almost identical.

At location 2 in the middle of the zone, the speed dependence is less pronounced; the temperature change here is only about 10% for the same speed ratio interval. The influence of burner size, however, is somewhat stronger. At low speed, the smallest burner has a temperature about 4% lower than the two larger burners. This difference is reduced to about 2% at blowoff.

Finally, at the downstream end of the recirculation zone, the temperature at location 3 shows a very small variation with the speed, and the influence of the burner size is also small. The smallest burner is again lower by about 2% at most speeds. However, at blowoff, the temperatures of the smallest and intermediate sizes agree closely.

The over-all temperature distribution is similar to that of burner (½ × 1 × 6) B discussed in the previous chapter. The temperatures in the present case are somewhat higher because of the reduction of heat transfer by the glass liner along the top wall. At the end region of the recirculation zone, however, the difference is surprisingly small. Figure 13 indicates that the aluminum-top burner has a temperature only a few per cent lower than the glass-top burner.

All temperature data discussed thus far have been obtained at stoichiometric operation of the combustor. The temperature in the recirculation zone is lower at the

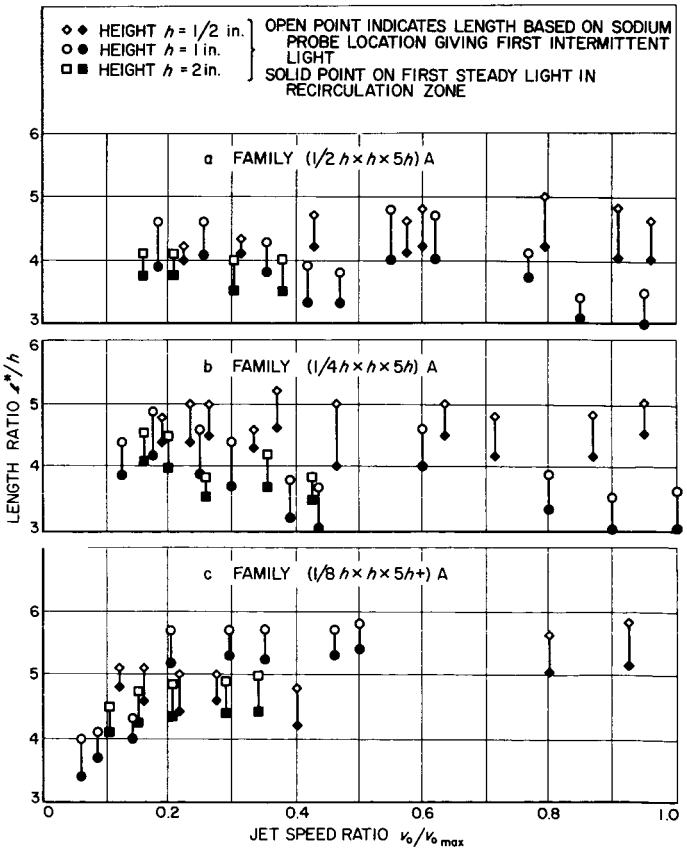

Fig. 19. Influence of Jet Speed on Recirculation Zone Length at the Lean Limit for Three Burner Families in Combustor Type A

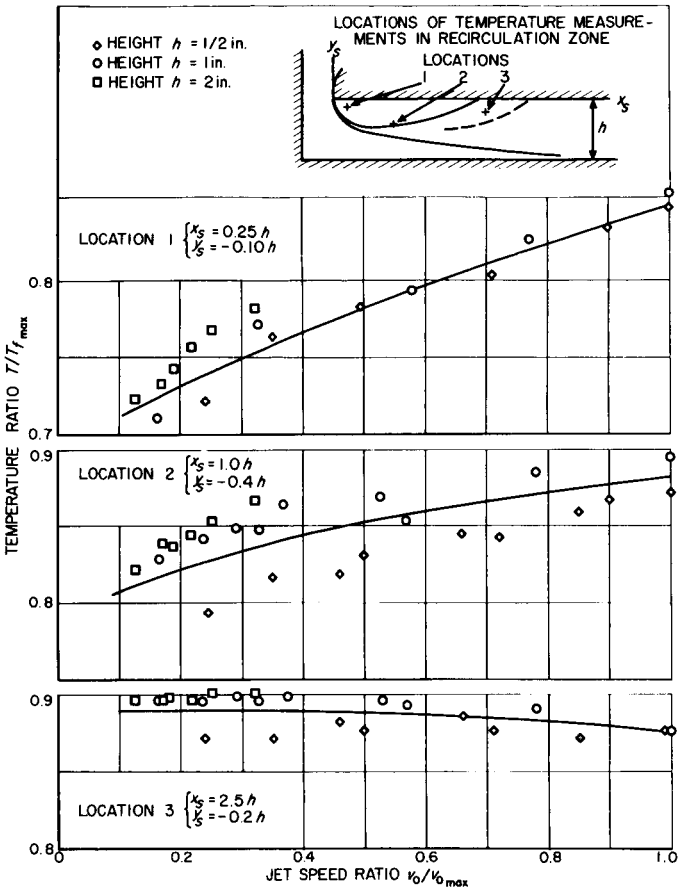

Fig. 20. Influence of Jet Speed on Recirculation Zone Temperature for Three Locations in Burner Family ($\frac{1}{2}h \times h \times 5h$) A at Stoichiometric Mixture Ratio

lean and rich limits than at stoichiometric operation; hence, the heat losses occurring during operation close to the lean and rich limits are smaller than those at stoichiometric mixture ratio. Measurements made at equivalence ratios of 0.7 and 1.3 support this view, since they indicate a higher ratio between actual temperature and corresponding adiabatic flame temperature than that obtained at stoichiometric operation.

Finally, the temperature measurements demonstrate that all burner sizes considered in family ($\frac{1}{2}h \times h \times 5h$) A exhibit almost identical temperature distributions over the full range of jet speeds. Also, the lack of dependence on scale suggests that the temperature distribution is unaffected by variation of slot ratio. Experimental results discussed in the next chapter confirm this suggestion. Thus it is evident that the changes in the flow parameters do not affect the recirculation zone temperature distribution, one of the important chemical parameters.

4. Stability limits. The stability limits expressed in terms of the blowoff speed and fuel–air ratio are presented in Figs. 21, 22, and 23 for the three burner families. The burners of family ($\frac{1}{2}h \times h \times 5h$) A exhibit a strong influence of the scale on the stability limits. As demonstrated by Fig. 21, the stable region of operation becomes a considerably expanded one as the combustion chamber size increases. The smallest burner has a maximum blowoff speed of about 500 ft/sec, while the intermediate size extends its blowoff limits to a maximum of 800 ft/sec. The data for the largest burner are incomplete, especially on the rich side, owing to limitations in the maximum fuel flow rates available. Judging from the location of the limits covered, it appears that the largest size would still have a stable operating range at sonic reference velocity in the jet.

Family ($\frac{1}{4}h \times h \times 5h$) A, in Fig. 22, shows the same general trend as the previous design, although the maximum blowoff speeds of the individual burners are larger. The smallest and intermediate size burners of this family are stable up to about 600 and 900 ft/sec, respectively, for stoichiometric mixture ratio. The stability limits of the largest burner are somewhat more complete in this case and indicate an increased stable region of fuel–air ratios at sonic jet speed as compared with the previous family.

At the smallest slot ratio, in family ($\frac{1}{8}h \times h \times 5h$) A, the limits are again extended towards higher speeds. As shown by Fig. 23, the smallest burner just about reaches sonic jet speed, while both the intermediate and largest size have wide, stable regions at sonic reference speed.

Because of the very great distortion of the wake geometry and velocity distributions which occur with pressure ratios higher than required for choking, no effort was made to operate in this regime. Consequently, the blowoff experiments were stopped when the jet speed reached the sonic value.

5. Correlation parameter for stability. The experimental results presented indicate that the flow conditions within each burner family are quite similar from a chemical and fluid mechanical point of view. The chemical parameters are basically the same, not only for burners within one family but also between different families, and the fluid mechanical parameters are fairly independent of burner size within each family. Because of the similarity within

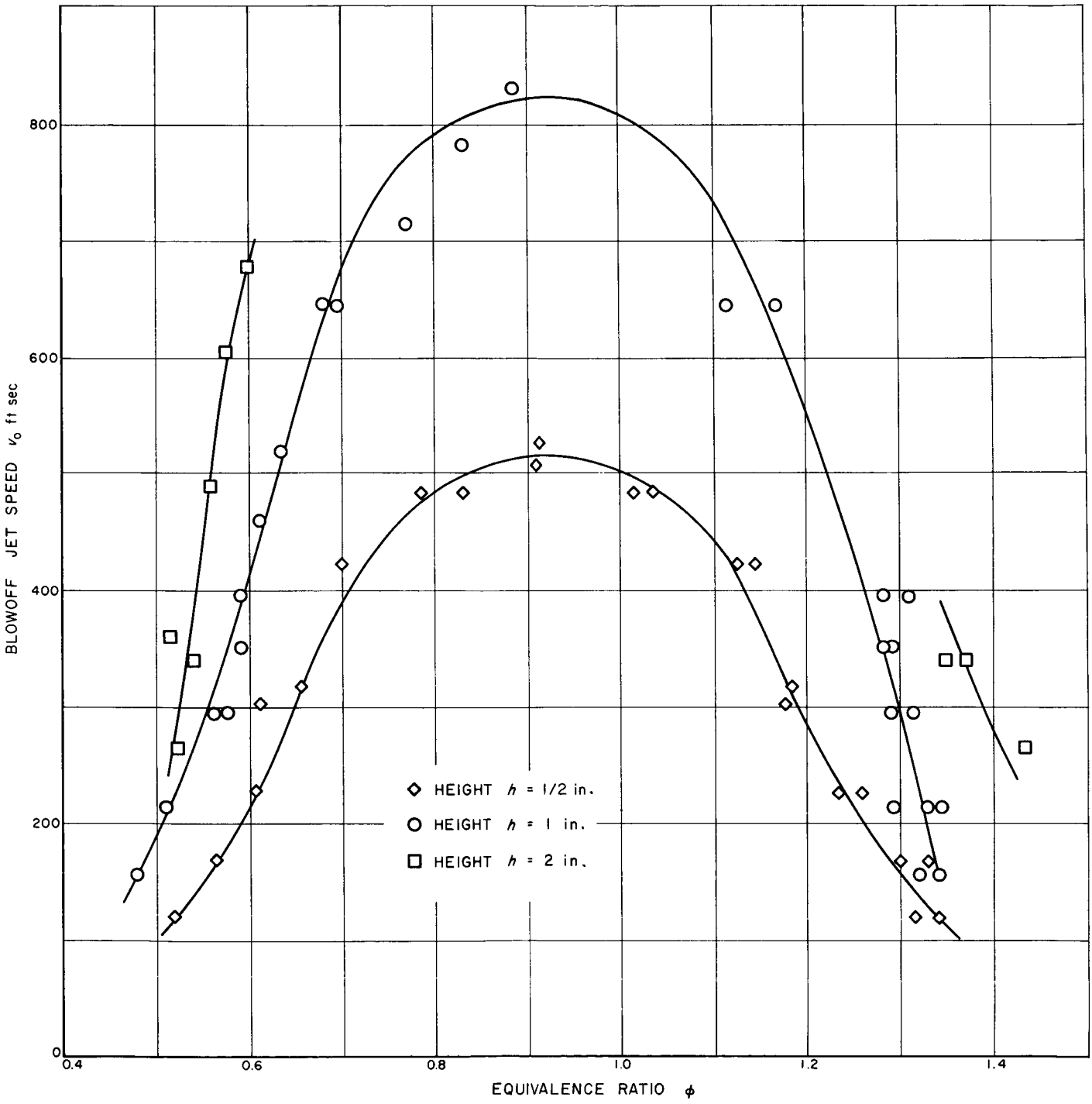

Fig. 21. Stability Limits Expressed in Terms of Blowoff Speed for Burner Family ($\frac{1}{2}h \times h \times 5h$) A

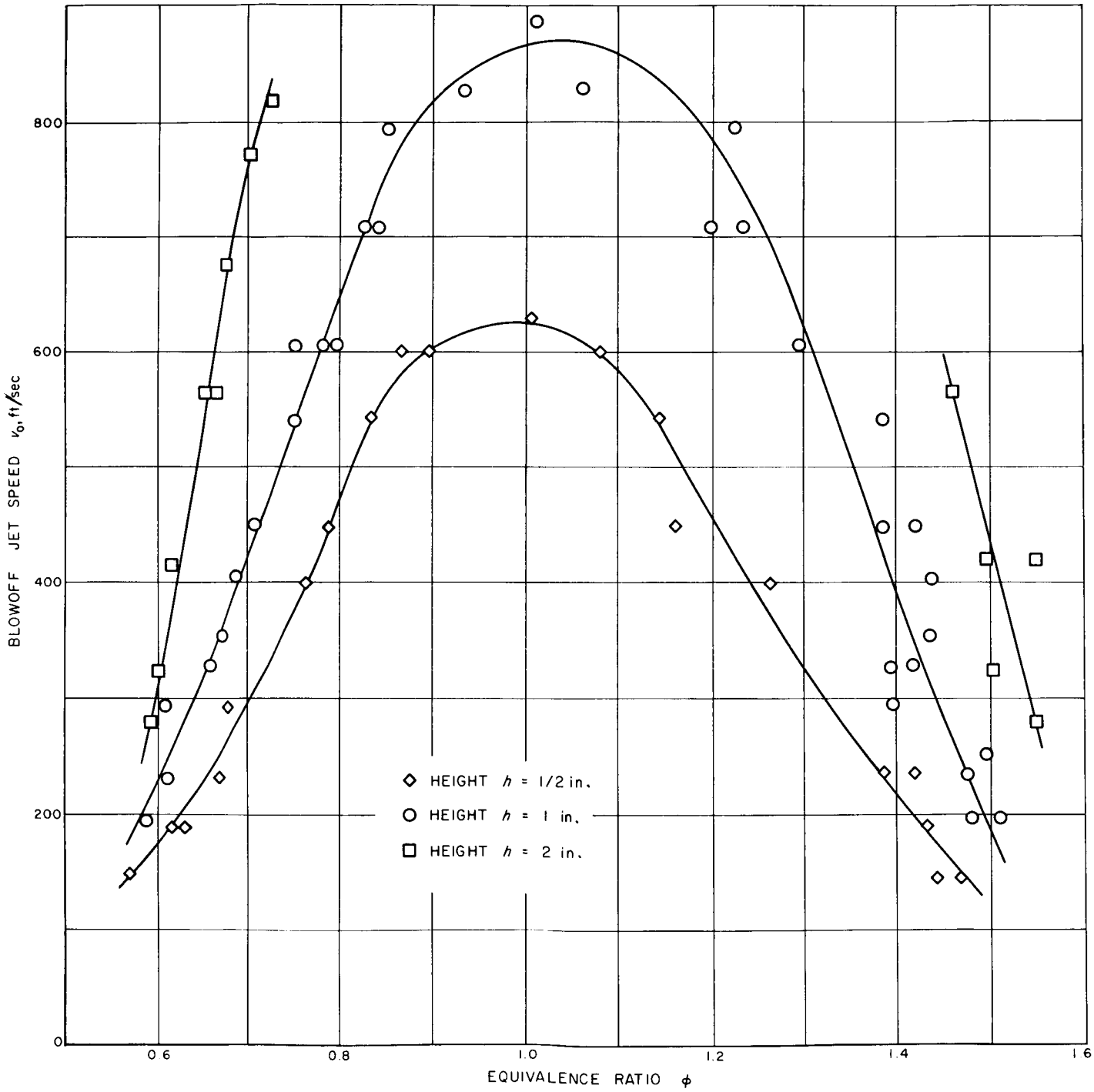

Fig. 22. Stability Limits Expressed in Terms of Blowoff Speed for Burner Family (¼ h × h × 5h) A

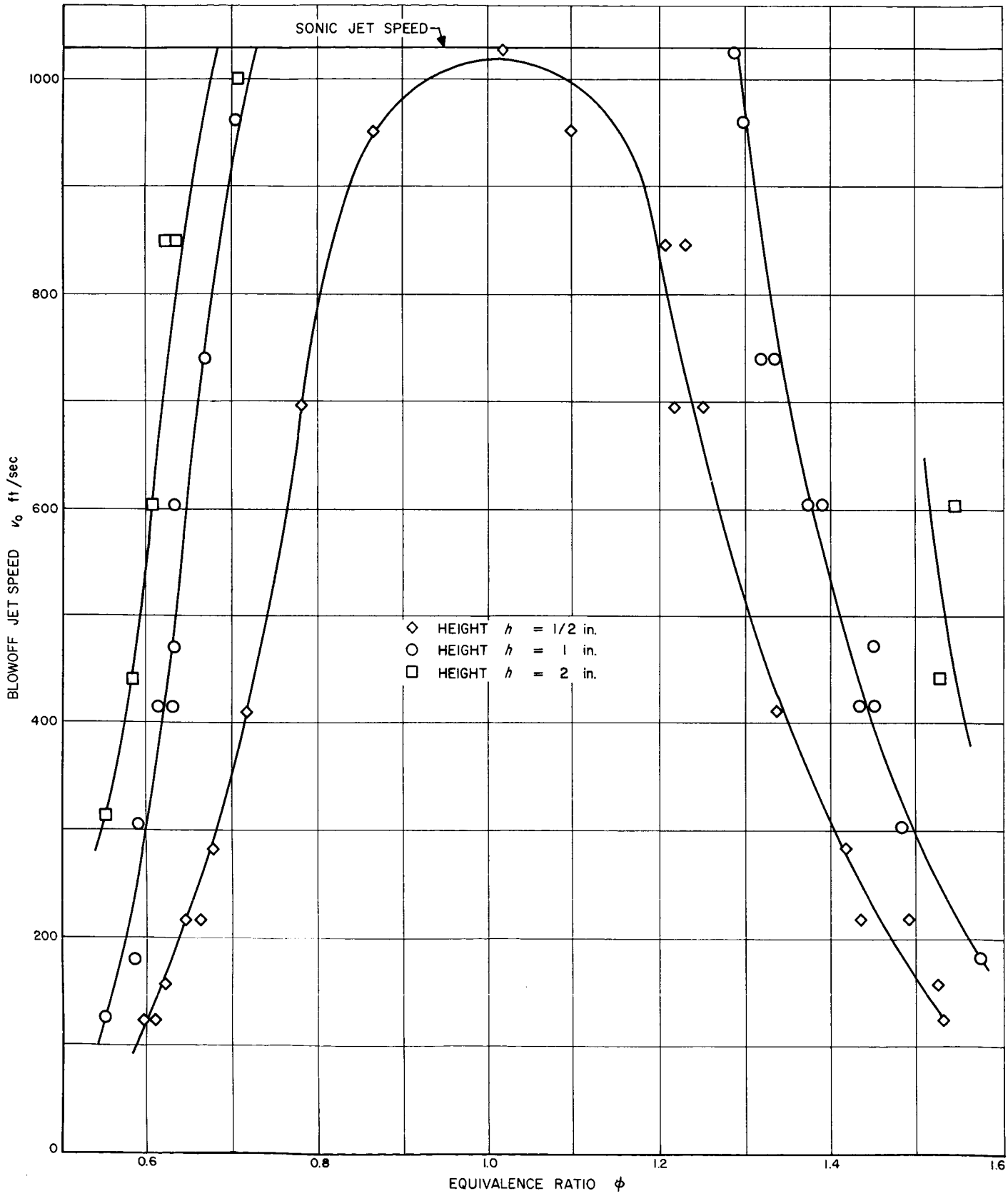

Fig. 23. Stability Limits Expressed in Terms of Blowoff Speed for Burner Family (⅛ h × h × 5h) A

each family of burners, it seems reasonable to assume that simple scaling laws for the stability limits may be found. The present discussion of correlation will be limited to the data of one geometry at a time because of the lack of flow similarity between the three burner families.

The stability limits in Figs. 21, 22, and 23 indicate that for a given fuel–air ratio the blowoff speed is approximately proportional to the burner size. This linear relationship holds within about ±15% for the family ($\frac{1}{2}h \times h \times 5h$) A, about ±25% for family ($\frac{1}{4}h \times h \times 5h$) A, and about ±20% for family ($\frac{1}{8}h \times h \times 5h$) A.

The approximately linear relation between blowoff speed and burner size implies that for a given fuel–air ratio there exists a similarity parameter of the form

$$\frac{\tau}{d} = \frac{d}{v_0}$$

where d is any linear dimension of the burner, and v_0 is the reference speed of the jet. Clearly, this parameter, or its inverse, will give an approximate correlation of the stability limits within each family.

The correlation parameter discussed has the dimension of time. It will be recalled that the correlation parameter found for the bluff body flameholder by Zukoski and Marble was a characteristic time

$$\tau_c = \frac{l^*}{u_0}$$

where l^* is the length of the recirculation zone, and u_0 is the blowoff speed of the cold flow along the boundary of the zone. Since these variables are well known for the present system, the next logical step would be to try a similar parameter of the form

$$\tau_0 = \frac{l^*}{v_0}$$

It should be noted that the reference speed v_0 represents the initial jet speed; the actual velocity along the boundary of the recirculation zone may change with position and certainly depends on the geometry of the flow field. Consequently, the time τ_0 is not directly comparable to the bluff body time τ_c.

The correlation of the stability limits by the new parameter τ_0 is illustrated in Figs. 24, 25, and 26 for the three families. The data show that within each family the stability limits for different sized burners are surprisingly well correlated over the complete range of operation. The correlation is most satisfactory on the lean side; the slight increase in scatter of the data on the rich side is probably due to the less stable character of the flow at rich blowoff.

The correlation obtained for each family by using the recirculation zone length is considerably more accurate than would be obtained by τ_d based directly on the burner size. The reason for the improved correlation lies in the fact that the deviations from the linear relationship between the blowoff speed and the size are compensated by the changes of the relative length of the recirculation zone (Fig. 19). Hence it is evident that the recirculation zone length is the correct characteristic dimension for the purpose of scaling the blowoff phenomena.

A comparison of the stability limit based on τ_0 reveals that the slot ratio parameter has a strong influence on the correlation. The minimum values of τ_0 are 0.33, 0.31, and 0.22 millisec for the ½, ¼, and ⅛ slot ratio families, respectively.

A qualitative interpretation of this trend can be obtained by considering the flame stabilization mechanism suggested for the bluff body flameholder. Zukoski and Marble based their characteristic time on the concept of a continuous ignition process taking place in the mixing zone. The mixture material has to spend a minimum of time, a so-called ignition delay time, in this reaction zone to make it possible for the flame to propagate from the downstream end of the recirculation zone.

If the stabilization mechanism for the present system is similar to that of the bluff body flameholder, as is suggested by the excellent correlation within each family, then the deviations in correlation between families can easily be explained. The reference speed used in the definition of τ_0 only is representative for the initial jet speed, and does not take into account the flow situation along the rest of the characteristic dimension. In burners with small slot ratios, the relative speeds in the downstream part of the mixing zone are lower than in burners with larger slot ratios. This follows from the fact that, for small slots, all of the fresh mixture enters the mixing zone before the downstream end of the recirculation zone is reached. Because the cross-sectional area of the duct is constant, the speed in the mixing zone at the end of the recirculation zone will be proportional to the mass flow rate. As the slot area is reduced, the mass flow rate for

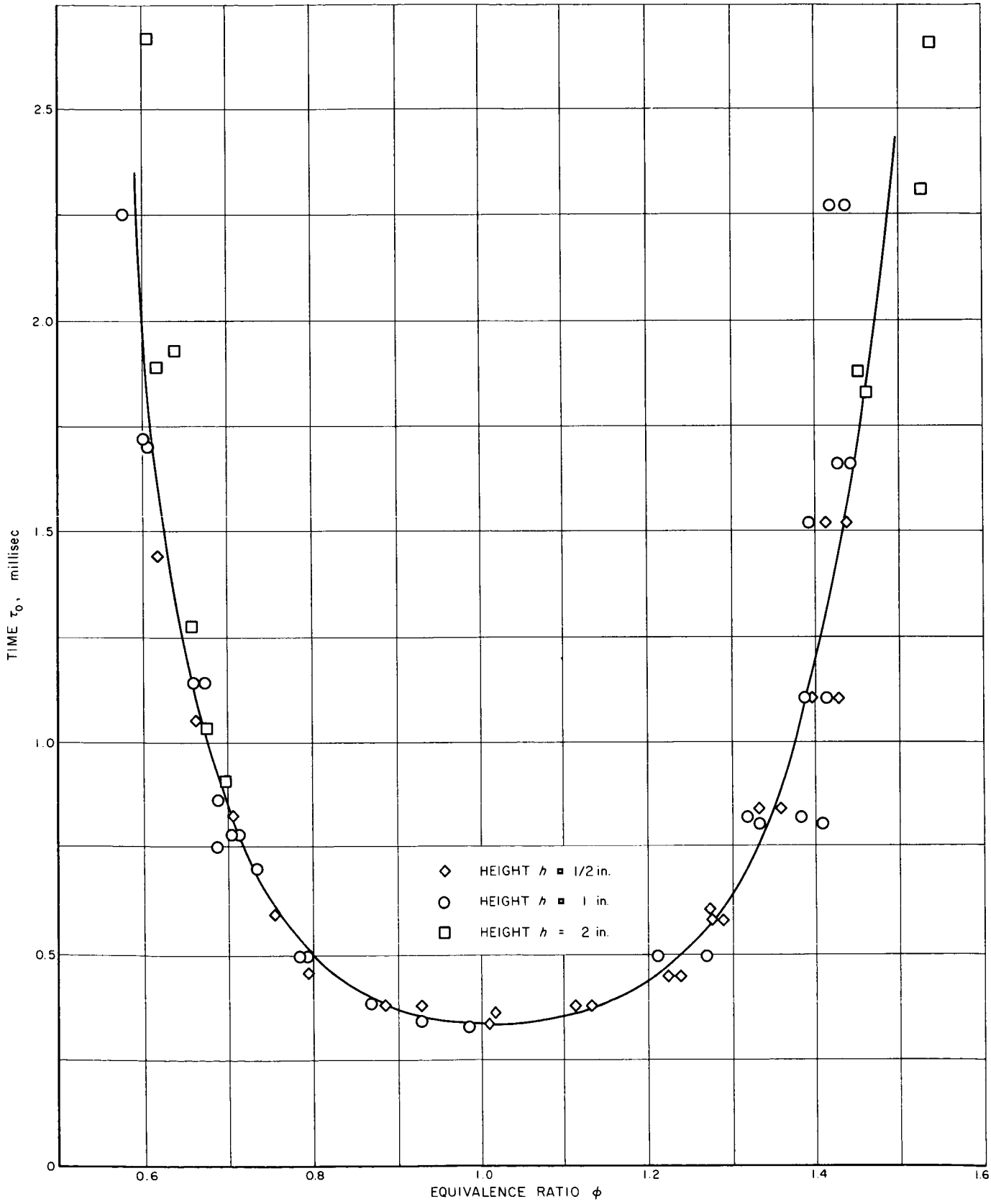

Fig. 24. Stability Limits Expressed in Terms of τ_0 for Burner Family ($\frac{1}{2}h \times h \times 5h$) A

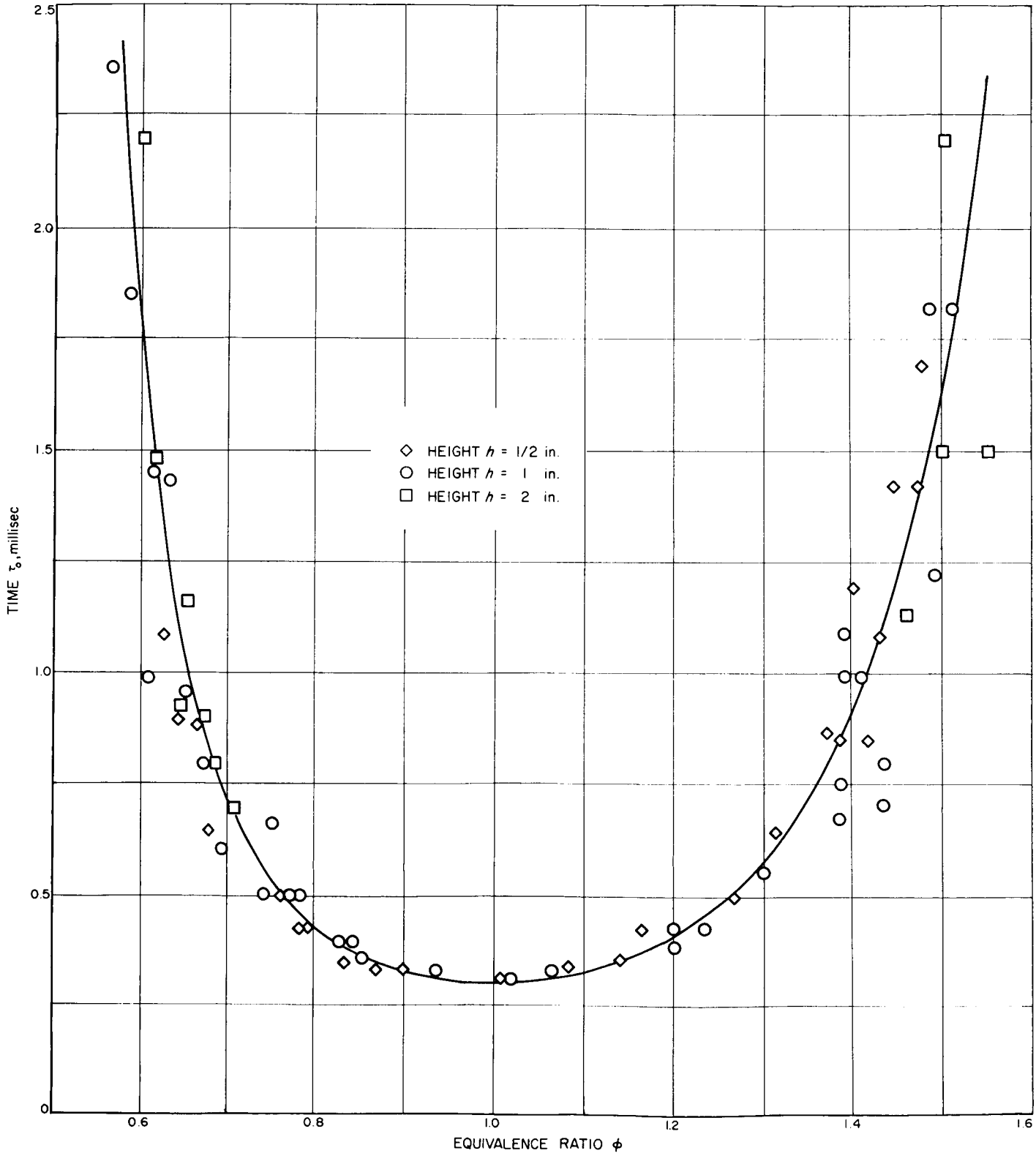

Fig. 25. Stability Limits Expressed in Terms of τ_0 for Burner Family (¼ h × h × 5h) A

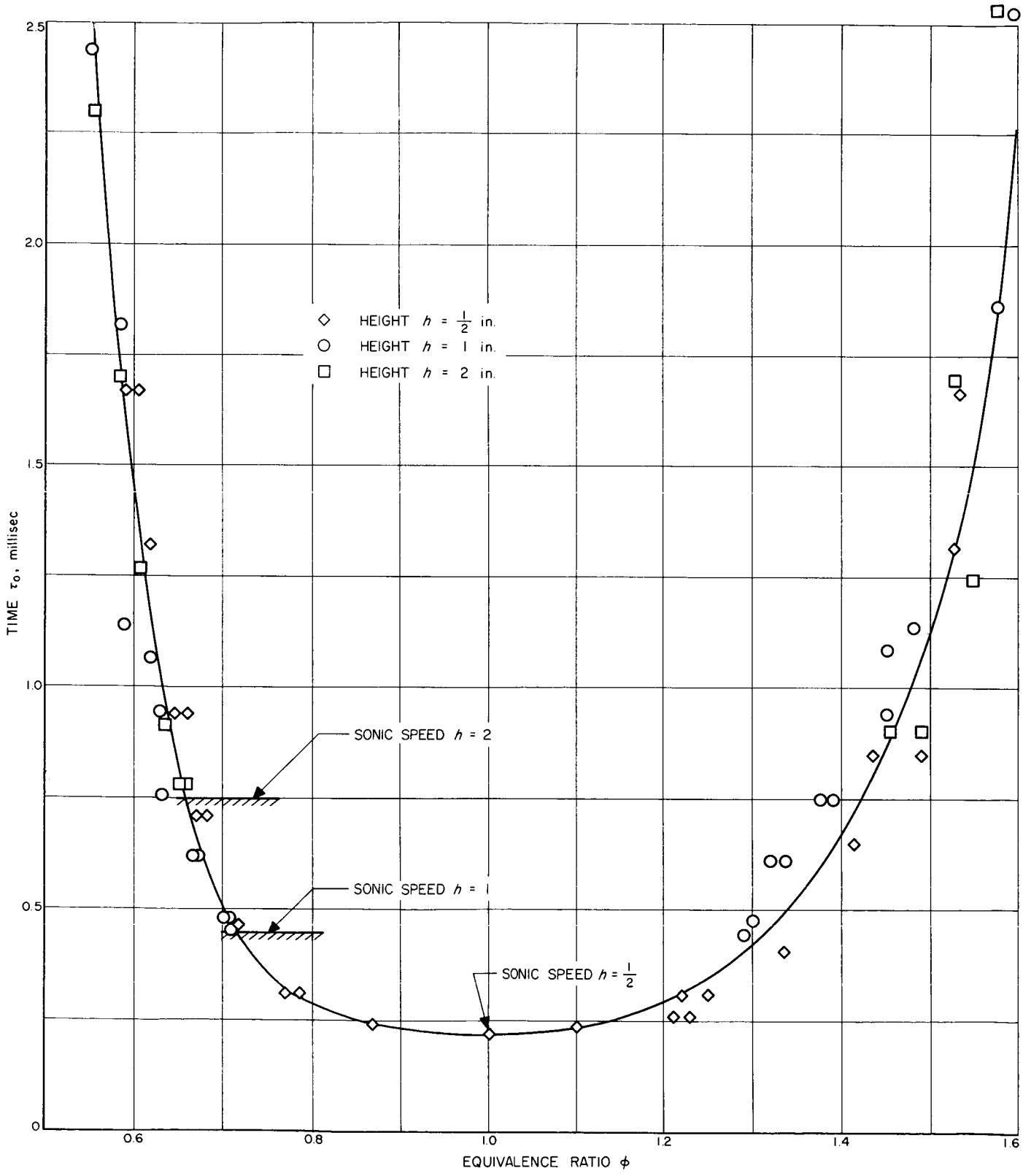

Fig. 26. Stability Limits Expressed in Terms of τ_0 for Burner Family ($\frac{1}{8}h \times h \times 5h$) A

a given jet speed decreases, and hence the flow speed in the mixing zone will also decrease. Consequently, the residence time for the material in the mixing zone will increase as the slot ratio is reduced for a constant jet speed. Under such circumstances, it is clear that the burner with the smaller slot can operate at higher initial jet speed, for any given fuel–air ratio, than a burner with a larger slot. Because τ_0 is based on the initial speed, lower minimum values would be expected for smaller slot ratios.

C. Summary

The objective of the scaling experiment has been achieved. The results demonstrate that the stability limits of geometrically similar combustion chambers subjected to the same situation from a chemical point of view can be accurately correlated by a parameter similar to the characteristic time found for the bluff body flameholder.

There are two direct implications of the successful correlation obtained. The first is that the length of the recirculation zone is the important characteristic dimension in flow. The second is that the stabilization mechanism is similar to that found for the bluff body flameholder.

The similarity parameter introduced, however, does not correlate the different families of burners except in a qualitative sense. The discrepancies, most noticeable for families with small slot ratios, are presumably caused by referring the correlation parameter to the initial speed of the jet without accounting for changes in the speed farther downstream. This conclusion is based on the assumption that the residence time in the mixing zone is the important parameter, as was suggested by the similarity of the process to that of the bluff body.

In order to elucidate the role of the residence time, more detailed information about the flow field must be obtained. For this purpose, it would be desirable to test a burner of a given size over an even wider range of slot ratios than studied during the scaling experiment. Such experiments will be described in Section V.

V. CORRELATION OF STABILITY LIMITS FOR COMBUSTION CHAMBERS OF VARYING GEOMETRY

The characteristic time introduced by Zukoski and Marble is a very convenient stability parameter for the bluff body flameholder, because in this case the complete length of the recirculation zone is covered by fresh mixture moving at constant speed. Hence the time spent in the mixing zone by an element of gas will be proportional to the characteristic time. Thus the stability limits can be correlated for flameholders of varying size and geometry by measuring only the recirculation zone length l^* and the speed in the isentropic flow past the wake.

Unfortunately, the situation is not as simple in the present case. The previous experiments have indicated that the flow field undergoes strong changes when the slot ratio of the burners is reduced below about ½. For these low slot ratios all of the fresh mixture enters the mixing zone before the end of the recirculation zone. The smaller the slot ratio, the earlier all of the fresh mixture is consumed by the spreading mixing layer. Consequently, in the downstream region of the wake the mixing is no longer sustained by the isentropic flow field. Thus it is clear that the characteristic time based on the jet reference speed does not represent a measure of the residence time in the mixing zone.

In order to facilitate a quantitative correlation of the stability limits of burners with small slot ratios, more information about the flow in the mixing zone is evidently required. The velocity as well as the temperature distributions through the mixing zone at various locations along the wake should be determined. Given these flow parameters, it will be possible to determine the actual residence time in the mixing zone.

A. Equipment and Experiments

The experiments were carried out using combustor type B, which was primarily designed to give a wide range of slot ratios for a burner of intermediate height, in this case, 1 in. It will be recalled that this combustion chamber has water-cooled aluminum top and bottom walls.

Even though the heat transfer rates are higher than in the glass-insulated combustor type A, it was found that the stability limits were more reproducible in the aluminum-wall burner. Since the burner size will be kept constant, the variation of heat transfer should not give rise to significant differences in recirculation zone temperature for burners of different geometry.

It was decided to extend the previously tested slot ratio range by a factor of 2 in both directions. The burner families tested in combustor type A had slot ratios from ⅛ to ½; the present study covers the ratios 1/16, ⅛, ¼, ½, ¾, 1.

Blowoff experiments were carried out with the burners of the different slot ratios mentioned. The previously described standard measurements were performed in each case.

Again, it was necessary to determine the temperature distribution in the recirculation zone to make sure that there were no pronounced differences in the chemical parameters between the individual burners. In the present case, the line reversal measurements were made at three different locations in the zone; namely, at the upstream end, the center region, and the downstream end.

In order to determine the local velocities in the mixing zone, the total and static pressure distributions were measured at several locations along the recirculation zone. The corresponding temperature distributions were also determined by using a thermocouple probe. In order to secure a satisfactory coordination of the locations of the pitot tube and the thermocouple, the two probes were mechanically coupled to one unit. The probe tips were located about ¼ in. apart in a plane parallel to the bottom wall of the burner.

The mixing zone temperatures were only measured at the stability limits. Actually, the operation along the stability limits is of primary interest, since the study of the mixing zone presumably will yield a correlation parameter for stability.

The inner region of the mixing zone reaches temperatures sufficiently high to require considerable correction for radiation losses from the thermocouple. Unfortunately, the speeds are low and often not very well defined in this region. Thus the speed as well as the temperature distributions in the hottest part of the mixing zone are somewhat inaccurate. In order to support the temperature data, a few line reversal measurements were made.

B. Results and Discussion

The experimental data obtained concerning the flow field parameters and the stability limits of the different burners are presented and discussed below. Attention will be concentrated on the mixing zone, because this region of the flow is of primary interest for the determination of a residence time. To make the picture of the burners more complete, the geometry of the flow field and the temperature of the recirculation zone are presented in the same way as for the previous burners.

1. Flow field geometry. Figure 27 presents direct flame and schlieren pictures of the combustion chamber ($\delta \times 1 \times 6$) B for the six different slot ratios ranging from 1 to 1/16. The pictures have been taken at maximum speed

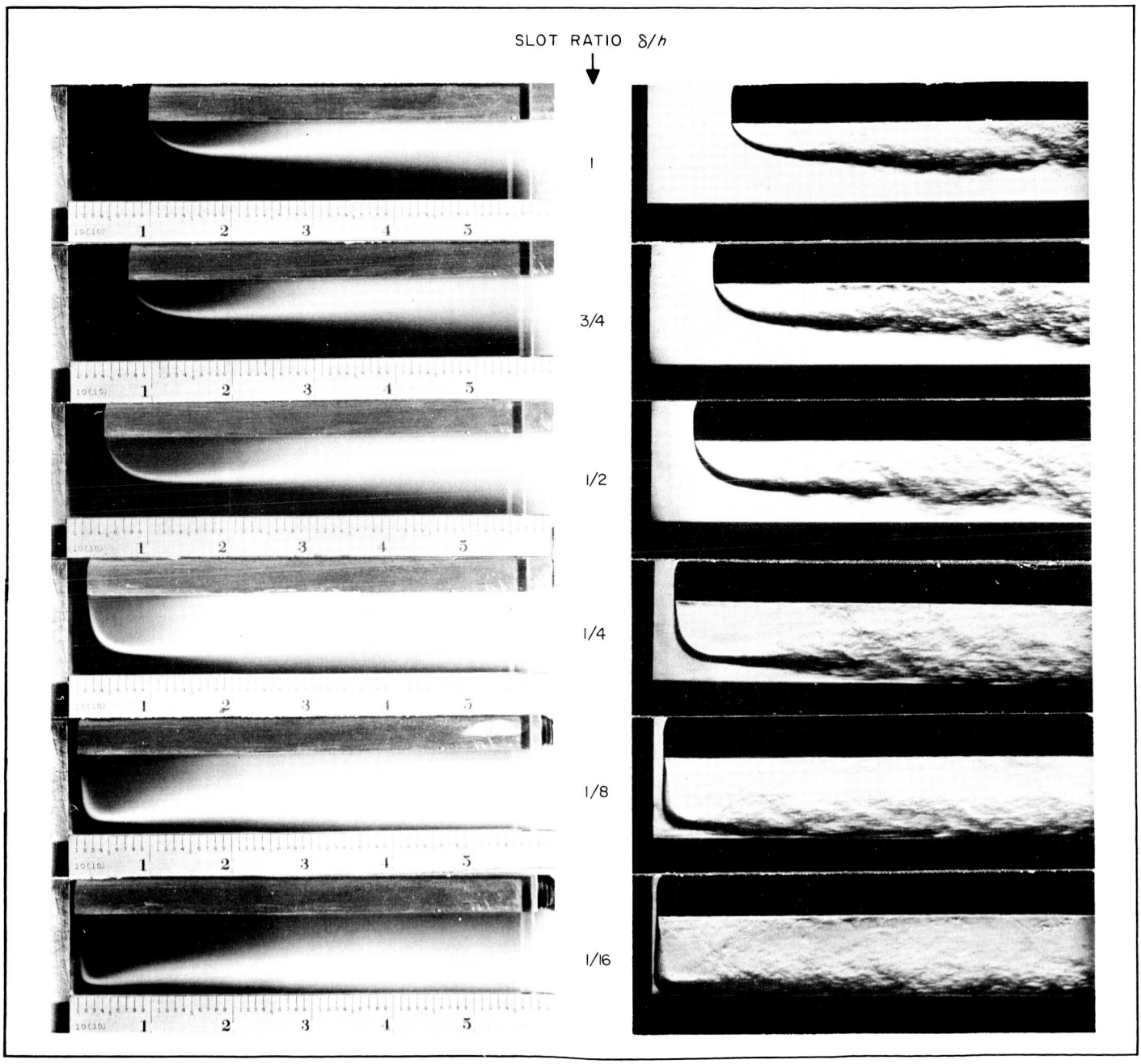

Fig. 27. Direct Flame and Schlieren Photographs of Combustion Chamber ($\delta \times 1 \times 6$) B for Various Slot Ratios and Stoichiometric Operation at Maximum Blowoff Speed

and stoichiometric fuel–air ratios and demonstrate the very pronounced change in flow configuration which takes place when the slot ratio varies over a wide range.

For the larger slot ratios, ½, ¾, and 1, both the flame and the schlieren pictures show that the wake is covered by a stream of fresh mixture along the total length of the recirculation zone. This length is about 4 in. on the scale shown in the flame pictures. The burners with smaller slot ratios, on the other hand, exhibit a direct contact between the mixing zone and the bottom boundary. Even though the lower surface of the flame appears at a small height above the bottom wall, the schlieren pictures clearly demonstrate that the mixing layer reaches down to the bottom wall. The point at which all of the fresh mixture has entered the mixing zone occurs further upstream as the slot ratio is reduced. At a slot ratio of ¼, this point is located at about the middle of the recirculation zone length; for ⅛, it has moved up to a short distance downstream from the deflection region of the jet; and finally, at slot ratio 1/16, all of the fresh mixture has entered the mixing zone immediately after the deflection of the jet.

The pictures in Fig. 27 also illustrate the manner in which the initial direction of the entering jet is affected by the slot ratio. For small ratios, the jet passes over more than half of the burner height before any deflection toward the exit takes place. As the slot ratio goes up, the jet becomes deflected earlier, until at large ratios a considerable initial deflection at the slot exit can be observed.

2. ***Recirculation zone length.*** The recirculation zone length for the various slot ratio burners is presented as a function of jet speed ratio in Fig. 28. As found earlier for other burners, the length of the zone is not strongly affected by the jet speed. Comparing the lengths for different slot ratios, it is found that the recirculation zone becomes longer as the slot ratio is reduced. For burners with large and intermediate slot ratios, the relative length is of the order 3.5–4.5 in. The smaller slots exhibit an increase in length to about 5 and 6 in.

3. ***Recirculation zone temperature.*** The temperature in the recirculation zone is presented as a function of velocity in Figs. 29 and 30 for locations at the upstream and downstream parts of the recirculation zone. The important facts demonstrated by these data are that the burners of different geometry not only show a very similar relative speed dependence, but also about the same absolute values of the temperature. For example, the temperature

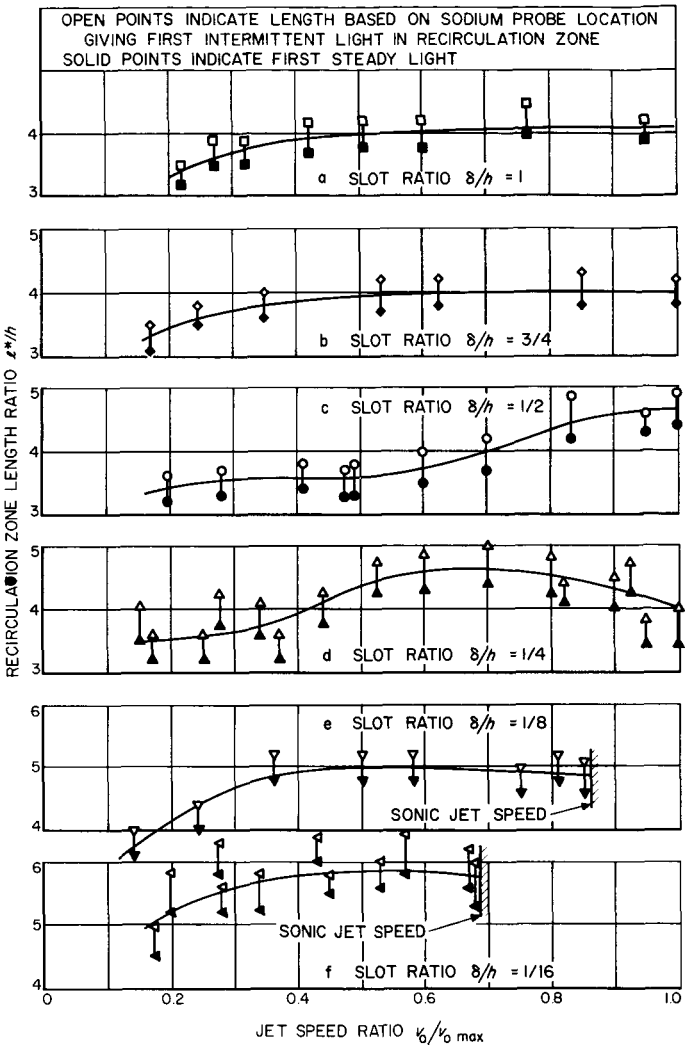

Fig. 28. Influence of Jet Speed on Recirculation Zone Length for Various Slot Ratios in Combustion Chamber (δ × 1 × 6) B Operating at the Lean Limit

difference at a given relative speed is less than ±1% for both sets of data.

The temperature variation with speed is about 10% for the upstream location and is negligible for the downstream location in the recirculation zone. The variation is caused by heat transfer to the top wall of the burner, and was previously discussed in detail for the combustion chamber (½ × 1 × 6) B.

Finally, these measurements have shown that the temperature levels in the recirculation zone are essentially independent of the burner geometry. Hence the chemical parameters governing the flame stabilization process are the same for all of the burners.

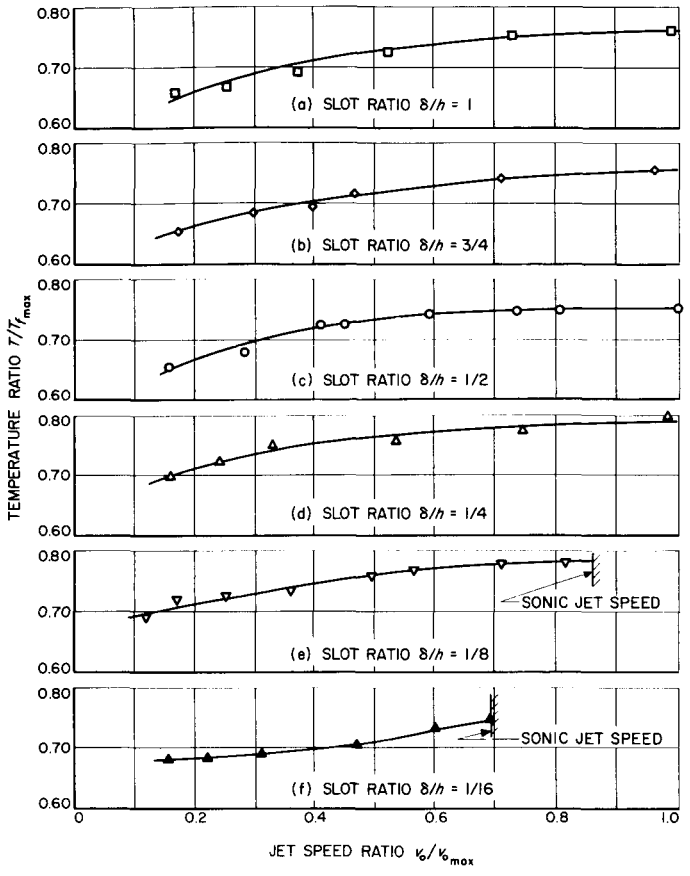

Fig. 29. Influence of Jet Speed on Temperature at the Upstream End of the Recirculation Zone for Various Slot Ratios in Combustion Chamber (δ × 1 × 6) B Operating at Stoichiometric Mixture Ratio

4. Stability limits in terms of τ_0. The experiments up to this point have established that the chemical parameters in the different burners are identical. The flow parameters, on the other hand, exhibit a great deal of variation between the burners, owing to the differences in slot ratio. Hence a comparison between the stability limits of the different burners will demonstrate the influence of the flow parameters only.

Figure 31 shows the stability limits in terms of τ_0 for the different burners, and demonstrates several very interesting effects of the burner geometry on the stability limits.

Burners with slot ratios ½, ¾, and 1 show a good correlation. This is perhaps not surprising because the mixing zone in these burners did not have any direct interaction with the bottom boundary before the end of the recirculation zone.

Reducing the slot ratio below ½ leads to a widening of the stability limits. Again, this effect may be expected because an increasingly strong interaction between the mixing zone and the bottom boundary was observed as the slot ratio was reduced.

Clearly, the trend observed here is the same as that found when comparing the different families of burners in Section IV. As was expected, the greater variation of geometry used in this case has led to a considerable amplification of the discrepancies in the stability curves expressed in terms of τ_0.

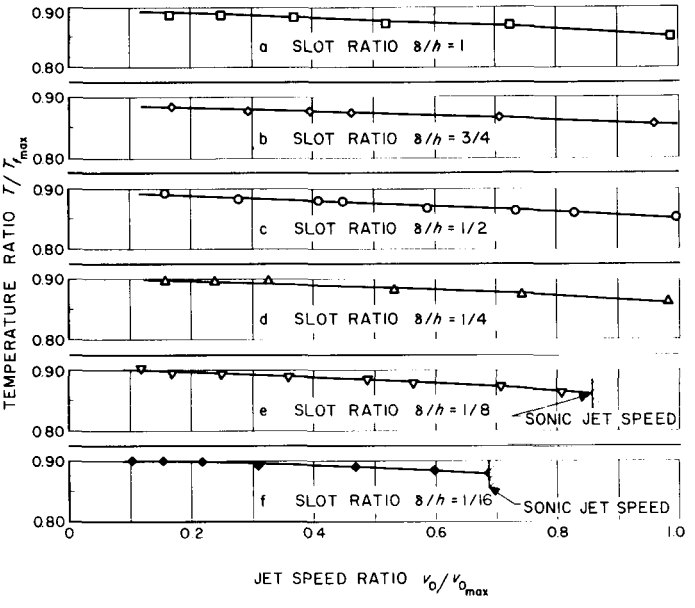

Fig. 30. Influence of Jet Speed on Temperature at the Downstream End of the Recirculation Zone for Various Slot Ratios in Combustion Chamber (δ × 1 × 6) B Operating at Stoichiometric Mixture Ratio

Previously, the trend in the discrepancies was explained by a qualitative comparison of the residence times in the mixing zone. In order to obtain a quantitative correlation, it will be necessary to actually measure these times. This requires a more detailed study of the flow field in the mixing zone.

5. Flow field in the mixing zone. The mixing zone structure is not very likely to be affected by the burner geometry for slot ratios equal to and larger than ½. The present investigation will therefore be limited to burners with slot ratios equal to ½ and smaller. Hence it will be possible to compare the flow in the mixing zone for a case without any interaction with the bottom boundary with cases in

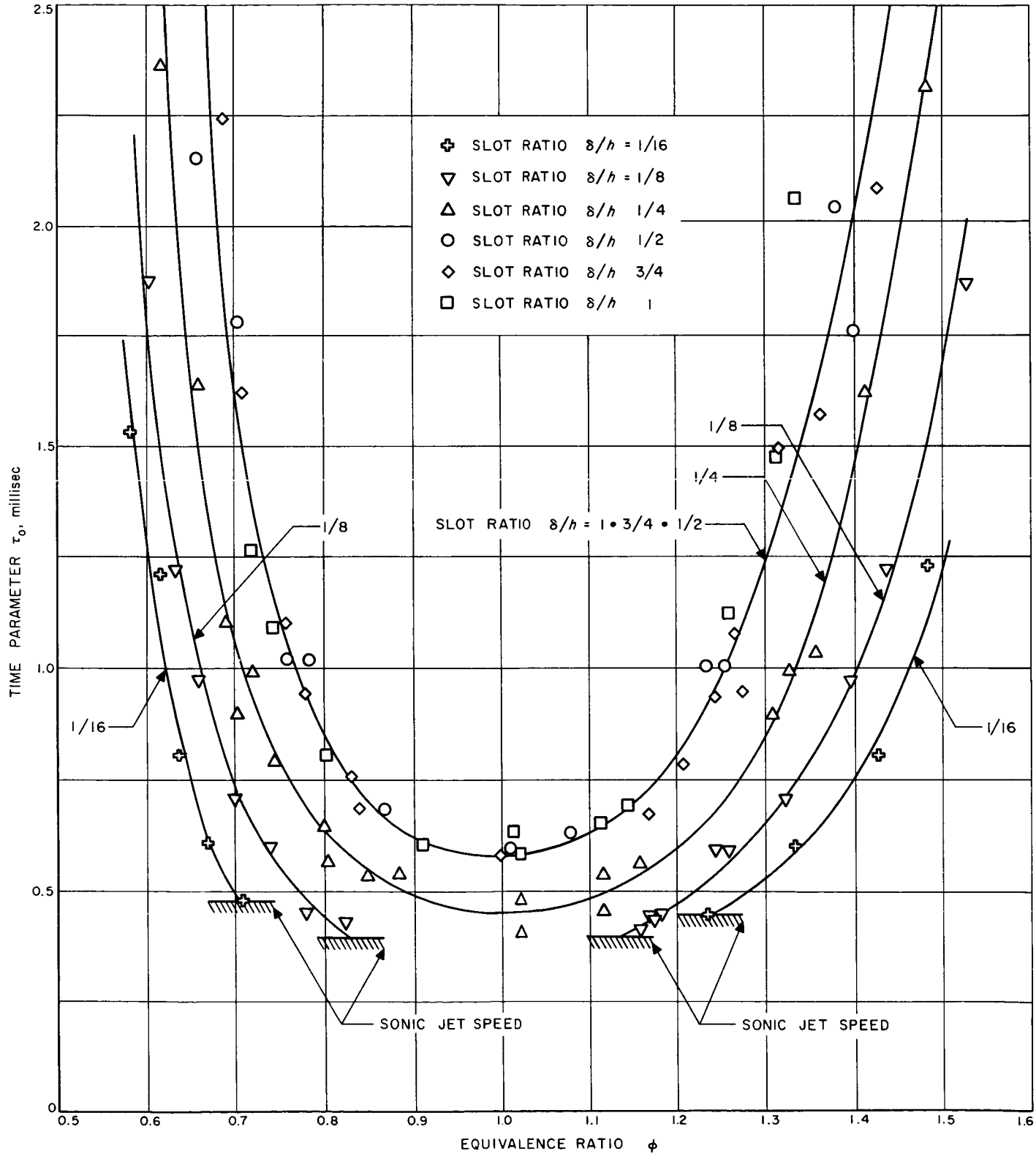

Fig. 31. Stability Limits Expressed in Terms of τ_0 for Combustion Chamber ($\delta \times 1 \times 6$) B with Various Slot Ratios

which a weak or strong interaction is present. The flow in the mixing zone of combustion chamber (½ × 1 × 6) B will be treated in some greater detail than for the smaller slots.

Slot ratio $\delta/h = ½$: The velocity distributions through several sections of the mixing zone at the lean limit and an intermediate jet speed in the burner (½ × 1 × 6) B are illustrated by Fig. 32. The local speeds are expressed in terms of the reference speed v_0. When going from the upstream. The latter sections also have considerably larger velocity gradients because of the smaller width of the mixing layer closer to the entrance of the jet.

The temperature distributions in the same sections are presented in Fig. 33. The temperature rises continuously through the mixing zone from the inlet temperature value at the stream of fresh mixture to the recirculation zone temperature level. Again, the temperature gradients are higher the farther upstream the traverse is made.

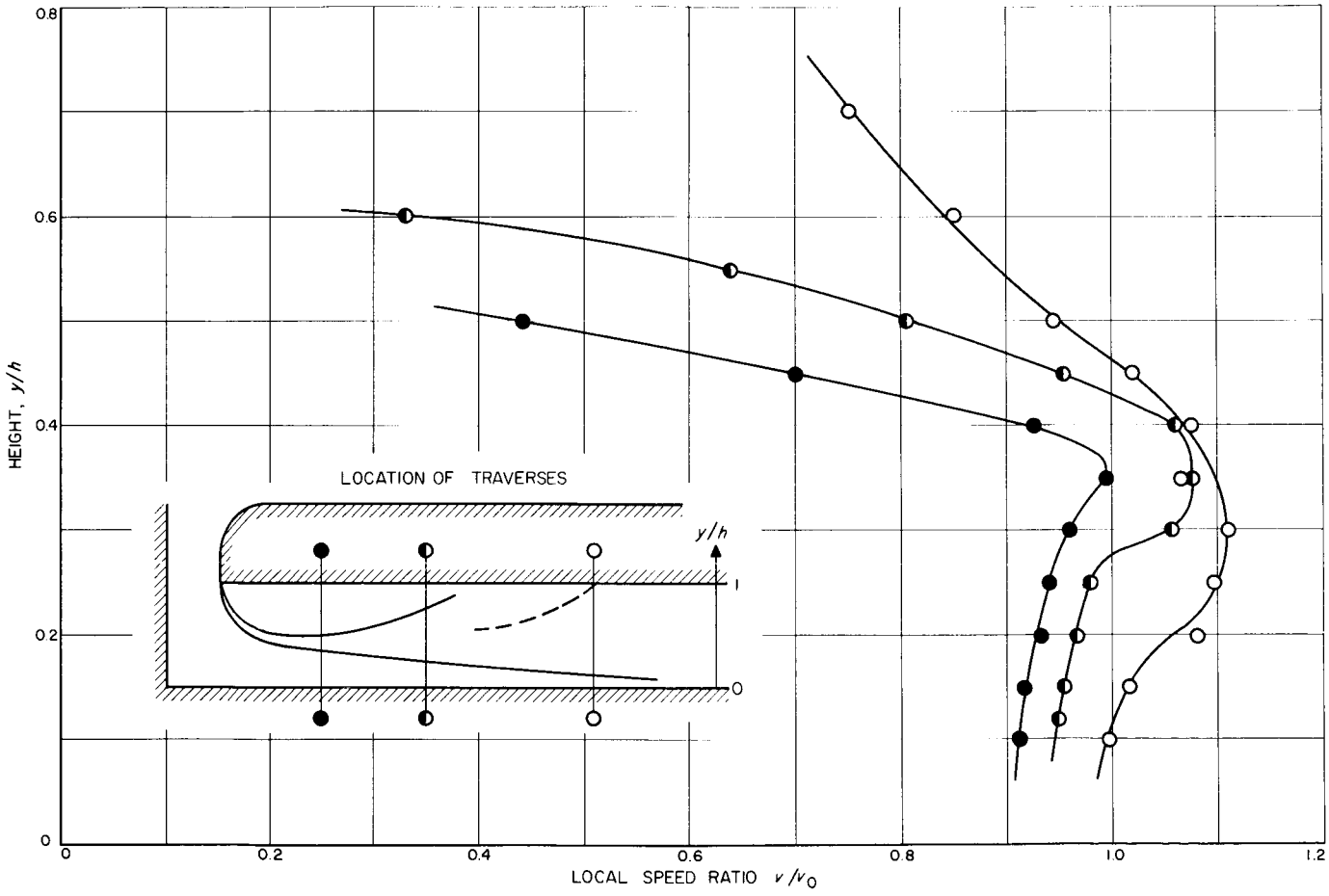

Fig. 32. Velocity Distributions in Mixing Zone of Combustion Chamber (½ × 1 × 6) B Operating Close to the Lean Limit and at Jet Speed Ratio $v_0/v_{0\,max} = 0.5$

isentropic flow of fresh mixture into the mixing zone, the speed first increases by about 10% to a maximum value which occurs fairly close to the boundary. Deeper in the mixing zone, the speed is gradually reduced to a very low value at the boundary of the recirculation zone.

The velocity distribution shows slightly higher speeds in sections farther downstream as compared with those

It is of interest to consider the speed of different temperature regions in the mixing zone. A diagram of the local temperature vs the corresponding speed facilitates a comparison of the flow at the various sections which have different mixer layer thicknesses. Such a cross-plot of the temperature and velocity profiles is shown in Fig. 34. The resulting $T(v/v_0)$ profiles are surprisingly similar at the different locations along the flow.

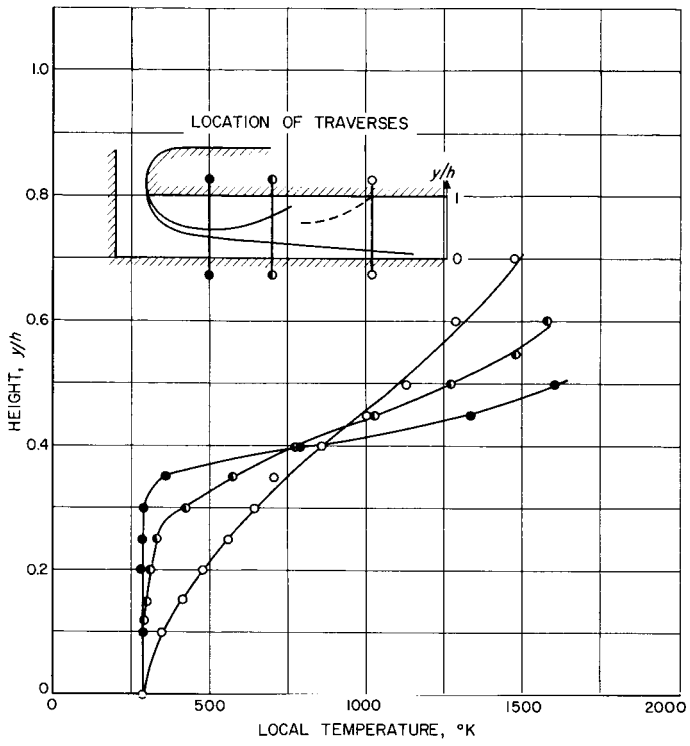

Fig. 33. Temperature Distributions in Mixing Zone of Combustion Chamber (½ × 1 × 6) B Operating Close to the Lean Limit and at Jet Speed Ratio $v_0/v_{0\,max} = 0.5$

The scatter observed for the section farthest upstream is probably caused by inaccuracies in the location of the probes. At this section, the velocity and temperature gradients are very high because of the small width of the mixing zone. Hence a small dislocation of a probe will give rise to large errors in the quantity measured.

Figure 34 shows that the material at about 600°K travels with the highest relative speed, which is equal to or slightly larger than the jet speed. The 600°K material is located fairly close to the lower boundary of the mixing zone; hence, at this location, the effect of the heat release on the speed is stronger than the losses in total pressure caused by the mixing. At higher temperatures the situation is reversed. The material at 1500°K moves with a speed of about half the jet speed.

The locations of isotherms in the flow field can be determined from the temperature distributions given in Fig. 33. Figure 35 indicates the locations of the isotherms for 500, 1000, and 1300°K in the mixing zone. It will be noticed that the 500°K isotherm has about the same shape as the lower boundary of the zone.

Thus far, the situation in the mixing zone has only been considered at a certain intermediate jet speed. The influence of the jet speed on the temperature distribution through the end of the recirculation zone is illustrated by Fig. 36. All data have been taken with the combustion chamber operating close to the lean stability limit. In the first case, the measurements were made at maximum speed and stoichiometric fuel–air ratio; in the second, the jet speed was about half of maximum, with an equivalence ratio of 0.8; and finally, the last case corresponded to a jet speed ratio of about 0.3 and an equivalence ratio of 0.7.

Considering the differences in recirculation zone temperature obtained with as widely different equivalence ratios as indicated above, the similarity in the temperature profiles, demonstrated by Fig. 36, is surprisingly good. A qualitative interpretation of the result can be obtained by introducing the residence time concept. Close to blowoff at stoichiometric equivalence ratio—that is, at maximum recirculation zone temperature—an element in the mixing zone spends a minimum amount of time in contact with the heat source of the flow field. On the other hand, at a lean equivalence ratio, e.g., $\phi = 0.7$, the same element spends a considerably longer time in contact with the recirculation zone owing to the reduced speed at the stability limit for this fuel–air ratio. Hence when an element reaches the end of the recirculation zone, its resulting temperature will be about the same in two cases, despite the much lower recirculation zone temperature at the lower fuel–air ratio.

An even more striking similarity is exhibited in the $T(v/v_0)$ profiles at the end of the recirculation zone for the three jet speeds studied. As demonstrated by Fig. 37, material of a certain temperature travels with the same relative speed close to blowoff. The similarity in $T(v/v_0)$ implies that the relative velocity profiles at the end of the recirculation zone also are similar, since it has been shown that the temperature profiles are similar.

Summarizing the results obtained from the investigation of the mixing zone in combustion chamber (½ × 1 × 6) B, it has been found that the flow field in the mixing zone close to blowoff exhibits a great deal of similarity in velocity as well as temperature distributions. The most striking similarity occurs in the $T(v/v_0)$ profiles, which seem to be relatively independent of jet speed as well as location along the flow. This implies that all elements at a given temperature level move with the same relative

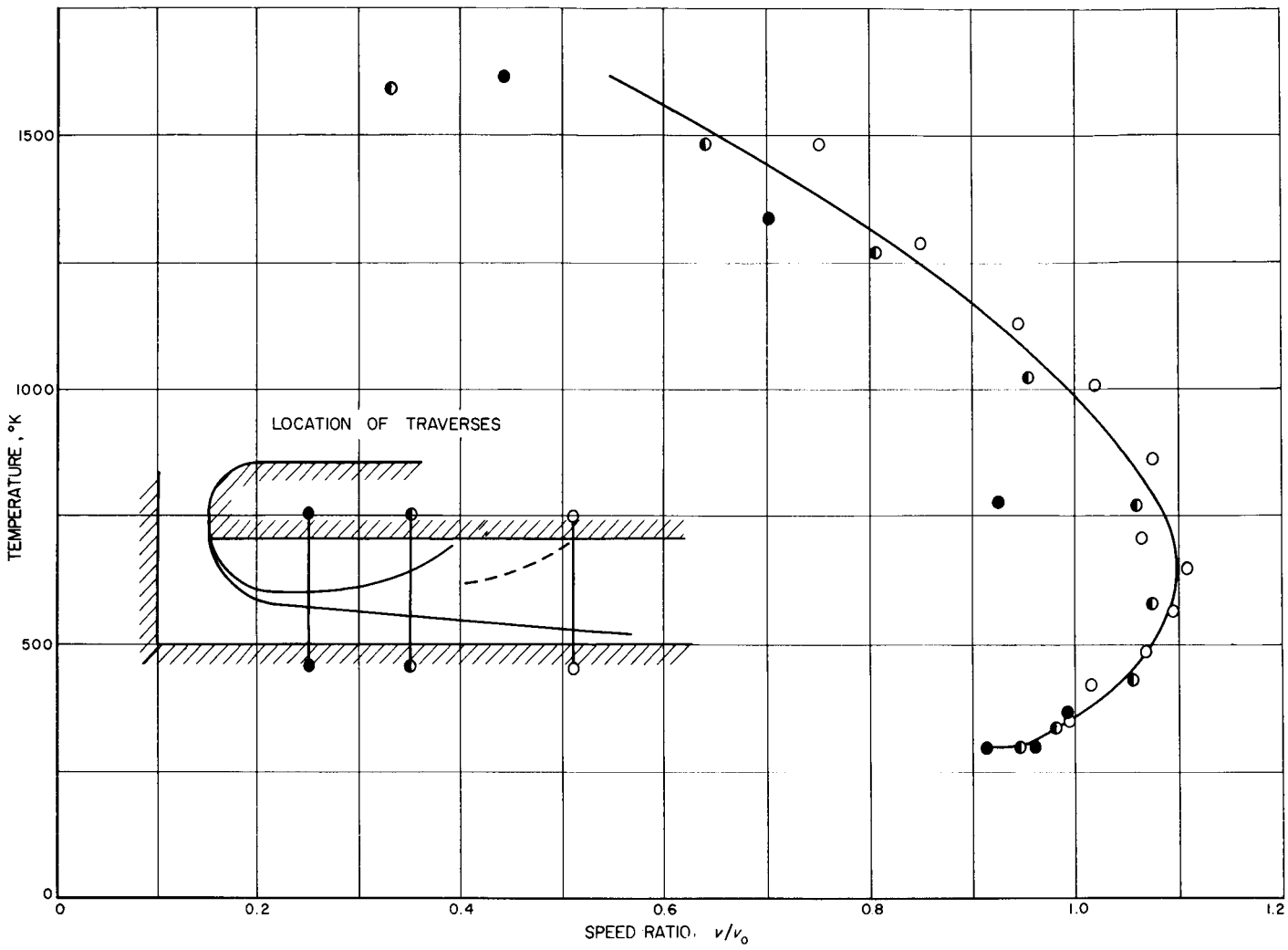

Fig. 34. Temperature vs Velocity Distributions at Several Locations in Combustion Chamber (½ × 1 × 6) B Operating Close to the Lean Limit and at Jet Speed Ratio $v_0/v_{0\,max} = 0.5$

speed regardless of absolute speed and location. It should be emphasized that this result is only valid for flows near the blowoff limits.

Under such circumstances, it is not surprising that the characteristic time τ_0 constitutes a useful stability parameter. Clearly, the actual residence time along a certain streamline in the mixing zone will be proportional to τ_0. Furthermore, the proportionality constant will remain the same for all flows near the stability limits.

It is likely that the similarities found in the flow field of the present burner will also appear in a geometrically similar burner of another size. If so, then the residence time in the mixing zone will again be proportional to τ_0 for the burner in question. This explains the correlation of the stability limits by τ_0 obtained for the burner family $(½ \times h \times 5h)$ A, as illustrated by Fig. 24.

The discussion has thus far been restricted to a flow field in which the mixing zone is covered by a flow of fresh mixture along the complete length of the recirculation zone. Even though only the burner with slot ratio ½ has been investigated, it is reasonable to assume that the burners with larger slot ratio will behave in an identical manner. For smaller slot ratios, however, the flow in the mixing zone will presumably be affected by the burner geometry. This case will be considered next.

Slot ratios $\delta/h = ¼, ⅛, 1/16$: The effect of the burner geometry on the flow in the mixing zone is best illustrated by the $T(v/v_0)$ profiles. Figure 38 shows these profiles at the end of the recirculation zone for all the slot ratios investigated. Each curve is based on traverses taken at an intermediate speed and mixture ratio, and again, the data are obtained at the blowoff limit.

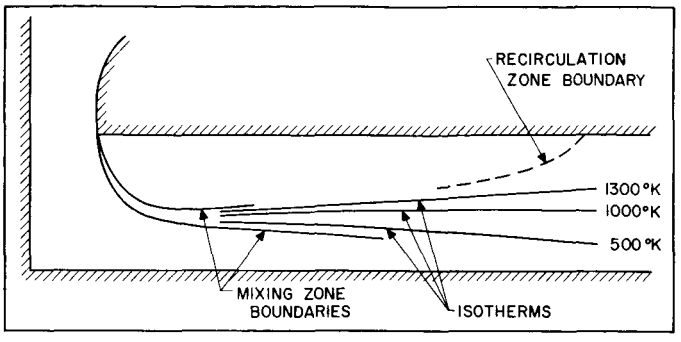

Fig. 35. Location of Isotherms for 500, 1000, and 1300°K in Combustion Chamber (½ × 1 × 6) B Operating Close to the Lean Limit and at Jet Speed Ratio $v_0/v_{0\,max} = 0.5$

The over-all trend exhibited in Fig. 38 gives indeed a confirmation of the repeatedly discussed interaction between the mixing zone and the bottom boundary of the burner. The smaller the slot ratio, the less the relative speed in the mixing zone. For example, Fig. 38 shows that for slot ratio ½ an element at 1000°K travels with almost exactly the same speed as the jet of fresh mixture. The weak interaction present at a slot ratio of ¼ reduces the relative speed of the same element to about 80% of the jet speed. Slot ratio ⅛ leads to a further reduction of the speed to about half of the jet speed; and finally, at slot ratio 1/16, the 1000°K element moves with a relative speed of only about 35% at the end of the recirculation zone.

The situation in the mixing layer at the middle of the recirculation zone is about the same as that at the end of the zone (see Fig. 39). The smallest slot ratio shows higher relative speeds at low and intermediate temperatures, indicating a stronger influence of the initial speed of the jet.

It is clear that if a traverse were taken even farther upstream, relatively close to the entrance of the jet, the relative speeds in the mixing zone would be about the same, independent of the slot ratio. Because of the extremely strong velocity and temperature gradients in this region, no attempt was made to actually measure the corresponding profiles.

This discussion demonstrates that the similarity in $T\,(v/v_0)$ found at slot ratio ½ for different locations along the mixing zone will no longer be present at small slot ratios. Thus for small slot ratios the similarity in $T\,(v/v_0)$ between different locations has been lost. Another type of similarity, however, may still be present for the small slot ratios. It will be recalled that slot ratio ½ showed similarity in $T\,(v/v_0)$ at blowoff for different speeds at the same location. The limited data available for the smaller slot ratios indicate that $T\,(v/v_0)$ at a given location is also fairly independent of the jet speed close to blowoff. A further indication in this direction is given by the satisfactory correlation of the stability limits obtained within the small slot ratio families by using τ_0 as was shown in Figs. 25 and 26.

C. Correlation of Stability Limits

An attempt at correlation of the stability limits shown in Fig. 31 is now made by considering the residence time in the mixing zone. This presents a problem as to what path to use for the determination of the time. The streamlines through the zone are not known. Even if they were, it is not very clear which part of the flow is the most significant one for the stability of the flame.

On the other hand, the measurements made yield the locations of the isotherms in the flow field, as was demonstrated in Fig. 35. In order to evaluate the effects of the residence time in different regions of the flow, it was decided to determine this time along three separate isotherms. The isotherms for 500, 1000 and 1300°K were chosen. The data above 1300°K are not sufficiently accurate to justify a study of higher temperature isotherms.

The isothermal residence time $\tau\,(T°\mathrm{K})$ was determined by graphical integration of the expression

$$\tau\,(T°\mathrm{K}) = \int_0^{\tau} \frac{ds}{v\,(T°\mathrm{K})}$$

where ds is a line element of the isotherm $T°$K, and $v\,(T°\mathrm{K})$ is the corresponding local speed. The integration range extends from the origin of the isotherm at the edge of the slot to the end of the recirculation zone.

The integrand is known from the traverses through the end and the middle of the recirculation zone. Because no experimental data were obtained to describe the initial state of the flow in the mixing zone at the edge of the slot, the reference speed was used as the initial speed for each isotherm. The isothermal speeds at this point are probably the same fraction of the reference speed independent of slot ratio. It is reasonable to assume that the spatial similarity in $T\,(v/v_0)$, valid for slot ratio ½ as shown by Fig. 34, holds up to a point close to the edge of the slot. Figure 34 indicates that the isotherms considered in

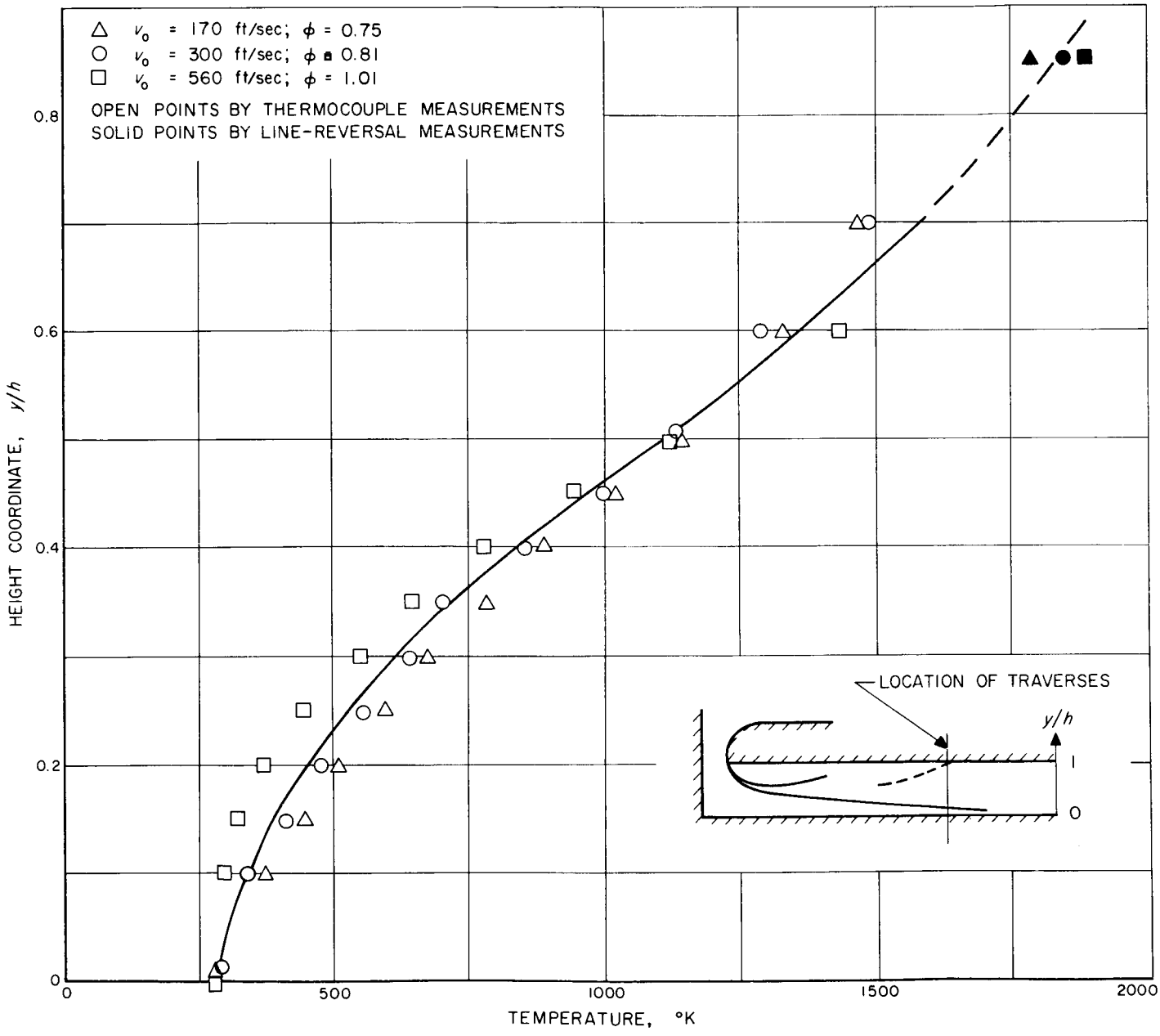

Fig. 36. Temperature Distributions at the End of the Recirculation Zone in Combustion Chamber (½ × 1 × 6) B Operating Close to the Lean Limit and at Several Jet Speeds

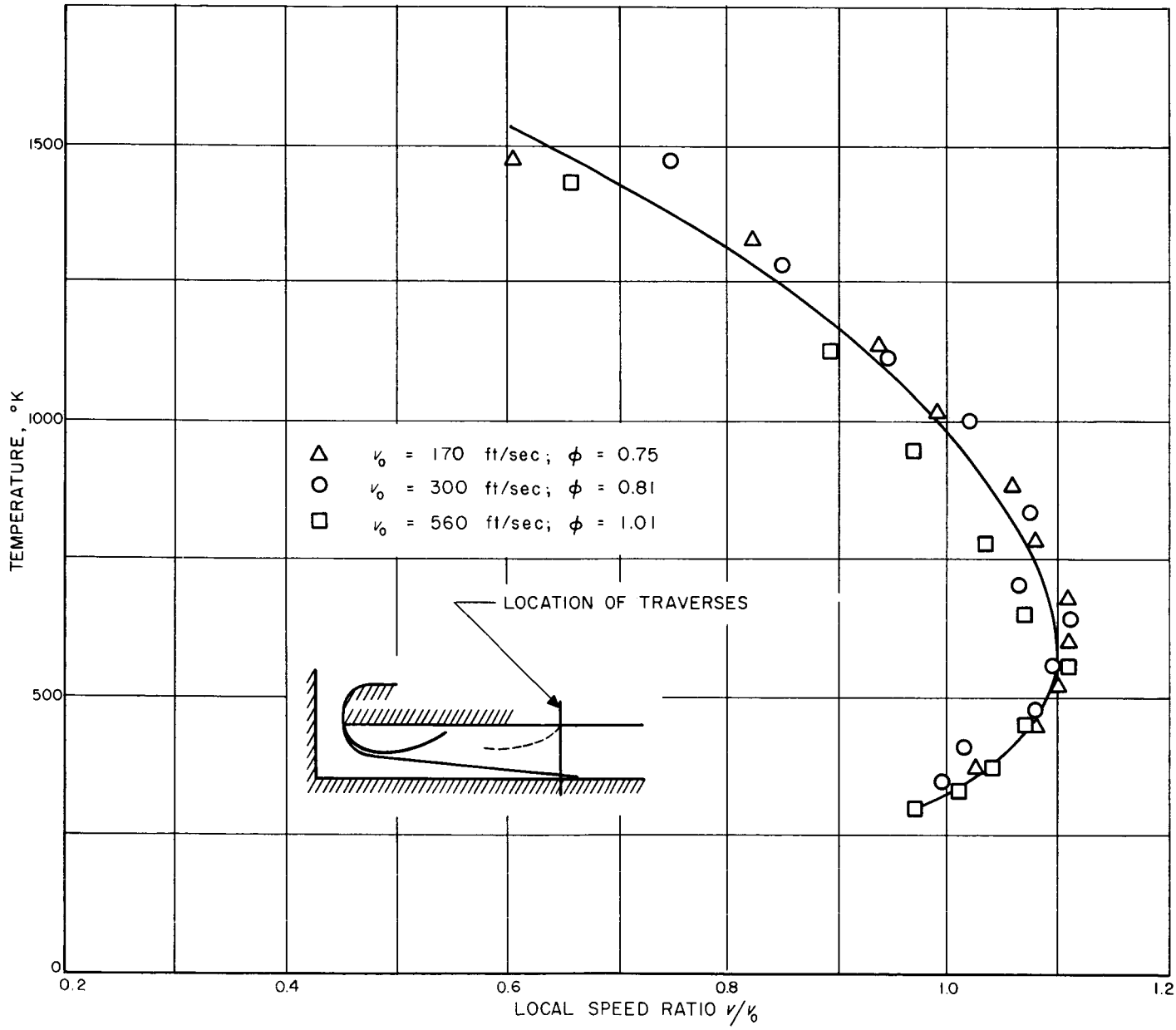

Fig. 37. Temperature vs Velocity Distributions at the End of the Recirculation Zone in Combustion Chamber (½ × 1 × 6) B Operating Close to the Lean Limit and at Several Jet Speeds

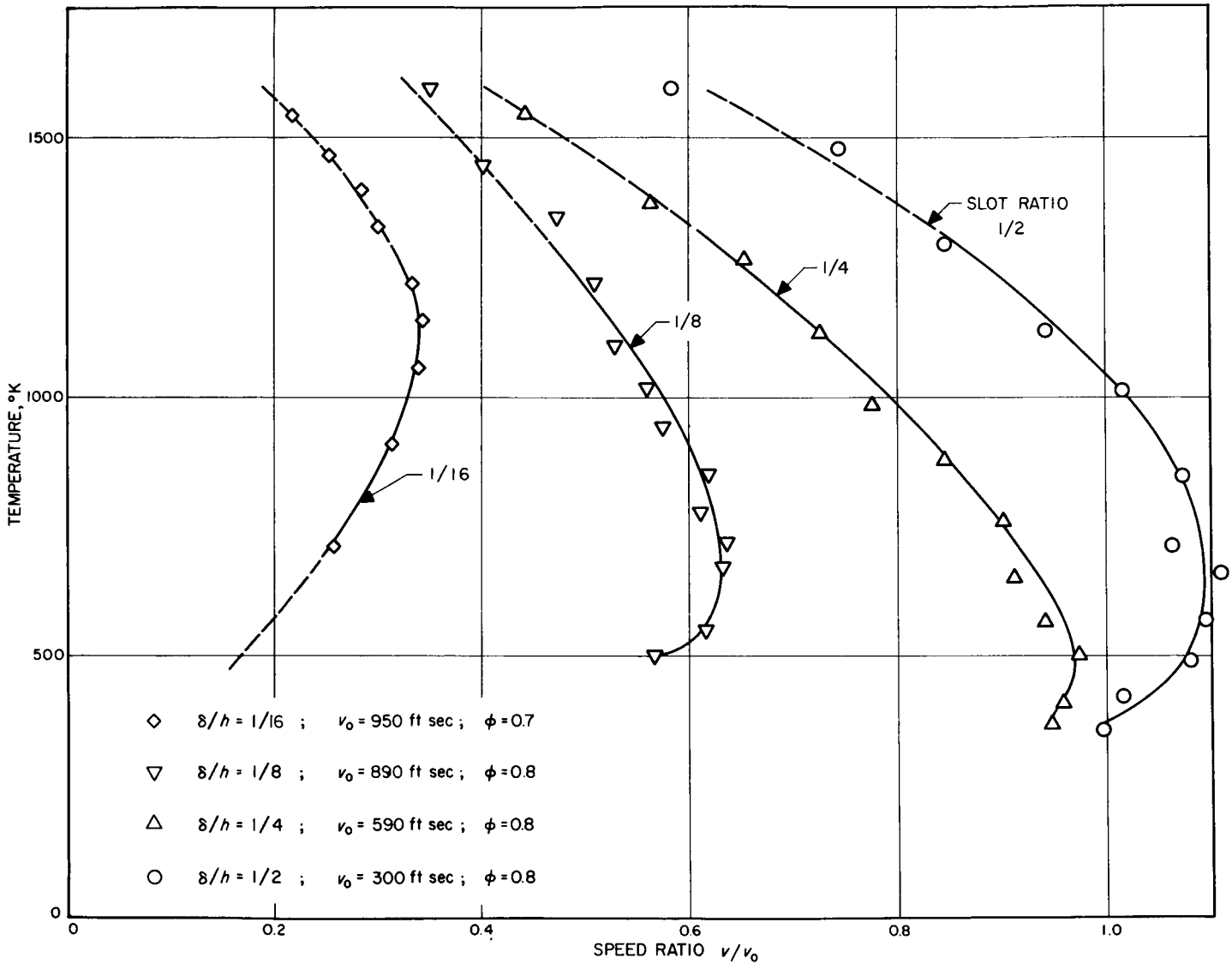

Fig. 38. Temperature vs Velocity Distributions in the Mixing Zone at the End of the Recirculation Zone for Various Slot Ratios in Combustion Chamber (δ × 1 × 6) B Operating Close to the Lean Limit

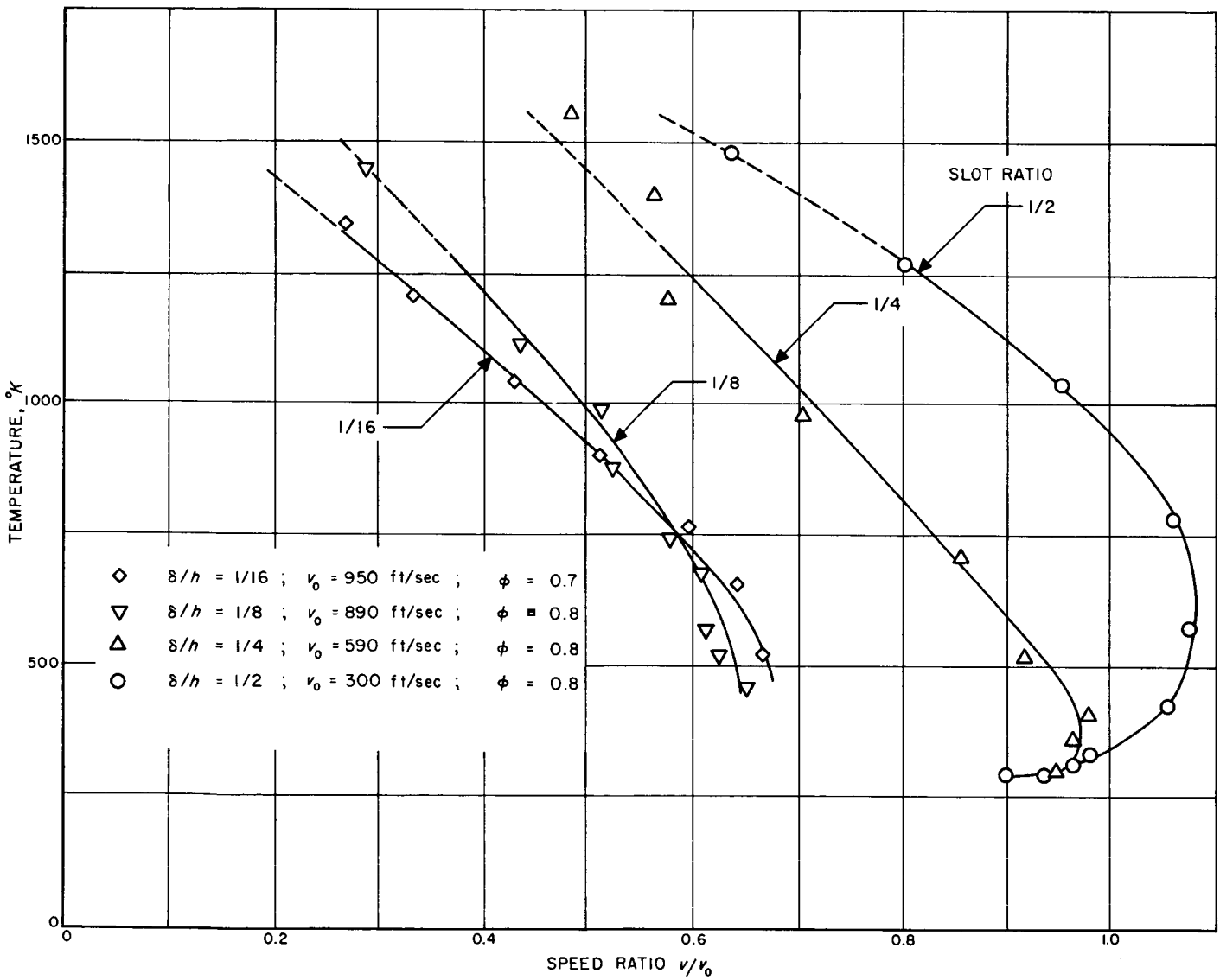

Fig. 39. Temperature vs Velocity Distributions in the Mixing Zone at the Middle of the Recirculation Zone for Various Slot Ratios in Combustion Chamber (δ × 1 × 6) B Operating Close to the Lean Limit

the present case have speeds fairly close to the reference speed. As the same approximation of the initial isothermal speed is made for all slot ratios, the error introduced will be negligible in comparisons between the burners of different geometry.

The results of the computation of the isothermal residence times are summarized in Table 1. At slot ratio ½, the isothermal time $\tau(T°K)$ is 5, 12, and 25% longer than the characteristic time τ_0 at 500, 1000, and 1300°K, respectively. The ratio $\tau(T°K)/\tau_0$ increases steadily as the slot ratio is reduced. At slot ratio 1/16, the isothermal times are 2–3 times longer than the characteristic time.

Table 1. Isothermal Residence Times for Various Slot Ratios in Combustion Chamber (δ × 1 × 6)B Operating Close to the Lean Limit

Slot Ratio	Characteristic Time τ_0 millisec	Isothermal Residence Time Ratio $\tau(T°K)/\tau_0$		
		500°K	1000°K	1300°K
½	1.01	1.05	1.12	1.25
¼	0.64	1.16	1.44	1.77
⅛	0.505	1.52	1.94	2.62
1/16	0.54	2.22	2.26	3.13

Up to the present point, the isothermal residence times have been determined at only one state of operation close to the lean limit for each burner. The following approach will be used for transforming the complete stability limits in Fig. 31 from the characteristic time τ_0 to the isothermal times $\tau(T°K)$.

It has been shown that the distributions $T(v/v_0)$ at blowoff are independent of speed. Consequently, the ratio $\tau(T°K)/\tau_0$ will be constant all along the stability limits as long as the recirculation zone length l^* remains unchanged. Relatively small variations in l^* are encountered in the present burners. Hence it is legitimate to transform the complete stability limits of a burner from τ_0 to $\tau(T°K)$ by multiplying the ordinate of the diagram in Fig. 31 by a constant factor $\tau(T°K)/\tau_0$, even though this factor has been determined at only one point of operation for each burner.

The resulting stability limits in terms of the isothermal residence times are presented in Figs. 40, 41, and 42 for 500, 1000, and 1300°K, respectively. The times based on the two latter temperatures give a remarkably good correlation of the limits as illustrated by Figs. 41 and 42. For 500°K, as shown in Fig. 43, there are certain deviations between the different burners and the trend is the same as for the limits based on τ_0 in Fig. 31. Even so, the correlation in Fig. 40 is considerably better than that in Fig. 31.

Actually, the streamlines in the mixing zone cross over the isotherms. This means that a certain element of gas entering the mixing zone close to the edge of the slot will first pass over the 500°K isotherm. Some distance farther downstream, it will reach 1000°K, and finally, at a somewhat later point, 1300°K. The actual residence time of this element in the mixing zone will consequently have a value somewhere in between the values of the time along the three different isotherms.

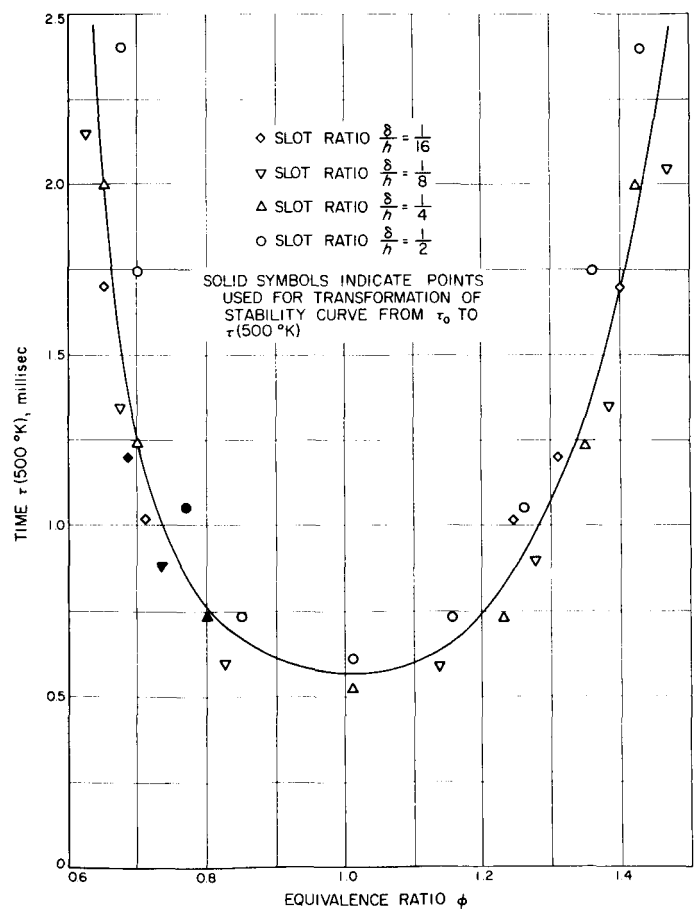

Fig. 40. Stability Limits Expressed in Terms of τ (500°K) for Various Slot Ratios in Combustion Chamber (δ × 1 × 6)B

Now consider another element of mixture entering the mixing zone at a somewhat later stage. This element may not reach a final temperature of 1000°K before the end of the recirculation zone. The residence time for this second element will then have a value closer to τ (500°K).

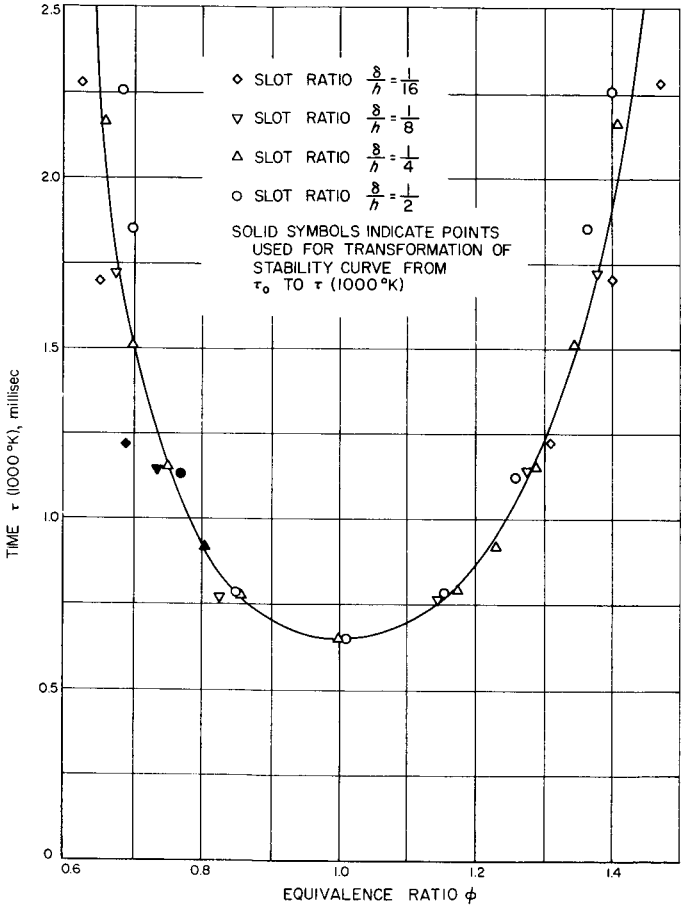

Fig. 41. Stability Limits Expressed in Terms of τ (1000°K) for Various Slot Ratios in Combustion Chamber (δ × 1 × 6) B

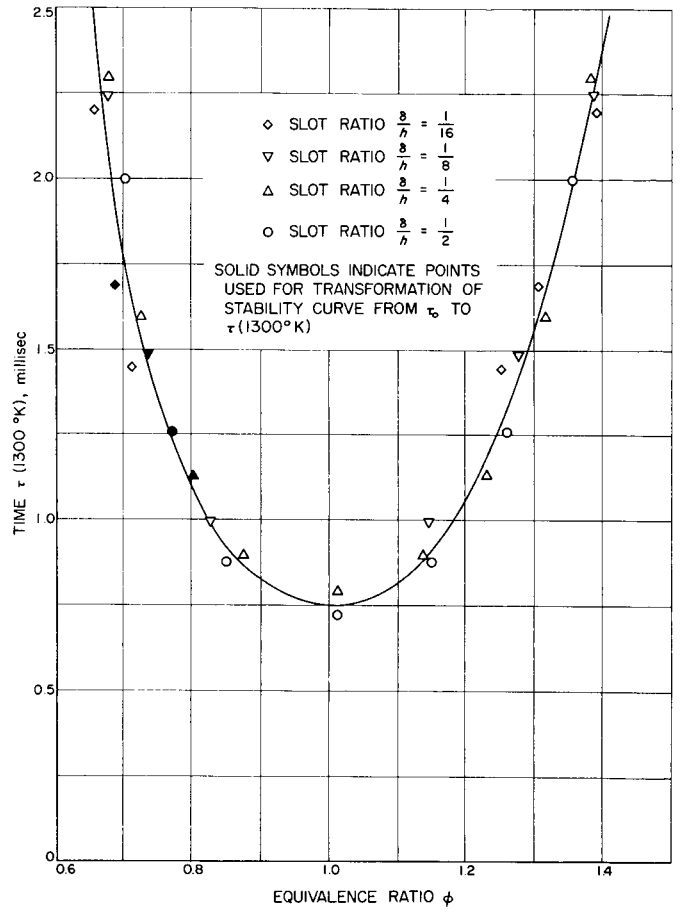

Fig. 42. Stability Limits Expressed in Terms of τ (1300°K) for Various Slot Ratios in Combustion Chamber (δ × 1 × 6) B

Judging from the degree of correlation obtained by the different isothermal times, it appears as though the first element considered above is the more significant one for the stability of the flame. Thus the results of the present investigation indicate that the inner part of the mixing zone is the important region of the flow field insofar as the flame stabilization process is concerned.

D. Summary

The discrepancies in the stability limits based on the characteristic time τ_0, which were observed when burner families of different geometry were compared in Section IV, have been explained by use of the residence time concept. Thus the present experiments with burners of varying geometry have clearly demonstrated that the residence time in the mixing zone is the proper correlation parameter for the stability limits. This parameter is not affected by the great variation the flow field encountered when the slot ratio was changed over a wide range. The experiment also has shown that the most satisfactory correlation is obtained by use of a residence time for the material in the inner part of the mixing zone.

In a burner with a slot ratio sufficiently large to prevent the mixing zone from reaching the bottom wall before the end of the recirculation zone, a great deal of similarity was observed in the flows close to the blowoff limit. This indicates that the residence time in the mixing zone is directly proportional to the characteristic time τ_0.

On the other hand, for small slot ratio burners in which all of the fresh mixture enters the mixing zone before the end of the recirculation zone, the same similarity is no longer present; hence τ_0 cannot be used as a comparative measure of the important parameter, the residence time. For flows of this type, the actual residence time has to be determined.

Finally, then, a stability parameter has been established which is completely independent of the flow parameters, and determined by the chemical parameters only.

The preceding sections have demonstrated the effects of the flow parameters on the flame stabilization process. The following section illustrates the influence of some of the chemical parameters.

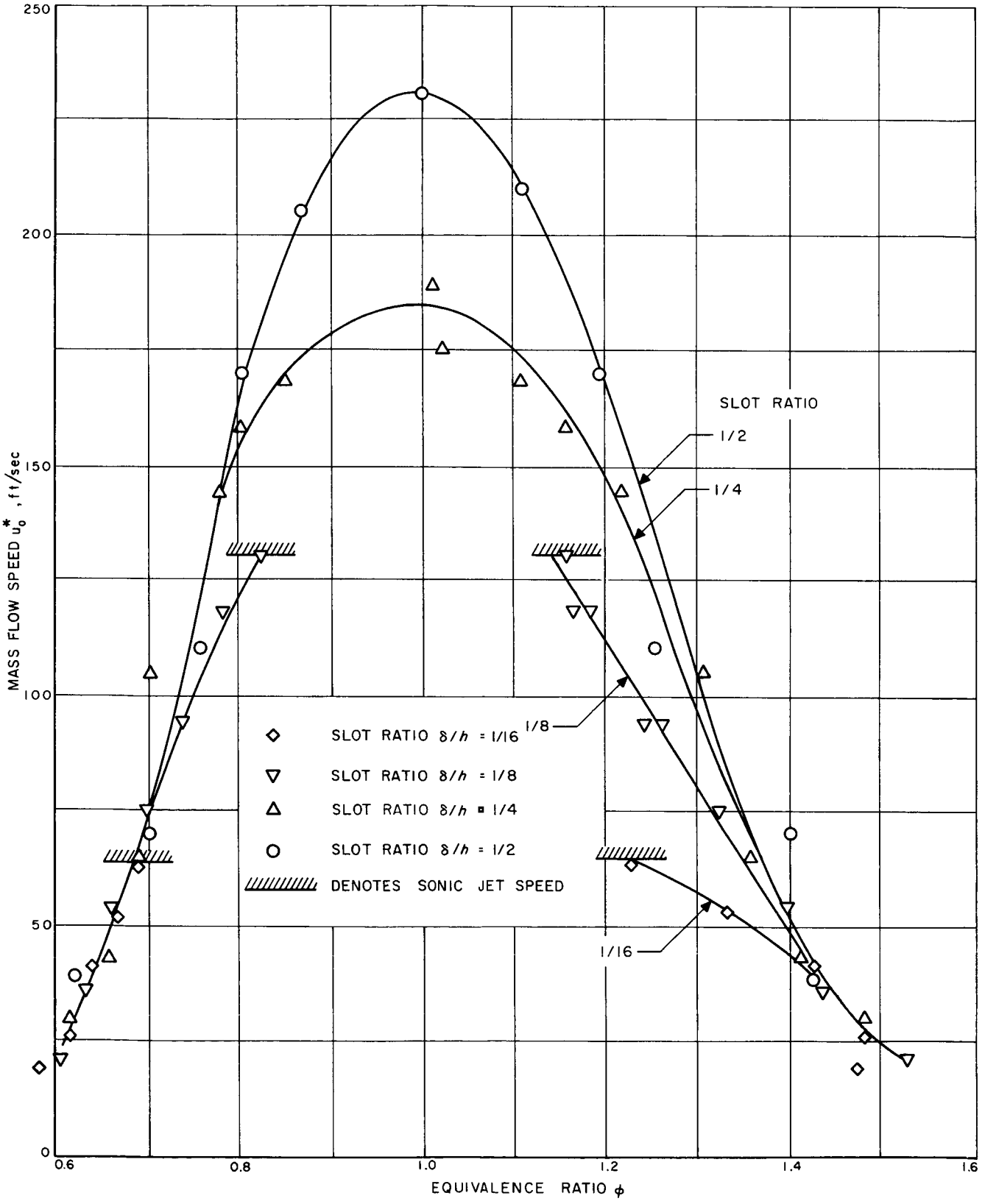

Fig. 43. Stability Limits Expressed in Terms of Mass Flow Speed u_0^* for Various Slot Ratios in Combustion Chamber (δ × 1 × 6) B

VI. TEMPERATURE EFFECTS ON STABILITY

The effects on the stability of changes in some of the chemical parameters such as mixture temperature at the inlet and in the recirculation zone are briefly considered in the following section.

The influence of the inlet temperature on the stability limits in one combustion chamber is studied. The previously presented data from the cooled and insulated burners will be analyzed to determine the effect of the recirculation zone temperature.

A. Influence of Inlet Temperature

The smallest of the burners in family ($\frac{1}{2}h \times h \times 5h$) A was chosen for the inlet temperature experiment. This combustion chamber, ($\frac{1}{4} \times \frac{1}{2} \times 2\frac{1}{2}$) A, blows off at a maximum speed of about 500 ft/sec at normal inlet temperature, $T_0 = 290°K$. Hence the burner has a considerable margin before sonic speed is reached in the jet. It is important to be able to reach maximum speed at stoichiometric mixture ratio, since it was decided to use the minimum time τ_0 for purposes of comparison.

The burner has a slot ratio sufficiently large to eliminate any interference between the mixing zone and the bottom boundary. Consequently, the parameter τ_0 is representative of the actual residence time in the mixing zone. Furthermore, the burner chosen is thermally insulated; thus it is possible to estimate the recirculation zone temperature without making further temperature measurements.

Tests were made at two elevated inlet temperatures, $T_0 = 420°K$ and $495°K$, and the blowoff experiments were performed in accordance with the standard procedure. The recirculation zone temperature, however, was not measured in this experiment.

The influence of the inlet temperature on the stability limits, expressed in terms of T_0, is demonstrated by Fig. 44. At a standard inlet temperature of 290°K, the burner reaches a minimum time of 0.35 millisec. As shown by Fig. 44, the increases in inlet temperature to 420 and 590°K reduce the minimum time to 0.20 and 0.145 millisec, respectively. Thus it is clear that the characteristic time is very sensitive to a change of the inlet temperature. Although the three curves of Fig. 44 are not exactly similar, the variation of the stoichiometric minimum point is typical of the behavior at other fuel–air ratios.

In Fig. 45, the logarithm of the minimum time has been plotted vs the inverse of the inlet temperature. The three points available indicate a linear relationship in the semilogarithmic diagram. It is interesting to notice that the corresponding curve obtained for a bluff body flameholder with a gasoline-like fuel is almost identical to that presented in Fig. 45. This is a further indication of the similarity of the two processes of flame stabilization.

B. Influence of Recirculation Zone Temperature

The earlier experiments with the cooled and insulated combustion chambers yield values of the minimum time τ_0 for the corresponding temperature levels of the recirculation zone. Again, only burners without mixing zone interference with the bottom boundary will be considered.

Figure 31 indicates that the water-cooled group ($\delta \times 1 \times 6$) B has τ_0 min = 0.58 millisec. The temperature distribution in the recirculation zone is presented in Figs. 29 and 30. The arithmetic average between the temperatures measured at the upstream and downstream ends of the recirculation zone was chosen as the reference temperature level of the zone. A value of 1780°K was found for this case.

The insulated burners of family ($\frac{1}{2}h \times h \times 5h$) A reach a minimum time of 0.35 millisec at standard inlet temperature, according to Fig. 24. For this family, the average recirculation zone temperature was 1925°K. In the case of the elevated inlet temperatures in the same burner, the corresponding recirculation zone temperatures have been calculated by assuming the same temperature ratio for the zone as measured at standard inlet temperature.

The relation between the minimum time and the reference temperature of the recirculation zone is plotted in Fig. 46. It is evident that the characteristic time is strongly influenced also by the recirculation zone temperature. A semilogarithmic diagram has been used to facilitate the estimate of the activation energy of the process. Assuming that the minimum chemical time is inversely proportional to the Arrhenius factor,

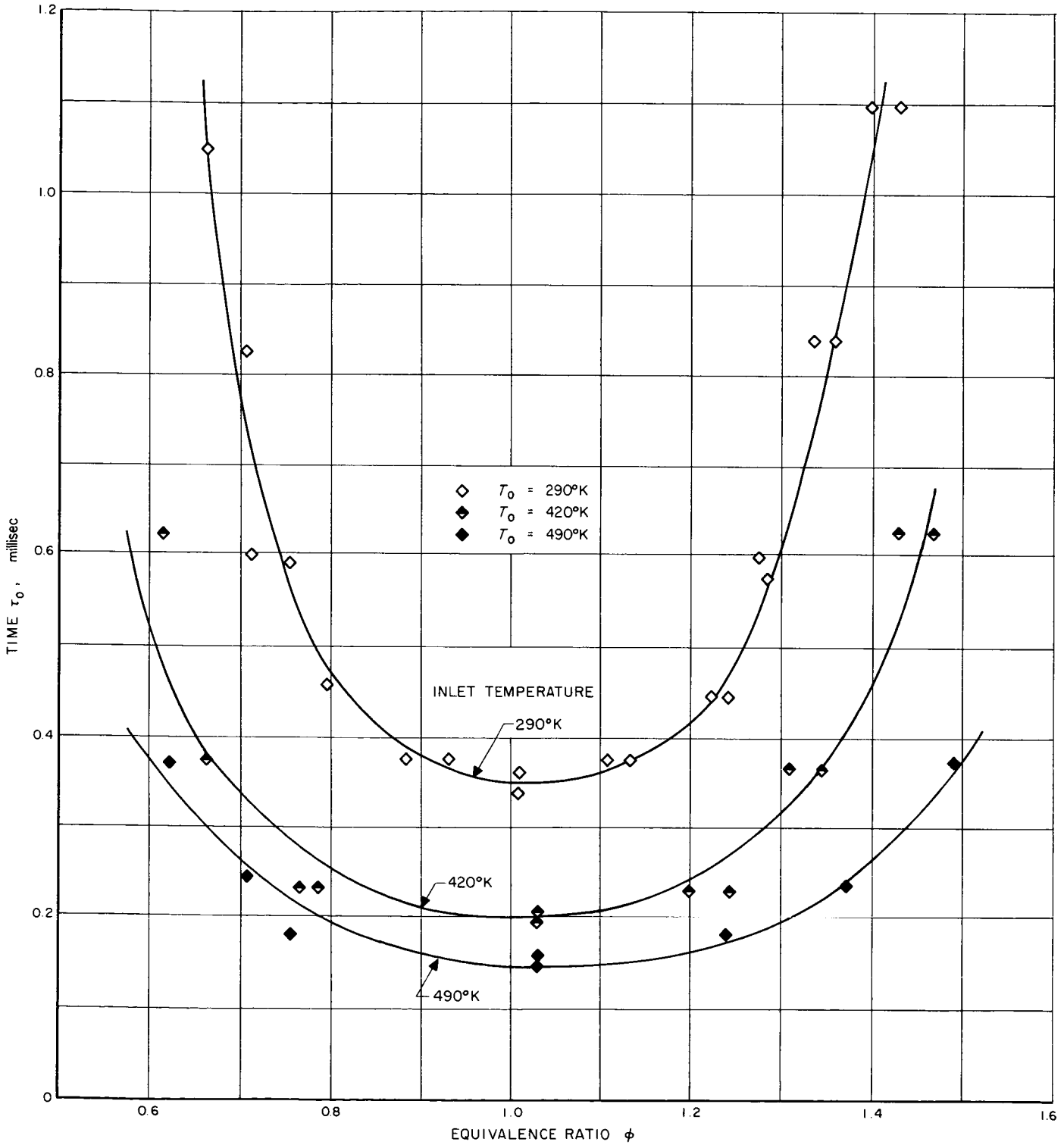

Fig. 44. Effect of Inlet Temperature on Stability Limits of Combustion Chamber (¼ × ½ × 2½) A

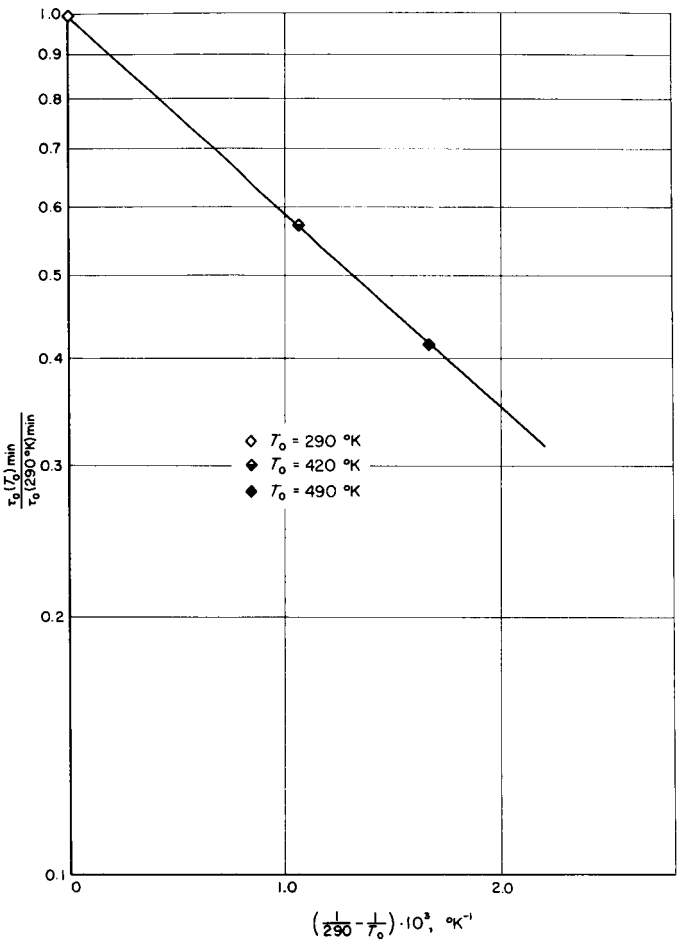

Fig. 45. Effect of Inlet Temperature on $\tau_{0\,min}$ for Combustion Chamber (¼ × ½ × 2½) A

$$\tau_{0}\,\text{min} \sim \exp(E/RT)$$

where E is the activation energy of the process and T the temperature of the reaction zone. In the present case, the reference temperature of the recirculation zone presumably controls the temperature of the mixing zone. Therefore, the former temperature will be used for T in the expression above.

If this approach is correct, the data of Fig. 46 should yield a straight line with the slope (E/R). In Fig. 46, a straight line based on the two points obtained by the measured temperature levels of the recirculation zone has a slope corresponding to an activation energy of 24 kcal/mole.

The computed recirculation zone temperatures for the inlet temperature experiment do not fit this line in a very satisfactory way. A line from the cooled burner point to the computed points indicates an activation energy of about 35 kcal/mole.

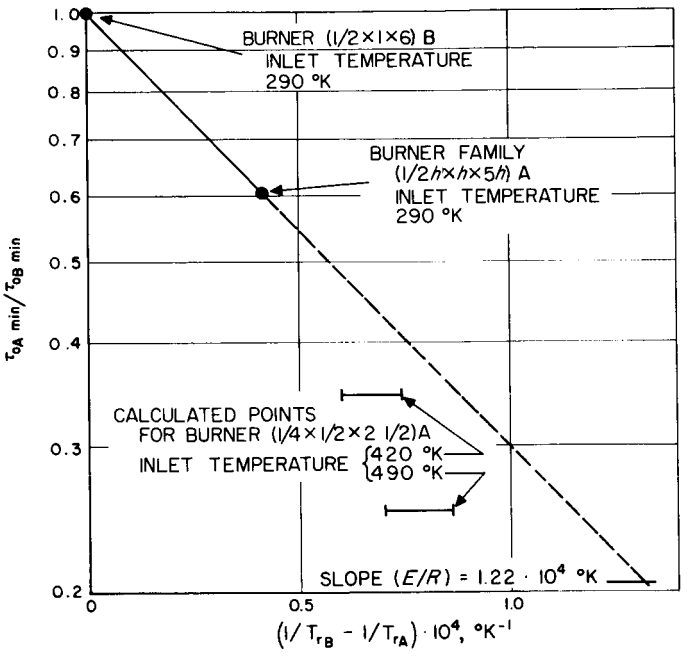

Fig. 46. Effect of Recirculation Zone Temperature on $\tau_{0\,min}$

The first value of the activation energy based on the measured recirculation zone temperatures agrees closely with a tabulated value of 26 kcal/mole in Ref. 13. However, the important result of this experiment is not a determination of an activation energy based on the tenuous arguments stated previously; rather it is that the stability parameter is very strongly affected by the inlet as well as the recirculation zone temperature.

VII. COMPARISON WITH BLUFF BODY FLAMEHOLDER AND CAN-TYPE COMBUSTION CHAMBER

The present burner gives a good illustration of some of the characteristics of other types of combustors. At large slot ratios, the burner exhibits a great deal of similarity with the bluff body flameholder. For small slot ratios, on the other hand, the slot burner has some features in common with the can-type combustion chamber.

A. Comparison with Bluff Body Flameholder

For slot ratios equal to or larger than ½, the mixing zone is free from contact with the bottom boundary. The resulting flow field is similar to that of the bluff body in the sense that all of the mixing zone is covered by a flow of cold mixture in both cases. The flow field for large slot ratios can be considered as approximately corresponding to the lower half of the flow field obtained behind a flat plate. The top wall introduced along the plane of symmetry represents a new boundary condition which will primarily affect the heat transfer from the wake. Because the wake is a relatively stagnant region in both cases, the rest of the flow picture will not be strongly affected by the presence of the new boundary.

The experimental results also indicate a great deal of similarity in the behavior of the two systems. For example, the blowoff occurs with a transition from a propagating to a residual flame in both cases. Also, the temperature levels of the recirculation zone show the same independence of speed. Finally, the characteristic time, based on the length of the recirculation zone and the speed in the cold flow past the wake, gives a good correlation of the stability limits for both systems.

No complete stability curve for propane at the present inlet conditions is available for the bluff body flameholder. Reference 14 presents two extrapolated values, 0.28 and 0.35 millisec, for the minimum characteristic time obtained with cylindrical flameholders working with propane–air mixtures at the same inlet conditions as in the present case. Figure 24 indicates a minimum time of 0.35 millisec for the insulated burners in good agreement with the bluff body values above. Actually, the heat transfer from the recirculation zone is larger in the present case than for the bluff body flameholder. Hence a slightly longer characteristic time would be expected for the slot burner.

The features in common between the flame stabilization process in the bluff body flameholder and in the present combustor suggest that the characteristic time concept can be extended to any combustor system exhibiting a free mixing zone. An example of such a system is presented in Ref. 15. A flame is stabilized in a duct by means of a recess in the wall. A wake is created in the recess and a free mixing zone develops along the boundary of the wake. Some qualitative trends supporting the view presented above can be observed in Ref. 15. However, the data of this reference are not complete enough to permit a quantitative comparison with the present results.

B. Comparison with Can-Type Combustion Chamber

In burners with slot ratios less than ½, the mixing zone reaches the bottom boundary before the end of the recirculation zone. The resulting flow field with a confined mixing zone requires knowledge of the actual residence time in the zone for the correlation of stability.

The small slot ratio burner shows several interesting similarities with the can-type combustion chamber. The primary similarity lies in the structure of the mixing zone, since there is good reason to believe that the mixing zone in the can burner also is covered by a flow of fresh mixture for only a short distance.

The impression obtained from the present slot-type burner suggests a flow field of the character shown by Fig. 47 for the can burner. The lower part of Fig. 47 illustrates the general flow pattern by two typical streamlines. This pattern, which was also indicated in Fig. 1, is in agreement with observations made by Way (Ref. 7) and by other investigators.

The upper cross section of the can burner in Fig. 47 shows the possible structure of the flow field. The jets of fresh mixture entering through the inlet holes meet at the central part of the burner. A stagnation point is located on the centerline in a perfectly symmetrical system. The flow of fresh mixture is divided into two streams about the stagnation point. A portion somewhat larger than half of the flow is deflected toward the exit of the

burner. The rest of the fresh mixture forms a similar axial jet in the opposite direction toward the upstream closed end of the burner.

Mixing zones are created along the boundary between the cold, fast-moving jets of fresh mixture and the hot, slower-moving material inside the burner. Judging from the spreading rates of the mixing zones in the slot-type combustor, all of the fresh mixture in the axial core, directed upstream, enters the mixing zone before or at the same time as the flow reaches the closed end of the can. From this point on, the mixing zone is in contact with the burner wall, hence, the notation "confined mixing zone" in Fig. 47.

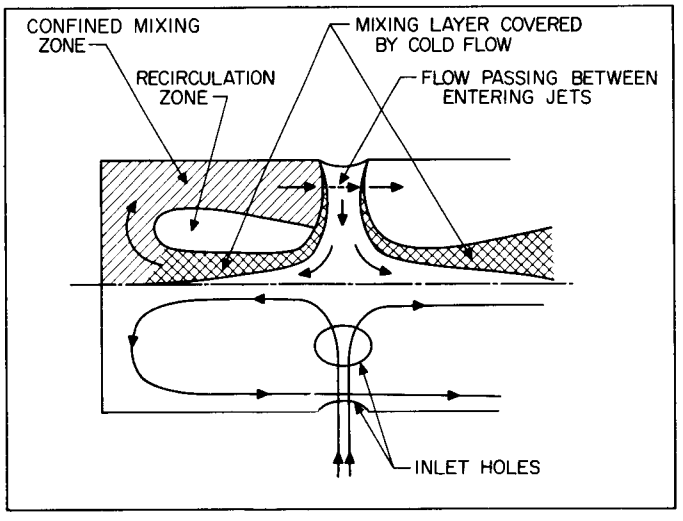

Fig. 47. Schematic Flow Diagram for a Cylindrical Can-Type Combustion Chamber

Because of the closed end, the flow turns and passes along the cylindrical walls toward the ports formed between the entering jets. A toroidal recirculation zone is enclosed by the mixing zone. The complete upstream closed-end region of the can is often referred to as the recirculation zone. As indicated by Fig. 47, only a limited part of this region constitutes a recirculation zone in the sense used for the slot-type burner.

The flow picture presented thus far has shown the presence of a mixing zone of the same general character as that found at small slot ratios in the slot-type burner. The two systems also show similarity in the processes taking place in the mixing zone at the end of the recirculation zone.

It is reasonable to assume that, in the slot burner, blowoff of the propagating flame occurs by convective heat transfer from an element of gas in the mixing zone. The situation in the can burner may be quite similar. Blowoff could conceivably be caused by the same type of quenching of the reaction in the mixing zone at the same point. When this occurs, no more hot material is available for the ignition of the entering jets. Hence the flame blows off.

If it is assumed that both processes require about the same state of the flow in the mixing zone for stability, then the flame stabilization process in the can burner will basically be governed by the same ignition delay time as that of the slot burner, and, hence, as that of the bluff body flameholder.

Available experimental data support this point of view. The can burner experiments by Weiss and Longwell (Ref. 6) demonstrate that the proper parameter for correlation of stability has the form D/u_0^*, where D is the can diameter, and u_0^* is a reference velocity based on mass flow. The latter parameter is defined by the expression

$$u_0^* = \frac{m_0}{\rho_0 A}$$

where m_0 is the rate of mass flow entering the first stage of inlet holes, ρ_0 is the density of the fresh mixture at inlet temperature and recirculation pressure, and A is the cross-sectional area of the burner.

It is very interesting to notice that the mass flow and not the jet speed enters the correlation parameter for stability. This observation can easily be explained in terms of the ignition delay time parameter suggested above. In a mixing zone covered only a short distance by a layer of fast-moving fresh mixture, the speeds in the initial part of the zone are determined by the speed of the fresh mixture along the boundary of the zone, while on the other hand, the speeds in the downstream part of the zone, which is in direct contact with the burner wall, are primarily determined by the rate of mass flow.

The time spent in the downstream part of the mixing zone is considerably longer than that spent in the upstream part owing to the reduced speeds in the former region. Consequently, the residence time in the mixing zone would be expected to be primarily determined by the rate of mass flow and the can size, which is indicative of the

length of the zone. This corresponds exactly to the parameter D/u_0^* found by Weiss and Longwell.

The experimental data provide an even more detailed elucidation of this point. For a given recirculation zone, length, and constant mass flow rate, the residence time should be somewhat reduced as the jet speed is increased for burner geometries with smaller inlet holes or slot areas. Hence, at a constant rate of mass flow, the stable region should actually be slightly reduced as the jet speed is increased.

The results presented in Ref. 6 give an excellent confirmation of this assumption. Even though Weiss and Longwell based their correlation parameter on the mass flow, the data of Fig. 8, taken from the same reference, demonstrate that there is indeed a slight influence of the jet speed as predicted.

In order to further illustrate the similarity between the can burner and the present slot burner, the stability limits for several slot ratios in the latter burner have been plotted as a function of the mass flow speed u_0^* in Fig. 43, which shows exactly the same trend as predicted by the residence time considerations above. For slot ratios less than ½, the mass flow parameter gives a reasonable correlation, particularly on the lean side. The secondary effect of the initial jet speed is clearly observable. Again it is found that for constant mass flow the limits converge slightly when the slot ratio is reduced, that is, when the jet speed is increased.

Because a stream of fresh mixture covers the mixing zone beyond the end of the recirculation zone at slot ratio ½, it is not surprising to find that the correlation based on the mass flow parameter is not very satisfactory any longer. At this geometry, the jet speed exclusively determines the residence time in the mixing zone.

The preceding discussion implies that the flame stabilization mechanism in the can burner may be the same as in the present slot burner. This would mean an even wider generalization of the ignition delay concept originally introduced by Zukoski and Marble for the bluff body flameholder. However, the process suggested for the can burner is essentially speculative; hence the picture has to be experimentally verified before any definite comparisons can be made with the other types of combustors.

VIII. CONCLUSIONS

The present investigation has demonstrated the manner in which the flame stabilization process in a deflected jet is affected by the flow parameters and the chemical parameters describing the system. The former parameters were varied over a wide range by changing first the size and, second, the geometry of the combustion chamber.

Two different types of flow fields were encountered during the experiments with burners of different geometry. The first type, exhibited by burners with large slot ratios, is characterized by a mixing zone covered by a flow of cold mixture along the complete length of the recirculation zone. In this case, the characteristic time introduced by Zukoski and Marble for the bluff body flameholder, was found to be a satisfactory correlation parameter for burners of different size and geometry. The flow in the mixing zone at blowoff conditions showed a high degree of similarity in temperature and relative speed profiles for different locations and absolute jet speeds. From this, it could be concluded that the residence time in the mixing zone is proportional to the characteristic time τ_0, and that the proportionality constant remains the same for burners of different size and geometry. Again, it should be emphasized that this conclusion only holds for burners with a mixing zone of the character described above and at blowoff conditions. A comparison between this type of flow and that of the bluff body flameholder revealed a high degree of similarity between the two systems.

A second type of flow field was found for slot ratios sufficiently small to make the entire amount of fresh mixture enter the mixing zone before the end of the recirculation zone. In this situation, part of the earlier-mentioned similarity in the flow field is lost; hence the characteristic time τ_0 is no longer representative of the residence time in the mixing zone of geometrically different burners. Therefore, the actual residence time along several isotherms in the mixing zone was determined. A satisfactory correlation of the stability limits for burners of a different geometry was obtained by using the isothermal residence times in the higher temperature range. It was also possible to correlate the small slot ratio group of burners with the large slot ratio group by the same parameter. This implies that the material traveling in the inner regions of the mixing zone, close to the boundary of the recirculation zone, constitutes the most important part of the flow for the stability of the flame.

The present investigation also demonstrated that the stability parameter is exclusively determined by the chemical parameters. This followed from the fact that the minimum residence time required in the mixing zone did not depend on the flow parameters. The next step was to determine the influence of some of the chemical parameters on the time required for stability. The effects of inlet temperature and recirculation zone temperature were found to be in reasonable agreement with chemical kinetics considerations.

Finally, a study of the blowoff mechanism supported the picture presented above of the flame stabilization process. It was observed that the blowoff of the propagating flame always preceded the quenching of a residual flame in the recirculation zone. In some cases, a steady residual flame was left after the blowoff of the propagating flame.

Summing up the results of the investigation, the following impression of the flame stabilization process in the present burner is obtained.

Under normal operating conditions far from the blowoff limit, the chemical reaction occurring along the inner boundary of the mixing zone produces hot gas which continuously enters the recirculation zone. The hot material in the zone diffuses out through the same boundary into the mixing zone. The net flow of material crossing the recirculation zone boundary is zero at steady-state operation. The exchange of material across the boundary makes it possible to maintain a high temperature in the recirculation zone at the same time that it provides a means of convective heat transfer from this zone to the mixing zone. The hot material diffusing out through the inner regions of the mixing zone initiates and sustains the chemical reaction. Part of the hot gas produced by the reaction returns to the recirculation zone; part moves farther out in the mixing zone, where it, in its turn, starts the chemical reaction by a continued mixing process extending out to the edge of the zone. By this process, a flame is ignited in the flow downstream from the wake.

The state of the flow at the same equivalence ratio but at a considerably higher speed close to blowoff is now considered. Assuming that the turbulent mixing process does not change character, material from the wake is supplied at about the same temperature as before. Because the chemical parameters are unchanged, the reaction starts with about the same reaction rate. The residence time of the flow exposed to hot material from the recirculation zone is now very much reduced. Consequently, the amount of heat evolved by the chemical reaction will be considerably less at the end of the recirculation zone.

Finally, for a further increase of the speed, the reaction in a finite amount of gas at the end of the wake will eventually be quenched by exposure to a too-large mass of cooler gas. This critical event is likely to take place in the inner regions of the mixing zone. Since the reaction has been quenched at this point, there is no hot material available for the ignition of a flame downstream; hence, blowoff of the propagating flame occurs.

The results discussed above have shown that the ignition delay time is indeed the proper similarity parameter for the stability of the present combustor. This implies that the basic stabilization mechanism is a continuous ignition process as suggested by Zukoski and Marble for the bluff body flameholder.

Because of the similarity between the flow field in the bluff body flameholder and that in the present burner at large slot ratios, it is not surprising that the stability is governed by the same characteristic time in the two cases. The detailed study of the flow field has, however, clarified the relation between the actual residence time and the characteristic time, which so far has been the only measure available of the basic parameter, the residence time.

Another important result is the fact that the original concept applies also to the second type of flow field with a confined mixing zone, which is encountered at small slot ratios. The flow in this case is very different from the flow for large slot ratios. For a given set of chemical parameters, however, the requirements for the stability of the flame are the same for both types of flow. Hence the concept of a continuous ignition process as the basic mechanism has been successfully extended to the flame stabilization in the present model of a deflected jet. Furthermore, the similarities proposed and found between the small slot ratio burner and the can burner imply that this mechanism is active also in the can burner.

NOMENCLATURE

A	cross-sectional area of combustion chamber
d	diameter of cylindrical can-type combustion chamber
D	linear dimension
E	activation energy
h	combustion chamber height
l	combustion chamber length
l^*	recirculation zone length
P	pressure
P_{0_t}	total pressure at combustion chamber inlet
p_{ref}	static pressure in recirculation zone
R	gas constant
s	arc length
T	temperature
T_0	inlet temperature
T_f	adiabatic flame temperature
u_0	velocity past wake of bluff body flameholder
u_0^*	reference velocity from Ref. 6
v	velocity
v_0	reference velocity based on p_{0_t} and p_{ref}
x_s	coordinate parallel to bottom wall and measured from edge of slot
y_s	coordinate normal to bottom wall and measured from top wall
δ	slot width
ρ	density
τ	time
τ_c	characteristic time (l^*/u_0) for bluff body flameholder
τ_d	characteristic time (d/v_0)
τ_0	characteristic time (l^*/v_0)
$\tau\,(T°\mathrm{K})$	residence time along isotherm $T°$K
ϕ	equivalence ratio, fraction of stoichiometric fuel–air ratio

REFERENCES

1. Zukoski, E. E., and Marble, F. E., "Experiments Concerning the Mechanism of Flame Blowoff from Bluff Bodies," *Proceedings of the Gas Dynamics Symposium on Aerothermochemistry* (held at Evanston, Ill., August 22–24, 1955), pp. 205–210, Northwestern University Press.

2. Longwell, J. P., "Combustion Problems in Ramjets," *Fifth Symposium on Combustion*, pp. 48–56, Reinhold Publishing Company, New York, 1955.

3. Mullins, B. P., "A Spontaneous Ignition Theory of Combustion Intensity and Combustion Stability Behind a Baffle," AGARD, *Combustion Researches and Reviews, 1955*, Butterworths Scientific Publications, London, 1955.

4. De Zubay, E. A., "Characteristics of Disk-Controlled Flame," *Aero Digest*, 61, (No. 1), pp. 54–56, 1950.

5. Wright, F. H., "Bluff Body Flame Stabilization: Blockage Effects," Progress Report No. 20-327, Jet Propulsion Laboratory, Pasadena, California, June 3, 1958.

6. Weiss, M. A., and Longwell, J. P., "Low Pressure Performance of Cylindrical Can Burners," *Jet Propulsion*, 26, pp. 749–756, September, 1956.

7. Way, S., "Combustion in the Turbojet Engine," AGARD, *Selected Combustion Problems II*, Butterworths Scientific Publications, London, 1956.

8. Herbert, M. V., "A Theoretical Analysis of Reaction Rate Controlled Systems, Part II," Report No. R 196, National Gas Turbine Establishment (England), 1957.

9. "Flow Measurement by Means of Standardized Nozzles and Orifice Plates" (in Ch. 4, "Measurements of Quantity of Materials"), *Information on Instruments and Apparatus*, PTC 19.5.4—1940. American Society of Mechanical Engineers, New York, 1939.

10. Scadron, M. D., and Warshawsky, T., "Experimental Determination of Time Constants and Nusselt Numbers for Bare-Wire Thermocouples in High-Velocity Air Streams and Analytic Approximation of Conduction and Radiation Errors," Technical Note 2599, National Advisory Committee for Aeronautics, Washington, D. C., January, 1952.

11. Zukoski, E. E., "Flame Stabilization on Bluff Bodies at Low and Intermediate Reynolds Numbers," Report No. 20-75, Jet Propulsion Laboratory, Pasadena, California, June 30, 1954.

12. Wright, F. H., and Becker, J. L., "Combustion in the Mixing Zone Between Two Parallel Streams," *Jet Propulsion*, 26, pp. 973–978, November, 1956.

REFERENCES (Cont'd)

13. Fenn, J. B., and Calcote, H. F., "Activation Energies in High Temperature Combustion," *Fourth Symposium on Combustion,* pp. 231–239, Williams and Wilkins Company, Baltimore, 1953.

14. Potter, A. E., "Effects of Pressure and Duct Geometry on Bluff-Body Flame Stabilization," Technical Note 4381, National Advisory Committee for Aeronautics, Washington, D. C., September, 1958.

15. Huellmantel, L. W., Ziemer, F. W., and Cambel, A. B. C., "Stabilization of Premixed Propane–Air Flames in Recessed Ducts," *Jet Propulsion,* 27, pp. 31–34, January, 1957.